The Impacts of Diamond Mining to Peatlands in the James Bay Lowlands

by

Peter Nicholas Whittington

A thesis
presented to the University of Waterloo
in fulfilment of the
thesis requirement for the degree of
Doctor of Philosophy
in
Geography

Waterloo, Ontario, Canada, 2013

Author's Declaration

I hereby declare that I am the sole author of this thesis, except where noted (see below).

This is a true copy of the thesis, including any required final revisions, as accepted by my examiners.

I understand that my thesis may be made electronically available to the public.

Exceptions to sole authorship:

Each chapter of this thesis has been submitted to a peer-reviewed journal, with chapters 2 and 3 already published. Some minor typographical or editorial differences may exist between the published version and the version that appears in this thesis.

Chapters 4, 5, and 6 will be subject to the requests of the reviewers and may differ substantially from those presented here.

For all chapters Dr. Price acted as an advisor, offering suggestions and insight as well as (usually) minor editorial changes. Chapters 3 and 4 are "Whittington and Price" chapters (i.e., no other co-authors).

Chapter 2 is published as:

Whittington, P.N., Ketcheson, S.J., Price, J.S., Richardson, M., and Di Febo, A. 2012. Areal differentiation of snow accumulation and melt between peatland types in the James Bay Lowlands. Hydrological Processes **26**(17): 2662-2671.

I was the lead author on this paper and did the majority of the writing and analysis. All authors contributed in some way to the written manuscript:

Mr. Ketcheson helped with the writing, mainly the introduction, as well as extensive field work.

Mr. Di Febo's and Dr. Richardson's contribution was related to the landscape classification and areal weighting. Dr. Richardson also helped with the discussion and statistical analysis.

Chapter 5 is submitted as

Whittington, P., Thompson, D.K., Price, J.S. submitted. Fire, rock and ice: a fire risk assessement of dewatered organic soils surrounding a bioherm at an open-pit diamond mine in the James Bay Lowlands. Submitted to Canadian Journal of Forest Research CJFR-2012-0499.

I was the lead author on this paper and did the majority of the writing and simple analyses (e.g., fuel loading, r^2, hydrology).

Dr. Thompson assisted with all things fire and provided guidance for the field methods. Dr. Thompson was responsible for the depth of burn model and results associated with that.

Chapter 6 is submitted as

Ali, K., Whittington, P., Remenda, V., Price, J.S. submitted. The role of permeable marine sediments in peatland-dewatering around a bioherm outcrop, James Bay Lowlands.

I wrote the majority of the study site and a lot of the methods, as well as early drafts of the Introduction. I discussed the objectives and theme of the paper at great length with Ms. Ali. We co-wrote (as applicable) the results and discussion at the early stages. Ms. Ali refined much of the text of later versions of the manuscript with comments from the other co-authors, including myself.

Ms. Ali did most of the analyses for the results of the marine sediment flows and as such is first author. This paper will also serve as a chapter in Ms. Ali's MSc at Queen's

Drs Price and Remenda acted as advisors, offering suggestions and insight as well as (usually) minor editorial changes.

All of the co-authors have read the above and agree with my (and their own) contributions.

Abstract

Approximately 7000 to 8000 years ago when Hudson Bay became ice-free the Tyrrell Sea flooded the Hudson basin and deposited fine grained marine sediments overlaying the previous glacial tills. Coincident with the ablation of the ice sheet isostatic rebound occurred causing regression of the Tyrell Sea and the emergence of a flat, relatively impermeable surface that would eventually host one of the world's largest wetlands: the Hudson Bay Lowlands. The low permeability marine sediments and low regional slope reduced recharge and runoff, respectively, so that basal tidal marshes were established, and with isostatic up lift were eventually replaced by swamp forests and then forested and non-forested bogs. Recent discovery of kimberlite (diamondiferous) pipes in an area of the lowlands has led the development of an open-pit diamond mine which requires dewatering of the regional aquifer. Dewatering is depressurizing the surrounding Silurian bedrock that underlies the marine sediments. It was hypothesized that these marine sediments would act as a confining layer, isolating the overlying peatlands from the regional bedrock aquifer. We tested this hypothesis by instrumenting a 1.5 km long transect located within the zone of the mine's influence that crossed various bogs and fens overlying these marine sediments, and was anchored at both ends by bedrock outcrops (bioherms), which represented areas of no marine sediment. Along this transect wells and piezometers were installed within the peat profile and upper marine sediments and bedrock to determine changes in water table and hydraulic head. The exposed bedrock outcrops (bioherms) did act as local drainage nodes, however, this effect was limited to ~30 m, beyond which water tables and hydraulic heads were similar to a control site located 25 km away. However, within this 30 m zone daily losses of water by the enhanced recharge often exceeded those of evapotranspiration (~3mm/day) representing a major local loss of water to the system. It is the distance to bedrock, rather than distance to bioherm, that determines strength of recharge. In areas of thinner marine sediments the daily fluxes were similar (but less) than those in the areas directly surrounding the bioherms, despite being 100s of meters away from the bioherms. The stratigraphy surrounding the bioherms lead to complicated flow regimes with higher conductivity layers (e.g., sands) circumventing the lower permeability marine sediments which may help extend the effect of the bioherms beyond the 30 m distance. The drying peat around the bioherms, and the elevated nature of the bioherms in a flat landscape, put them at increased risk for lighting strikes and thus fires; however, very little viable fuel exists in the peatlands around the bioherms and any fires that might occur would be confined to the bioherm and not spread into the surrounding peatland. Overall, at least within the first 5 years of aquifer

dewatering, seasonal weather played the dominant role in affecting the hydrology of the peatlands; a heavy snow pack and cool, wet summer can mask, or at least minimize the effects of aquifer dewatering.

Acknowledgments

I started my undergrad at Waterloo in 1999 and in the following decade (and a bit) I have made some incredible friends and colleagues, too numerous to mention them all by name here, but you know who you are.

To De Beers Canada, particularly the Victor Mine Environment Lab. The opportunity you have presented us to understand the James Bay Lowlands is unparalleled. Your unwavering commitment to science has not gone unnoticed, as it seems you are now overrun with other schools and agencies doing work on and around site; sorry about that. Special thanks to Brian Steinback for facilitating everything and the many late night conversations at the mine.

To the UW Guard Team and Rebecca Boyd, thank you for all of the opportunities (for procrastination and general theses avoidance) you have presented me. I will look back at my time with Campus Rec with very fond memories.

To the Wetlands Hydrology Lab students, both past and present, thank you for pestering me with countless questions about hydrology, data loggers, Microsoft Excel, and life in general; you have made me a much better researcher and teacher because of it and for that I offer a very sincere “Thank You”.

I would be amiss to lump you, Scott, in with the rest of the lab rats. You’ve been around since basically the beginning and have provided much support and advice that an extra “thanks brother” is due. Please note that the bar has been set at 5.3 years…

To Jean Andrey: thank you for the many random chats we’ve had over the years and the equally many opportunities you’ve presented me with.

To my advisor, Dr. Jonathan Price, who has obviously failed miserably in this role: I still do not drink coffee or scotch, nor do I play hockey, and I still consider The Tragically Hip to be one of the greatest bands ever.

To my friend, Jon: what an amazing “tenyear” it has been since Fall 2002. We have shared many laughs and countless adventures. Words truly cannot express the depth of my gratitude to you. Your keen wit, insightful comments, and commitment to academia are *nulli secundus*. You have set the bar high for me, and for that I ~~begrudge~~ thank you.

To my old employee, turned roommate, turned best friend, best-man, and more recently landlord, Adam. You are truly an good friend and a awesome guy. Thank you for all of the discussions about this, that and the other, particularly *K*.

To my parents: being a parent myself I can truthfully say that I cannot begin to express that debt that I owe you for setting the building blocks in motion at a young age that would allow me to get to this point in my life.

To my wife, Carly, I know this is a bit late, but will you marry me? Since this thesis came a few years later and we've already tied the knot I might as well praise you a little more. You are a remarkable woman. After giving birth to our wonderful son you managed to complete an entire Masters degree, plan and execute the best wedding ever, all while still being an incredible mother and raising a wonderful little boy. Anderson and I are truly lucky to have you in our lives. But let's be honest, the most impressive feat is that you've managed to put up with me all these years…

Dedication

This thesis is dedicated to my family, both new and old; particularly my son, mum and dad.

Table of Contents

List of Figures

List of Tables

1 Introduction

The Hudson-James Bay Lowlands (HJBL) represent about one-third on Ontario's landmass and are the largest sources of fresh water to the saline James Bay; they store nearly 35 gigatons of carbon and provide about a tenth of the globe's cooling benefits from peatlands. Despite these impressive statistics, a dearth of information exists about how the lowlands function hydrologically, ecologically, and biogeochemically. Until recently this lack of knowledge was not relevant to the majority of Ontario's (and wider) audiences. However, with the discovery of many mineral rich deposits (e.g., De Beers Victor Mine, Ring of Fire) leading to resource extraction, as well as a changing climate, it is now critical to understand how these vast peatland systems couple hydrology, ecology, biology and chemistry and how changes would manifest themselves within the complex ecosystem.

Bog and fen peatlands comprise the majority of the surface area of the lowlands, occupying ~ 90% of the lowlands. Bog peatlands are ombrogenous, meaning they receive inputs of water from precipitation (P) only. Fens, by contrast, may receive surficial waters (streams) as well as groundwater discharge. The dominant water loss from both peatland types is evapotranspiration (E_t). Thus a simple water balance of $P-E_t$ would indicate that P must exceed E_t and that other water losses from these system (e.g., groundwater recharge) would need to be minimal to sustain the high water tables that typify these environments. Thus the factors that are important for peatland development are the wet and cool climate, flat landscape and restricted vertical seepage losses.

These factors have combined on an immense scale to give rise to the world's second largest wetland complex, the Hudson-James Bay Lowlands. Annual precipitation is 700 mm/year in a cool subarctic climate which helps limit evapotranspiration to ~430 mm/year. The extremely low relief (<1% slope) in the HJBL delays lateral runoff (e.g., streams). In fact, higher rates of isostatic rebound (~1 cm/year) near the coast of James/Hudson Bay, where the ice was present the longest, is continually reducing the regional gradient, further reducing runoff (Glaser et al., 2004a; Glaser et al., 2004b). Thick (10s to 100s of meters) low permeability marine sediment deposited at the bottom of the Tyrrell sea from the last glaciation supressed groundwater seepage loss so that the inflow of fresh water from rivers and glacial melt helped reduce the salinity and peat started to form on the mineral base, quickly separating it from the saline water underneath (Glaser et al., 2004a; Price and Woo, 1988a). Thus bog and fen peatlands have continued to grow, relatively uninhibited, for the last 6000 years and now dominate the landscape.

The delicate balance of these factors is changing with the demands for the natural resources of the HJBL, as well as the warming climate. Discovery of kimberlite (diamondiferous) pipes in an area of the James Bay Lowland has led to open-pit diamond mining, which requires substantial groundwater pumping to dewater the mine thus causing depressurization of the regional bedrock aquifer. Early modelling reports predicted a daily pumping rate of approximately 85,000 m^3/day in the middle of the mine's life (year 5 of 12), of which nearly 50% is predicted to be "additional recharge from muskeg [peatland]" (HCI, 2004a). This depressurization has the potential to significantly affect the peatlands, as the groundwater seepage losses (previously shown to be minimal) (HCI, 2004a) will depend on the nature and strength of the connection between the surficial peatland aquifer and the regional (bedrock) aquifer, which will ultimately be controlled by the properties of the marine sediments between them. Complicating matters are the presence of scattered bioherms (ancient coral reefs) that protrude to the surface as exposed bedrock outcrops and represent a direct peat-bedrock interface (i.e., no marine sediments) where enhanced seepage was predicted (HCI, 2004a).

Given the dearth of information noted previously we needed to speculate at how these peatland systems functioned so that we could begin to understand what a loss of 42,500 m^3/day (i.e., the recharge from muskeg) might do the hydrology and biogeochemistry of the lowlands and what changes may occur so that we could instrument accordingly.

A generally accepted theory is that bogs are storage features of the landscape and that fens are the conveyors of water (Quinton et al., 2003) and are important in understanding runoff. Patterned fens have a repeating pool, lawn, ridge topography and when exposed to water table drawdown, the pools and lawns subside the most and the more densely packed ridge peat subsides the least, deepening the pool (Whittington and Price, 2006). Concurrent with this are increased water table fluctuations due the lower specific yield found in the recently compressed peat; these increased water table variations cause enhanced decomposition of the peat and therefore more subsidence (Whittington and Price, 2006). Ubiquitous to all larger bogs in boreal zones are the presence of internal fen water tracks (Glaser et al., 1997) (typified with the pool, lawn, ridge topography) which appear to drain the tops of large, heavily pooled, domed bogs. Water table drawdown could essentially disconnect these pools from contributing to runoff, lowering stream levels and thus fish habitat.

This same process was anticipated to occur to the marine sediments underlying the peatland aquifer; if the clay content is high, then we would expect to see significant subsidence due to dewatering in areas with thick marine sediments, essentially creating non-pre-existing depression storage features in the landscape

(i.e., larger scale depressions than the small ponds), these, combined with the pools noted earlier, would create a “fill and spill” (Spence and Woo, 2003) environment requiring more water to contribute to runoff (i.e., water levels in the ponds and depressions would need more water to raise the level up to a point that the water could ‘spill’ over into the adjacent pond). Therefore, potential changes in runoff from the peatlands would be dependent on two main things: 1) any vertical drawdown experienced in the peatlands causing surface subsidence, and 2) any subsidence of the marine sediments. Both of these are dependant largely on the properties of the marine sediments.

Of great concern to the First Nations communities are mercury concentrations in fish. Mercury is a naturally occurring global pollutant, however total mercury concentrations in the waters of the HJBL are low, and are largely in an inorganic form (Kirk and St. Louis, 2009). This inorganic mercury has the potential to transform via anaerobic bacterial respiration to the organic neurotoxin methylmercury, which occurs in wet, reducing environments. The majority of such methylation occurs in the anaerobic zone, especially within the zone of water-table fluctuation, where carbon and terminal electron acceptors are abundant, and Sulphate Reducing Bacteria (SRB) thrive (Ullrich et al., 2001). If the peat subsides, and fluctuations in the water table increase in frequency and magnitude, this has the potential to enhance methylmercury production. However, with the lower water tables that are anticipated, the methylmercury would be unable be exported from the system until all of the pools were once again connected and able to ‘spill’ into each other, contributing to runoff. If the subsidence is considerable, then methylmercury concentrations in streams could decrease while concentrations in disconnected pools could increase. When dewatering of the mine ceases and water levels return to pre-mining conditions, a pulse of increased mercury concentrations to the tributaries could occur (but would still be well below drinking quality guidelines) as the pools become connected once more.

Therefore, the overall objective was to characterize the changes in peatland structure, hydrological connectivity and mercury fate and transport in response to mine dewatering. This ultimately became a Collaborative Research and Development (CRDPJ 360525 - 07) grant with NSERC (Natural Science and Engineering Research Council) awarded to Dr. Jonathan Price at the University of Waterloo, Dr. Victoria Remenda at Queen’s University and Dr. Brian Branfireun at Western University (previously at University of Toronto, Mississauga).

This thesis is one part of that project; it focuses on peatland processes and its hydrological connectivity.

1.1 General methods

To determine the changes in peatland structure, hydrological connectivity, and mercury dynamics, an area expected to be impacted by the mine in the early years of dewatering was selected. The area selected also needed to cross various peatland forms (bogs and fens indicative of the area), as well as covered various stratigraphies (no marine sediments (i.e., bioherms) and thin to think marine sediments) to allow an overall assessment of the role of the marine sediments in dewatering to various peatland types. This was achieved by instrumenting a 1500 m long transect that crossed various fen and bog peatland that was also anchored at both ends by bioherms but traversed areas of thick marine sediments in the middle of the transect. The transect also crossed two small streams allowing for stream discharge (and thus runoff) measurements.

1.2 Specific Objectives

The NSERC-CRD proposal sub-objective that formed the basis of this thesis was to identify and characterize the hydrological linkage between upper (peatland), intermediate (marine sediments: sand and fine-grained overburden) and lower (bedrock) systems and determine the change in recharge and discharge flow pathways resulting from aquifer dewatering. Ultimately this objective was addressed in Chapter 4 where we assessed the impacts of dewatering across our entire study area. It was clear early on that including the bioherm impacted areas (i.e., start and end of the transect) in with the rest of the transect area was misleading as a different set of processes were occurring. Therefore the bioherms required a special set of objectives due to the minimal presence of the marine sediments in these areas. Chapter 3 focused solely on the peatland hydrology surrounding the bioherms and it was clear from the results of Chapter 3 that further investigation was warranted into the hydrogeology of the marine sediments that were present in the near bioherm areas and that became the focus of Chapter 6. Because of the localized dewatering occurring around the bioherms, and some wildfires that were occurring in close proximity to the mine, the decision to assess the fire risk of dewatered bioherms was made, as it is also an impact of the dewatering and had the potential to disturb various biogeochemical cycles.

Finally, it became apparent early in the project that seasonal weather, particularly snow accumulation and spring melt, was extremely important for characterizing hydrological and chemical results and thus the need to adequately determine the snow pack and melt regimes for the various landscapes (bog and fen) became the focus of Chapter 2.

2 Areal differentiation of snow accumulation and melt between peatland types in the James Bay Lowland

This chapter is published as:

Whittington, P.N., Ketcheson, S.J., Price, J.S., Richardson, M., and Di Febo, A. 2012. Areal differentiation of snow accumulation and melt between peatland types in the James Bay Lowlands. Hydrological Processes 26(17): 2662-2671.

2.1 Overview

Snow accumulation and melt between various peatland types in the James Bay Lowlands is poorly understood despite being a significant source of fresh water to the saline James Bay. Many topographical factors that control snow accumulation and melt (e.g., slope, aspect) are not relevant in the James Bay Lowlands due to the extremely low relief. Thus vegetation characteristics (e.g., winter leaf area index, tree density), which are strongly linked to peatland type, may dictate spatial patterns of snow accumulation and melt across the landscape. A 1.5 km long transect that bisected 5 peatland types representative of the local area was used to determine average snow depth, density and water equivalence for each of the landscape units. The peatland types were classified, in part, due to the density of treed vegetation and were named open bog, open shrub fen, low density treed fen, medium density treed bog, and high density treed fen. Those with medium or high-density treed vegetation accumulated significantly more snow than those with low or open densities. Snow density, however, showed no correlation with landscape unit and snowmelt proceeded at similar rates between all landscape units due to the relatively open canopy typical of this environment. A randomization test showed that the areally weighted basin average snow depth estimates varied by less than 10 cm as a result of the small but statistically significant differences in snow accumulation among landscape units. These differences are therefore relatively unimportant for accurately quantifying basin-wide snow depth in this landscape.

2.2 Introduction

The James Bay Lowlands (JBL) represent a significant contribution of the fresh water runoff to the saline James Bay (Rouse et al., 1992), yet there is a dearth of information on how different types of wetlands

behave hydrologically in terms of snow accumulation and melt. Determining the average snow depth, density and water equivalent for large basins can be critical for an accurate understanding of the hydrological processes (e.g., runoff) in these basins (Hamlin et al., 1998; Pietroniro et al., 1996; Pomeroy et al., 2002; Woo, 1998), yet doing so can be expensive and labour intensive. However, landscape units within the same climatic region tend to accumulate snow with repeatable patterns (Steppuhn and Dyck, 1974; Woo and Marsh, 1978) and thus targeted surveying in easily identifiable landscape units can improve our regional generalizations from a few measurements (Adams and Roulet, 1982) in targeted terrain types (Woo and Marsh, 1978) versus a simple random sample (Elder et al., 1991).

At the regional (Steppuhn and Dyck, 1974) or macroscale (Pomeroy et al., 2002) (10 – 1000 km) snow accumulation is controlled by latitude, elevation, orographic influences, atmospheric circulation, and large water bodies; at the local or mesoscale (100-1000 m) it can be controlled by terrain variables such as elevation, slope and aspect and vegetation variables such as vegetation type, canopy and tree density; and at the micro scale (10 – 100 m) by interception, surface roughness and redistribution along airflow patterns. Despite differences in snow accumulation at the micro scale, Pomeroy and Gray (1995) note that snow accumulation patterns are still evident at the stand (meso-) scale. These accumulation patterns typically vary with the effective winter leaf area index (LAI; total horizontal area of stems, needles and leaves per unit area of ground) (Pomeroy et al., 2002) and the impact of wind redistribution of snow (Benson and Sturm, 1993), both of which should be affected by differences in the relative tree density between different landscape units in the JBL.

Snow interception in forested canopies is impacted in part by the leaf area and tree species (Hedstrom and Pomeroy, 1998), and in combination with sublimation losses directly from the canopy can greatly reduce snow accumulation in forested sites (Koivusalo and Kokkonen, 2002). In areas where the LAI is low, snow accumulation patterns are similar to open areas (Pomeroy et al., 2002). Further, wind-blown snow from adjacent open areas will accumulate in stands of more dense vegetation where surface wind speeds are reduced (Benson and Sturm, 1993). The JBL is dominated by low LAI landscape units (e.g. sparse trees in bogs) that have yet to be suitably characterized but will likely result in much subtler differences in snow accumulation patterns compared to forested watersheds with higher average LAI and also higher spatial variability in LAI.

Relatively little research on snow accumulation and melt processes has been conducted in low relief and sparsely vegetated landscapes typical of Canada's northern lowland regions. Adams and Roulet (1982) studied snow accumulation in a small sub-arctic drainage basin and found that average snow depth was

greatest in areas with the closest spacing of trees (e.g., 146 cm with 2-6 m spacing and 126 cm with 7-12 m spacing) and shallowest in open tundra environments (e.g., 77 cm with shrub covered tundra). Sturm et al. (2001) found that the deepest snow packs were found in areas with the tallest, densest shrubs in a tundra site in arctic Alaska. Additional research is required to accurately characterize spatial variability of snow accumulation in JBL sub-arctic lowland environment.

The rate of snowmelt at the micro and macroscale is controlled and also strongly influenced by the vegetation canopy LAI, hence tree density, and its effect on the energy available for snow ablation (Boon, 2009). A forest canopy will reduce the net radiation and turbulent transfer contributions to snow ablation. Similar to accumulation processes mentioned above, the relatively open canopies in the JBL may not be notably different than open areas resulting in similar snow melt rates across landscape units.

Many studies have used the landscape unit approach in their snow studies, however, these have largely been used in the Western boreal forest (e.g., Pomeroy et al., 2002), Southern Ontario forest (Adams, 1976), Sierra Nevada alpine (Elder et al., 1991), disturbed forest (Boon, 2011), sub-Arctic (Adams and Roulet, 1982), and high-Arctic (Woo, 1998; Woo and Marsh, 1978; Woo and Young, 1997) systems. Few studies have employed the "landscape unit" approach in wetland dominated basins, especially in the James Bay Lowlands where more than 60% of the landscape is covered by bogs and fens (Riley, 2011). Many of the terrain factors that can affect snow accumulation at the mesoscale are irrelevant in extremely low relief areas such as the JBL. Vegetation factors, however, vary with peatland type, and are likely to influence snow accumulation and ablation patterns. Different peatland types are, in part, a function of vegetation structure and unambiguously classifying them is difficult (Di Febo, 2011). While the Canadian Wetland Classification System (NWWG, 1997) categorizes wetlands with a three level hierarchical system based on 1) class (e.g., bog or fen), 2) form (e.g., peat plateau bog or channel fen), and 3) type (e.g., treed bog or graminoid fen), these hierarchical structures, especially form, are often difficult to identify. Riley (2011) offers an alternative system which ignores form and focuses mostly on class and type, where type is predominantly vegetation based. Therefore, using Riley's (2011) classification scheme would conveniently divide the landscape into relatively homogenous "landscape units".

Considering the limited understanding of snow dynamics between and within different "landscape units" in peatland dominated basins, the objective of this paper is to determine the snow pack and melt regime characteristics of various peatland types in the James Bay Lowlands.

2.3 Study Site

The study site is located 500 km north-north-west of Timmins, Ontario; 90 km west of Attawapiskat, Ontario in the Hudson-James Bay Lowlands (lat. 52.8349, long. -83.9290). The study area comprises part of the North Granny Creek (NGC) watershed, which is a tributary of the Nayshkootayaow River and subsequently the Attawapiskat River Figure 2-1. North Granny Creek splits into two distinct channels which we have labelled south-North Granny Creek (SNGC) and north-North Granny Creek (NNGC).

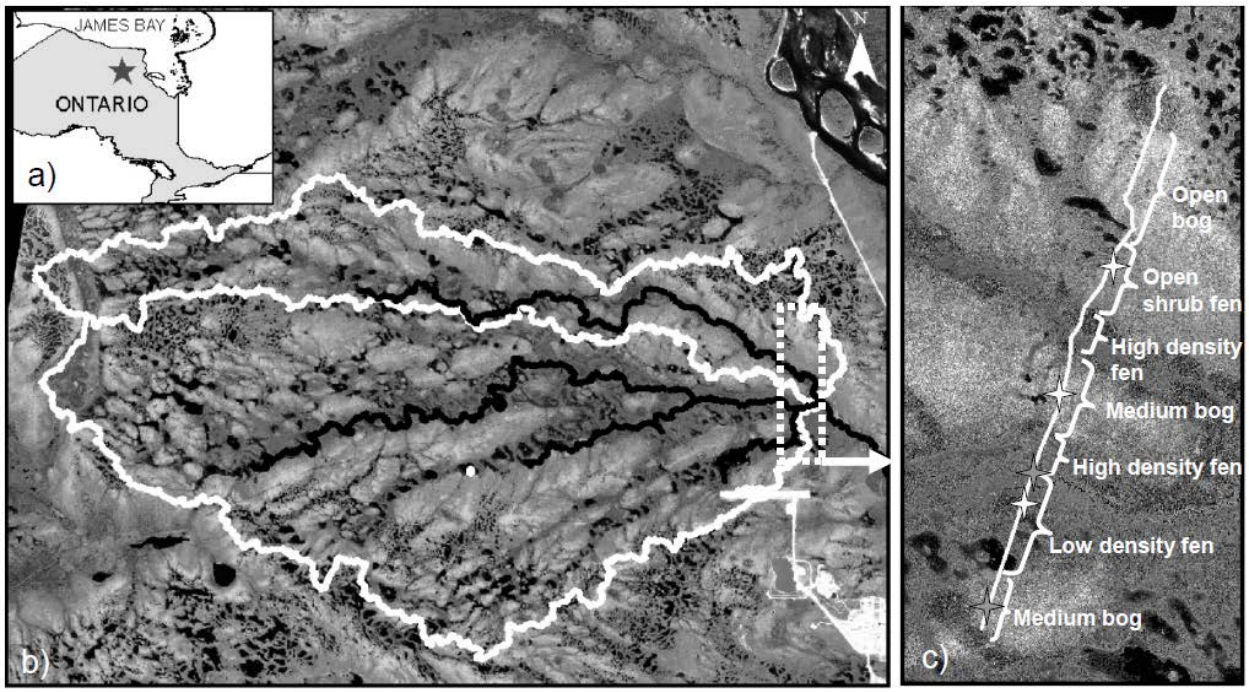

Figure 2-1 Site Map. a) Location of study area within Ontario. b) IKONOS image showing part of the NGC watershed divided into the NNGC and SNGC subwatersheds (white lines) and the streams (black lines). The De Beers Victor mine camp is visible in the lower right hand corner; the pit is located ~1km further to the right. The image is approximately 9 km across C) IKONOS image of the snow survey transect (solid white line), ablation lines and snow pits (all stars 2009, grey stars 2011) and landscape types along the transect. The transect is 1500 m long. Note: Some high vegetation density fen sites do exist in the low density fen areas but have been omitted in this figure and Table 2-1 for simplification. They were classified correctly for all analyses.

The snow survey transect was 1.5 km long and bisected 5 different peatland types common to the area. The start of the transect was a medium density treed lichen-rich bog which led into areas of low density treed fen and high density treed fens in the riparian areas near the streams. The bog that separates SNGC and NNGC is similar to that at the southern end of the transect. At the north end of the transect is an open

shrub fen water track classified as open shrub fen. Lastly, there is an open, lichen-rich low shrub bog at the northern-most end. Table 2-1 provides a key to the nomenclature (including transect locations).

Table 2-1 Landscape classification class and type. The superscript T^5 is a quantification of how open the area is, e.g., <5% tree cover. The letters can be deduced from the classification column. Tree distance was determined from the manual tree density survey. Height was determined as the average of non-zero returns from the canopy height model. % treed was calculated as the number of non-zero returns for that landscape type/total returns (zero and non-zero) for that landscape type x 100.

				Tree properties		
Distance along transect (m)	Classification (Riley, 2011)	Official	This paper	Height (m)	Distance (m)	% treed
0 to 145; 615 to 810	Medium density treed lichen rich bog	T(md)lrB	Medium bog	3.3	16	50
145 to 580	Open treed or low density treed fen	T^5F-T(ld)F	Low density fen	3.9	17	18
580 to 615; 810 to 866	High-density Treed Fen	T(hd)F	High density fen	3.9	4	63
886 to 1200	Open shrub fen	OsF	Open shrub fen	3.0	29	6
1200 to 1500	Open, lichen-rich low shrub bog	OlrlsB	Open bog	3.7	35	12

The two closest stations with long-term meteorological records were Lansdowne House (inland 300 km west-south-west) and Moosonee (near the coast, 250 km south-east). The average annual January and July temperatures for Lansdowne House are -22.3 and 17.2 °C, respectively, and for Moosonee are -20.7 and 15.4 °C, respectively (Environment Canada, 2008). Annual precipitation for Lansdowne House is 700 mm with ~35% falling as snow; for Moosonee precipitation is 682 mm with ~31% falling as snow.

The study site is located at the De Beers Victor Mine and therefore the possibility of dust enhanced melt (from blasting in the open pit) must be addressed (Drake, 1981). Drake and Moore (1980) studied dust loading around a mine in Schefferville, Quebec and noted that prevailing winds were a large control on dust fall and that within a distance of 1 km cross-wind from the disturbed area, dust fall returns to a "…presumably normal background level." The normal background values by Drake and Moore (1980) are reported as 2 g/m^2 over the winter season (~6 months). The study area at the Victor Mine is located several (3-4) kilometers directly upwind of the mine and thus dust fall is likely not an issue. In addition, as part of De Beers' monitoring requirements dust fall is collected at 4 orthogonal locations around the mine. At the location nearest the transect dust fall for 2008, 2009, and 2010 for May were 0.8, 1.8 and 1.2 g/m^2/30 days (Steinback, personal communication; 2011 data were not ready for release, but as the pit continues to get deeper, the risk of dust contamination diminishes), which, while slightly higher, are in-line with those reported by Drake and Moore (1980).

2.4 Methods

2.4.1 Meteorological

A weather station was erected ~ 1 km south of the Victor Mine in March 2000, this weather station was decommissioned when a new weather station was erected ~2 km north of the Victor Mine near the study area in April 2008. Both weather stations measured precipitation, temperature, relative humidity, net radiation, wind speed and direction.

2.4.2 Snow surveys and ablation lines

Snow surveys were conducted every 4-5 days from April to May in 2009 and 2011 along the research transect. In 2010 there was an abnormally low snowfall and early melt, and is not considered in this paper. Depth measurements using a metal ruler were taken every 15 paces (~10 m) with depth and snow water equivalent (SWE) every 30 paces using an ESC-30 (Eastern Snow Conference) plastic snow tube (1.2 m by 0.07 m i.d.) and hanging mass scale. SWE was calculated based on the mass of the snow in the tube and water density of 1 g/cm^3; snow density was calculated using the volume (depth of the sample and tube dimension). At each SWE measurement location a GPS reading (± 4m) was taken to locate the landscape type sampled (a separate ground truthing survey for landscape classification was completed in November 2009). To measure the rate of snowmelt, measurements of the change in snow surface elevation were made at 0.5 m intervals along 6.5 m to 10.5 m ablation wires. In 2009 (all stars, Figure 2-1) they were erected in medium bog (x2), low density fen (x2), and open shrub fen (1) (Figure 2-1) and in 2011 (grey stars only, Figure 2-1) in medium bog (1) and low density treed fen (1). Snow pits were used to measure density and temperature profiles in the area near each ablation line in both years, however they were only completed once in 2011. Density samples were taken using a fixed volume cutter (6x3x5.5cm=99cm^3) centered at every 5 cm for the entire snow pit depth. Ablation lines and snow pits were measured when they were reached along the snow survey transect. Different snow pits in roughly the same area (within 5 m) were used each time.

2.4.3 Tree canopy properties

Starting at the southern end of the transect, the distance and the diameter at breast height (DBH) was measured for the closest tree in each quarter (following the point-quarter method (Cottam and Curtis, 1956)) at a point every 50 m along the transect. Due to the stunted growth of trees in the James Bay Lowlands the definition of tree was extended to those with a DBH of 6 cm, rather than 10 cm. Where

canopy cover was very open (e.g., north end of the transect) and trees would be double counted (i.e., the same tree would be the closest for the subsequent quarter) the spacing was increased, or the survey stopped.

To create the canopy height model, a 5 m resolution digital surface model (DSM) was first interpolated using the maximum elevation of all LiDAR returns using a 5 m by 5 m moving window that followed the snow survey transect. The ground surface elevation was subtracted from this DSM using the 5 m resolution bare earth DEM (digital elevation model, see below). Areas with no classified vegetation returns were assigned a height of 0 m.

2.4.4 Landscape classification

The watershed boundaries and landscape composition are based on classification of LiDAR and IKONOS remote sensing imagery (Di Febo, 2011). Briefly, a maximum likelihood classification was conducted on the IKONOS red, green, blue and near-infrared bands as well as several topographic derivatives computed from a 2.5 m resolution LiDAR derived DEM that were shown to improve the classification accuracy. The final cross-validated accuracy of the classification (using separate training and validation classes and excluding water, which is relatively easy to discriminate) was approximately 80%.

2.5 Results

The average April temperature (when the majority of the melt occurs) based on the 8 year record located on site (2000-2007) fell between those at Lansdowne House and Moosonee, suggesting that those stations could be used for the long term average. The average daily temperatures for April 2009, 2011 and the 30 year Lansdowne House and Moosonee averages were, -2.9, -2.2, -2.4 and -1.6 °C , respectively, making 2009 slightly cooler than average and 2011 average. The first half of April 2009 averaged -6 °C whereas for 2011 it was -3 °C, in part due to a warm period (average daily temperatures >0) for 4 out of 5 days (and the <0 day daily temperature was only -1.8 °C) from April 8 to April 13, 2011; the second half of April was similar for both years (Figure 2-2).

In 2009 a 5 day warm period occurred from April 13 to April 18, with April 16, 2009 having a daily average and max temperature of 7.4 and 15.3 °C, respectively. Wind speeds were higher for the start of melt in 2009, but were similar between years after ~April 18. For 2009 and 2011 snow accumulation at the end of March (i.e., near the start of melt) was 133% and 71%, respectively, of the normal values reported at Lansdowne House (inland station), though snow melt in 2011 had started prior to our arrival.

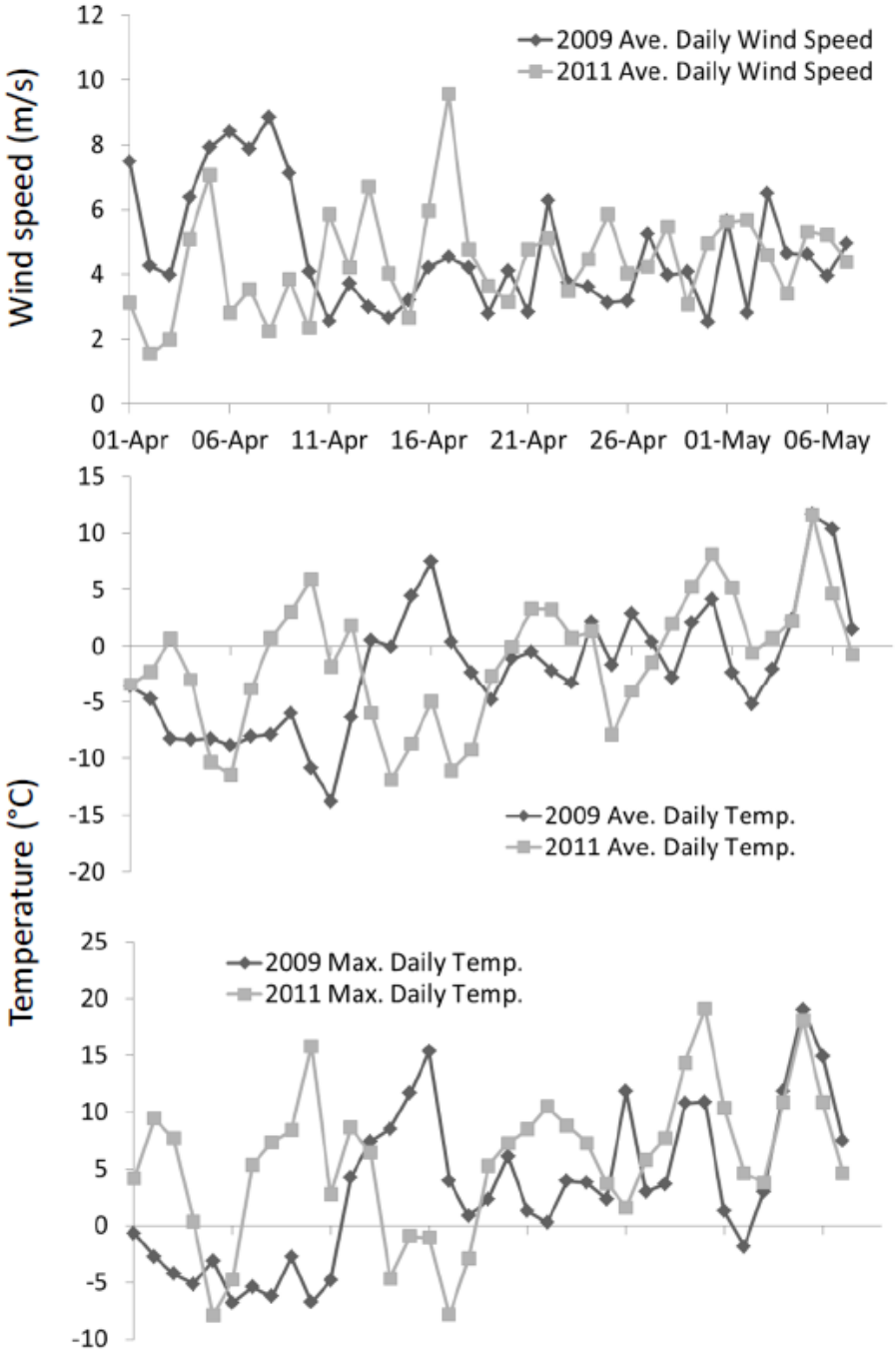

Figure 2-2 Meteorological variables for the 2009 and 2011 melt seasons.

In 2009 snowmelt started on April 9, and continued until ~ May 7. Average snow depth across the site was 75 cm at the onset of melt, ranging from 63 cm in the open shrub fen to 90 cm in the medium bog (Figure 2-3). In 2011 snow melt had started before we arrived on site and some ripening and settling of

the snow pack had occurred, however, very few bare patches were present (the tops of a few hummocks at the northern end of the transect were visible). Average snow depth upon arrival in 2011 was 39 cm, ranging from 27 cm in the open bog to 47 cm in the high density fen (Figure 2-4). The completion of melt was not well documented in 2011 due to limited field personnel but the site became snow free ~April 28. For both years the medium bog and high density fen were above average in snow accumulation and were statistically significantly different than the open shrub fen, low density fen and open bog which were below average (Table 2-2).

At the onset of melt in 2009 snow density ranged from 0.17 g/cm^3 to 0.20 g/cm^3 in the open bog and low density fen, respectively, but offered no real trend with landscape type (Figure 2-4). Snow water equivalence ranged from 12 cm in the open shrub fen to 18 cm in the medium bog. The site remained completely snow covered until April 13 and became functionally snow free ~May 7 (some small, isolated drifts in heavily treed areas remained) (Figure 2-3). In 2011 snow density ranged from 0.28 g/cm^3 in the low density fen to 0.36 g/cm^3 in the open bog on the first day of measurement (Figure 2-4). Again, no real trend with landscape type was observed. SWE was highest in the medium bog at 16 cm on the first day of measurements and was lowest in the low density fen with 11 cm. In both years the medium bog had the highest SWE followed by high density fen. Open bog was the second lowest in both years.

The rate of snow surface lowering beneath the ablation lines in 2009 and 2011 were very similar between landscape types for the same time period for both years and ranged between 0.5 cm/d and 10 cm/d (Figure 2-5a/b). The large increase in the second medium bog location was due to some small patches of relatively deep snow remaining that melted to nothing very quickly. For 2009 these corresponded to melt rates of between 2.3 and 0.24 cm/day (Figure 2-5c) and again were similar between all landscape types. The fewer points are a result of no snow pits being conducted on the last measurement days due to a very shallow snow pack.

Temperature profiles (not shown) in the snow pits in 2009 showed the snow profile in all 5 of the pits becoming isothermal and ripe (~0 °C) around April 21 shortly after the warm period noted previously (Figure 2-2). In 2011 the first (and only) snow pits (April 12) showed an already isothermal and ripe snow pack, again, corresponding with the end of the warm period (Figure 2-2).

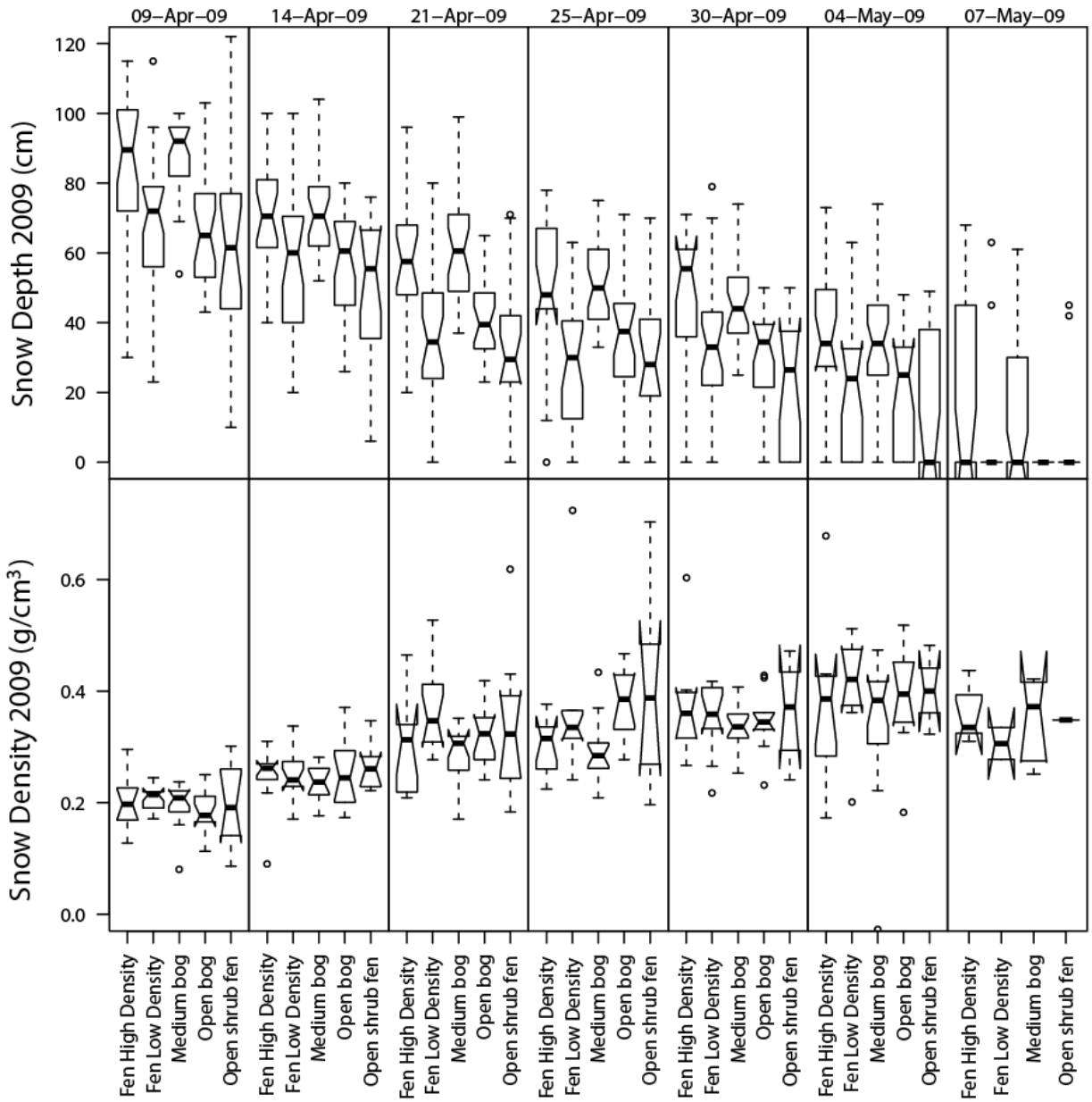

Figure 2-3: Box plots of snow depth (top) and density (bottom) through the melt period for 2009. The whiskers (upper and lower lines) show the 5% and 95% values, and open circles are outliers. The notches above and below the median can be used as a visual test of significance: where the notches do not overlap (e.g., low density fen, medium bog), they are significantly different at 5%, but where they do overlap (e.g., open bog and open shrub fen) they are not significantly different (R Development Core Team, 2009).

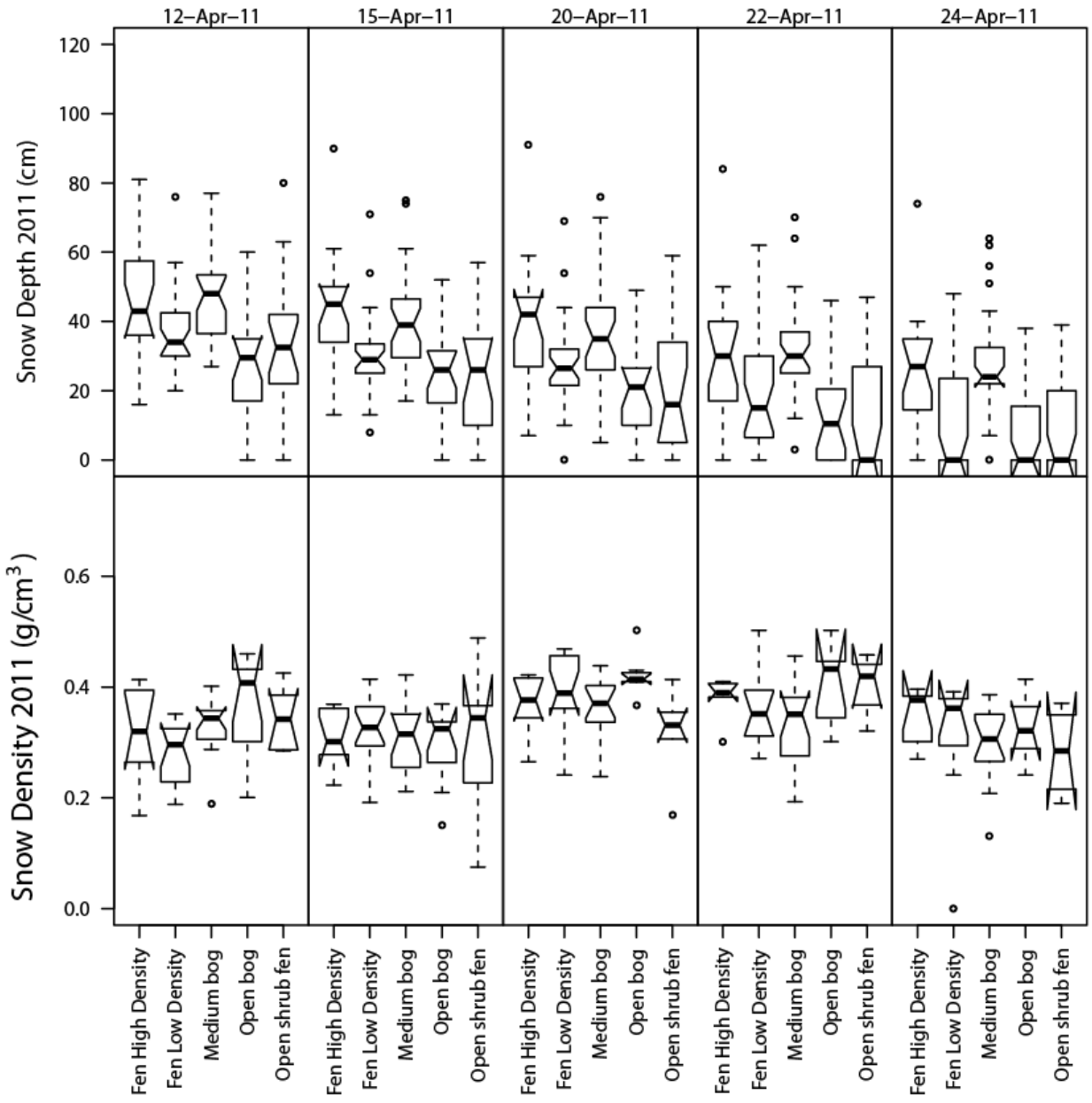

Figure 2-4: Snow depth (top) and density (bottom) through the melt period for 2011. See comment for Figure 2-3.

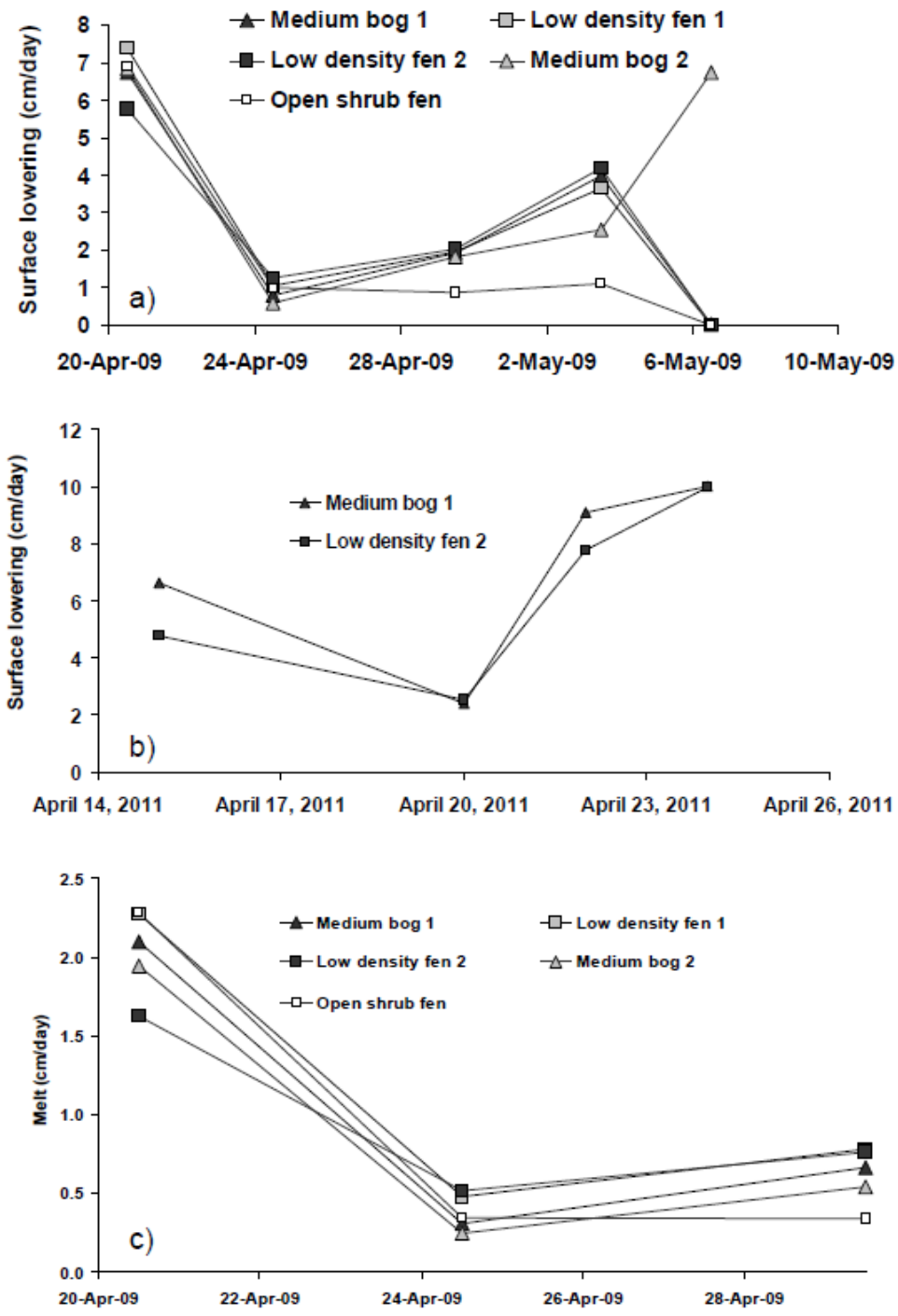

Figure 2-5 Snow surface lowering determined from ablation lines for 2009 (a) and 2011 (b) and the corresponding melt rates for 2009 (c). Snow pits were not completed on the last day.

The average distance to a tree (which is an inverse surrogate for tree density) is being used in this paper instead of tree density as it removes the need for dividing by an arbitrary area (e.g., hectares) to convert distance to a density. Snow depth at the onset of melt (or first survey for 2011) was inversely correlated to average distance to tree (Figure 2-6). The open bog point was artificially placed at 35 m distance as the tree density survey was stopped due to very low tree density (35 m was the furthest distance recorded in the open shrub fen before the survey was terminated). The R^2 values excluding the open bog point for 2009 and 2011 are 0.52 and 0.56, respectively. The open fen and open bog had 6 and 12% tree coverage, based on the canopy model created by the LiDAR, compared with 50 and 63% coverage for the medium bog and high density fen locations, respectively (Table 2-1). Shrub heights were not part of the original tree survey, however, personal observations show that in the medium bogs' shrubs were ~<60 cm tall and spaced similarly to the trees. In the open fen and open bog shrubs were much more prevalent than trees, however less frequent that in the medium bog locations, and were smaller (~<45 cm).

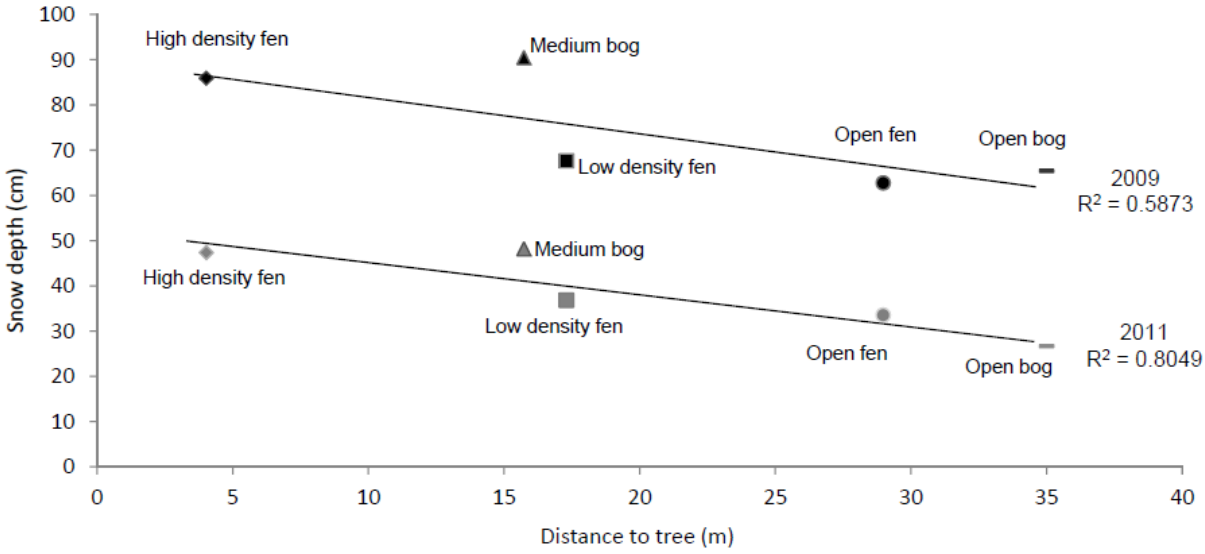

Figure 2-6 Average distance to tree versus snow depth for the different landscape types for 2009 (dark) and 2011 (white) initial snow survey. Recall tree being defined at a DBH >6cm.

2.6 Discussion

Classification of any landscape into "landscape units" is difficult, especially low relief environments like the JBL. Riley's (2011) system offers more flexibility over the NWWG (1997) as many of the types are scale dependant on the density of treed vegetation. Snow depth in this peatland complex varied by site (Figure 2-3, Figure 2-4) and was statistically significant between those with higher density and those with

lower density (Table 2-2). For instance, low and high density fen were different, however, low density fen and open bog or open shrub fen were not. This is also supported by the strong correlation between snow depth and tree distance (Figure 2-6). Sites with high or medium tree densities had snow depth above the overall average and those with low tree densities were below; this trend was consistent for both years' data. Snow density, however, was similar among landscape types and almost none were significantly different.

Table 2-2 p-values of Wilcoxon rank sum difference of means test for snow density (below diagonal) and snow depth (above diagonal) at onset of snowmelt (2009/2011). Bold entries significant at 95% or better.

	Fen High Density	Fen Low Density	Medium Bog	Open Bog	Open Shrub Fen
Fen High Density	-	**<=0.01/<=0.01**	0.95/0.90	**<=0.0001/<=0.0001**	**<=0.001/0.013**
Fen Low Density	0.90/0.43	-	**<=0.0001/<=0.0001**	0.45/0.24	0.29/0.32
Medium Bob	0.73/0.79	0.76/**<=0.05**	-	**<=0.0001/<=0.01**	**<=0.0001/<=0.001**
Open Bog	0.29/0.22	0.10/**<=0.05**	0.20/0.20	-	0.48/0.03
Open Shrub Fen	0.86/0.53	0.87/0.10	0.91/0.71	0.53/0.23	-

Melt rates were similar between landscape types and most proceeded at very similar rates (Figure 2-5), regardless of tree density. While the snow is deeper in areas with denser tree cover, shading by the canopy of these stunted, relatively well-spaced trees is minimal, and at almost all points along the transect there is always a clear view of the sky. Reifsnyder and Lull (1965) showed that in forested environments (red pine), reducing canopy cover from 1.5 m average distance to tree to 7.7 m increased light intensity from 15 to 60 percent. As the tree distance is much larger in our study area (16 to >35 m) and the stunted black spruce typical of the JBL would have an already more open canopy than red pine, it is not surprising that melt rates proceeded similarly among landscape types. Exceptions to this are the very dense forested areas near the streams (average distance to tree of <4 m), but these represent a small proportion of the area (about 3% (Di Febo 2011)). Therefore, the denser tree cover generally encourages snow deposition, likely due to lower wind speeds (Benson and Sturm, 1993; Ketcheson et al., 2012), but is insufficient to markedly reduce the radiation budget and thus the rate of melt. While we do not have meteorological instruments in the forested sections to quantify the wind speed differences, field observations support lower wind speeds in the treed areas compared to the open fen and bog. Therefore the duration of the snowmelt period in the JBL is ultimately dependant on how much snow was present at the start of the melt and the radiation balance.

Our results indicate small but statistically different snow depths between the majority of the landscape units at this JBL study site. In order to test whether these differences were *hydrologically* important at the

scale of the entire drainage basin, a simple reallocation experiment was conducted. Based on the analysis of Di Febo (2011) we were able to relate our landscape units to Di Febo's (2011) to areally weight the snow depths for the entire basin for the snow melt period. These areally weighted basin average snow depth values were always within 0.8 cm (Table 2-3) of the field snow survey average, suggesting that the snow survey chosen was representative of the basin as a whole (see below and Table 2-3). To test the importance of the differences between landscape units, observed snow depths were re-assigned to different land cover types iteratively until all possible permutations of land cover type/snow depth observations were satisfied. The basin average snow depth was re-calculated each iteration and recorded. There are 5 landscape units and therefore there are 120 (5! = 5x4x3x2x1=120) ways (permutations) of reallocating the depths to the landscape unit areas. Table 2-3 shows an example for the first day of snow surveys in 2009. The snow survey average was 74.5 cm at the onset of melt, which compared well with the average of the "correct" order of areally weighting the depths of 73.7 cm. The maximum (Max column, Table 2-3) would be 1 outcome (of the 120) where the depths arranged themselves ascending with ascending area (i.e., the shallowest snow depths with the smallest areas), whereas the minimum (Min column, Table 2-3) would occur when they were arranged in reverse. For example the 62.8 cm average depth for open shrub fen was applied to the area for high density fen (Max) and then to low density fen (Min) (Table 2-3). The outcomes of the other 117 (min, max, correct) cases are summarized using box plots (Figure 2-7). The range (max – min) varied between 5.2 cm and 8.3 cm with an average range of 6.9 cm. The inter-quartile range (upper – lower quartile) where 50% of the outcomes would occur ranged from 2 to 3.6 cm, with an average of 2.8 cm. Given the large natural variability of snow depth within a landscape type (see Figure 2-3 and Figure 2-4), these ranges are well within the expected error of measurement, implying that while landscape types do, generally, have statistically significantly different snow packs than each other, this difference is not important to the basin's average snow depth.

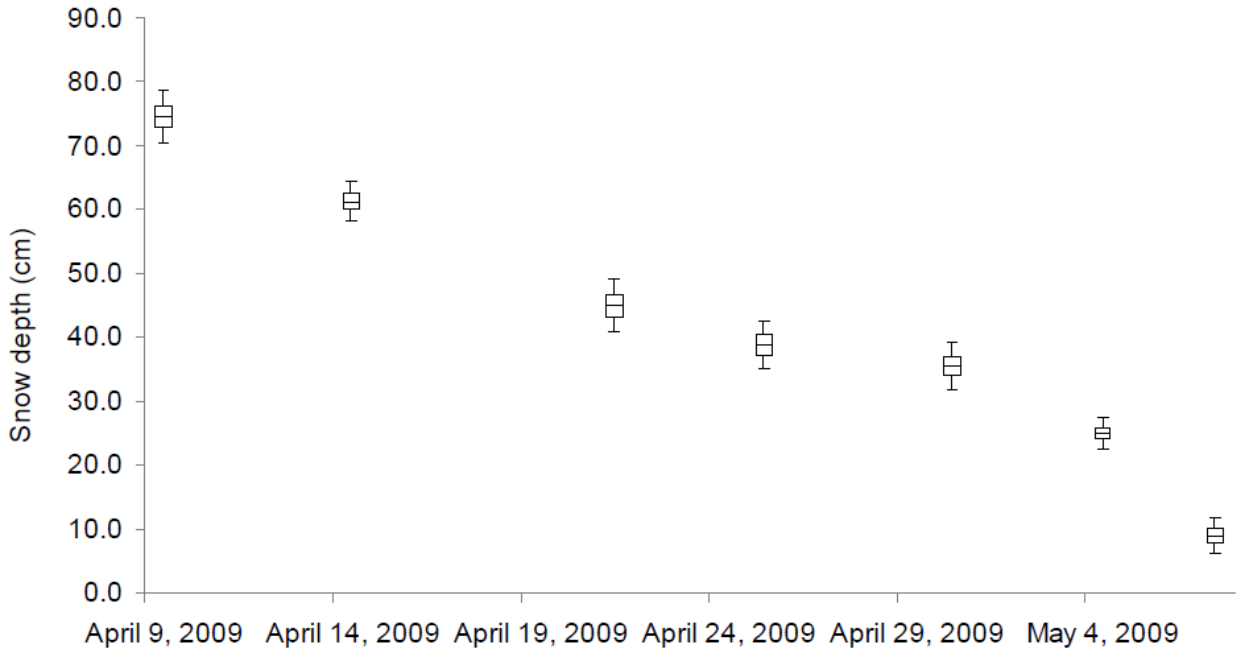

Figure 2-7 Randomized areally weighted average snow depths for the NGC basin. Whiskers in these box plots represent min and max.

Table 2-3 Percent area for each of the landscape units of the NGC basin and an example of the randomization for April 9, 2009. e.g., The high density fen occupied 8% of the area and contained 85.9 cm of snow based on the field survey and therefore contributes 0.08 * 85.9 cm = 6.9 cm of the 73.7 cm basin average for the "correct" areally weighed allocation column. This value is only 5 cm for the "Max" areally weighed allocation (0.08 * 62.8), when the snow depth for the open shrub fen (i.e., 62.8 cm) is applied to the area of the high density fen (0.08) (i.e., shallowest snow depth with smallest area). All values in cm.

		Snow depths April 9, 2009			
			Areally weighed		
Landscape Unit	Area	Survey	Correct	Max	Min
High Density Fen	8%	85.9	85.9	62.8	90.5
Open Bog	17%	65.4	65.4	65.4	85.9
Open Shrub Fen	19%	62.8	62.8	67.7	67.7
Medium Bog	26%	90.5	90.5	85.9	65.4
Low Density Fen	30%	67.7	67.7	90.5	62.8
	Average	74.5	73.7	78.6	70.4

2.7 Conclusion

In this area of the JBL, snow depth is controlled mostly by land cover type and its associated vegetation characteristics, as opposed to other landscapes where topography, aspect and slope have a much stronger

influence on snow depth. Despite differences in snow depth, melt rates were similar across all landscape types, in part due to the relatively open canopy cover throughout this sparsely vegetated landscape. Due to the similar proportions of open bog/fen and low/medium fen and bog, and small area of high density fen, changing the distribution of snowfall by re-allocating it did not significantly affect the average basin snow depth. Our findings contrast those of many other studies that have shown that topography and vegetation strongly influence the spatial pattern of snow accumulation and melt and must be specifically addressed as part of any snow sampling strategy designed to estimate basin wide snow depth. Here we found that a simple snow survey that transects some open and treed areas is sufficient to estimate basin wide snow depth.

2.8 Acknowledgments

The authors wish to thank Dave Fox, Chris Cook, Tom Ulanowski, Melissa Leclair and Emily Perras for assistance in the field. Special thanks must be given to the Environment Lab at the De Beers Victor mine for everything they have done for us. Thanks also to the keen eye of one of the reviewers of this paper. Funding was provided in part by De Beers Canada and an NSERC CRD grant to J. Price.

3 Impact of mine dewatering on peatlands of the James Bay Lowland: The role of bioherms

This chapter is published as:

Whittington, P., and Price, J.S. 2012. Effect of mine dewatering on peatlands of the James Bay Lowland: the role of bioherms. Hydrological Processes 26(12): 1818-1826.

3.1 Overview

The James Bay Lowland host one of the largest wetland complexes in the world in part due to the low permeability of marine sediments that suppress groundwater seepage losses. Dewatering of an open-pit diamond mine in the area has depressurized the regional bedrock aquifer. Bioherms, fractured limestone outcroppings formed from ancient coral reefs that protrude to the peatland surface lack this mantle of low permeability sediments, and provide a direct connection between the peatland (surficial) and regional (bedrock) aquifers. Well transects and piezometer nests were installed around 7 bioherms in the depressurized zone and one in an non-impacted zone (control) to monitor the water table drawdown and change in hydraulic gradients around the bioherms. Water tables in the impacted bioherms decreased between 2 and 4 m in the first four years of dewatering. The drawdown in the bioherms caused a localized water table drawdown in the peat surrounding the bioherms that extended to ~30 m from the edge of the bioherm during a dry period. Under wet conditions drawdown was similar to that at the control site. Hydraulic gradients in the peat (which typically are very small) increased over the field seasons and in a few locations exceeded 1. These gradients represented significant losses to the local, near bioherm, system as at many of the locations surrounding the bioherms vertical seepage losses ranged between 1 and 4 mm/day, which are similar to the seasonal average evaporative water loss of ~3 mm/day. The bioherms are acting as efficient drainage nodes; however, their influence is localized to the peat immediately (< ~30 m) surrounding them.

3.2 Introduction

Peatlands (mostly bogs and fens) cover nearly 90% of the Hudson Bay Lowland (Tarnocai, 1998) and are formed by the high water tables that are a consequence of the extremely low relief and thick low permeability marine sediment deposits that suppress runoff and groundwater seepage loss, and the cool subarctic climate which limits evapotranspiration. In addition, isostatic rebound (greater near the coast) continually lowers the regional gradient away from the coast which Glaser *et al*. (2004b) determined to be

a key factor in the development of the landscape. The Hudson Bay Lowland represent one of the largest wetland complexes in the world (Riley, 2011) and understanding their hydrological response to environmental stressors is important since they affect freshwater discharge to major river systems and Hudson Bay itself, and thus the transport of nutrients and contaminants (Kirk and St. Louis, 2009), regional climate (Rouse et al., 1992) and the global carbon cycle (Gorham, 1991; Roulet, 2000).

Discovery of kimberlite (diamondiferous) pipes in an area of the James Bay Lowland (which is part of the Hudson Bay Lowland) has led to open-pit diamond mining, which requires substantial groundwater pumping to dewater the mine thus causing depressurization of the regional bedrock aquifer. This depressurization has the potential to significantly affect the peatlands, depending on the nature and strength of the connection between them and the regional (bedrock) aquifer. Due to their hydrogeomorphic setting peatlands can be isolated from a more permeable bedrock substrate (Price and Woo, 1988a) and because vertical hydraulic gradients in peatlands are typically very small (see Fraser et al., 2001; Price and Maloney, 1994), in the order of 0.01 – 0.0001 are not uncommon, any connection would not result in a significant loss of water from the system (direction dependant, of course). However, this is not to say that there is no connection with the fine-grained marine sediments that typically underlie peatlands. Fen peatlands often have a groundwater input component bringing with it nutrient rich geogenous water (Glaser et al., 2004c). Reeve et al. (2001) determined that mechanical dispersive mixing with shallow mineral soils as a result of lateral groundwater flow (in part from the raised water table of bogs supplying water to the bordering fens) can be the dominant mass transport mechanism in large peatlands. They concluded that these flows can be a determinant for the formation of bogs: where these fluxes are significant, bogs will not form (Reeve et al., 2001).

However, the presence of bioherms, fractured limestone formed from ancient coral reefs, that protrude from the surface as partially vegetated mounds of exposed bedrock (Cowell, 1983), could provide a direct and efficient connection between the aquifers, bypassing the marine sediments. The presence of peatlands that surround the bioherms indicates that, currently, vertical recharge near the bioherms is sufficiently small for saturated conditions to be sustained to a degree favourable to peatland development. The fact that many of the peatlands are bogs (ombrogenous) implies groundwater discharge (i.e. upward flow from the aquifer) is either minimal or at least localized.

Horizontal groundwater flow in peatlands can efficiently shed water through the relatively undecomposed, high permeability upper layer of the peat deposit (acrotelm) in times of high water tables; mainly spring melt. At other times, flow is directed mostly through the relatively well-decomposed low

permeability deeper peat (catotelm). The low permeability catotelm inhibits drainage of peat beyond 30 m from a drainage ditch (Boelter, 1972; Silins and Rothwell, 1998). Consequently, lateral flows toward drain nodes (e.g. bioherms) through peat may be low.

The area that bioherms affect may be double the total surface area that the exposed portion of the bioherms occupy; about 21% of the area (North Granny Creek Zone, see below) pertinent to this paper (or ~0.5% of the total model domain area) (HCI, 2004a). This paper will examine how complexities in the geological structure (notably bioherms) influence the potential impacts of mining development.

Therefore, the specific objectives of this paper are to 1) determine if bioherms promote drainage of the peatlands in response to aquifer depressurization, and if so, 2) quantify the lateral extent of this effect and 3) determine the recharge rates through the peat towards the bioherms both horizontally and vertically.

3.3 Study Site

The study site is ~500 km north of Timmins, Ontario, at the De Beers Canada Victor Diamond mine (N 52° 49' 15", W 83° 53' 00") (Figure 3-1). There are a complex arrangement of bogs and fens with peat up to 4 m thick (Sjörs, 1963) overlying fine-grained clay-sized marine sediments, which can be up to several hundreds of metres thick, mantling Silurian bedrock of the Upper and Lower Attawapiskat formation (Martini, 1981; McDonald, 1989). Bioherms resting on the Upper Attawapiskat formation either protrude to the surface where exposed limestone is visible (cropping bioherms), or do not extend above the surface (subcropping bioherms) but may be visible due to vegetation community anomalies (e.g., tree density increases). The main study area is approximately 90 km from the James Bay coast (0 masl) and the surface of the peatland within the study area is generally located between 85-87 masl (higher on-top of bioherms). The headwaters of the Attawapiskat are ~600 km from the coast at an elevation of ~241 masl. Near the study site the Attawapiskat river has an elevation of ~65 masl. A regional flow map completed by HCI (2007) shows that over a distance of ~100 km (50 km radius from the mine) water levels, pre-mining, at the top of bedrock change from ~130 masl to 40 masl or a rate of about 0.9 m/km.

Data on the regional extent of bioherms are scarce. However, using a DEM created from LiDAR data which covers ~500 km^2 in a ~12 km radius around the mine, a topographic derivative was computed showing local patterns of relief within a 150m x 150m moving window (30 pixel x 30 pixel at 5m resolution). The resulting map clearly emphasized local topographic highs. From this it was possible to identify more than 100 "topographic highs" in three distinct bands (about 2 km wide) running north-west to south-east, approximately 10 km apart. We believe the majority of these to be bioherms based on

personal observations during helicopter flights. Unfortunately, palsas would also show up as “topographic highs” causing an over-estimate of the number of bioherms; conversely, subcropping bioherms would not show up. In the study area immediately surrounding the mine the number of palsas is roughly the same as the number of sub-cropping bioherms and the ratio of bioherms:palsas/sub-cropping is about 7:1, meaning that it is probably reasonable to assume that the majority of the “topographic highs” are bioherms.

Within the area the mine is predicted to impact HCI (2004a) identified 6 enhanced recharge zones, typified by a local abundance of bioherms (i.e., located in one of the bands noted earlier). This paper focuses mostly on one of these zones (North Granny Creek Zone, see the heavily pooled area in the top half of Figure 3-1) that is located ~2.5 km north west of the open pit mine. Within this area there are at least 4 cropping and 2 subcropping bioherms. This paper will focus on data from 5 cropping bioherms: North Bioherm (NB), South Bioherm (SB), North Road Bioherm (NRB), South Road Bioherm (SRB), and North North Bioherm (NNB); 2 subcropping bioherms: North Middle Bioherm (NMB) and South Middle Bioherm (SMB). A sixth cropping bioherm, Control Bioherm (CB), is located ~25 km south west of mine (about 100 masl), outside the zone of influence. (Note: SB is outside of the North Granny Creek Zone mentioned earlier.) The height and lateral extent of each of these bioherms is shown in Table 3-1. A non-bioherm site is located in a fen water track (FWT) also shown in Figure 3-1.

Long-term meteorological records are available from Lansdowne House (inland 300 km west-south-west) and Moosonee (near the coast, 250 km south-east). The average annual January and July temperatures for Lansdowne House are -22.3 and 17.2 °C, respectively, and for Moosonee are -20.7 and 15.4 °C, respectively (Environment Canada, 2008). Annual precipitation for Lansdowne House is 700 mm with ~35% falling as snow; and for Moosonee is 681 mm with ~31% falling as snow.

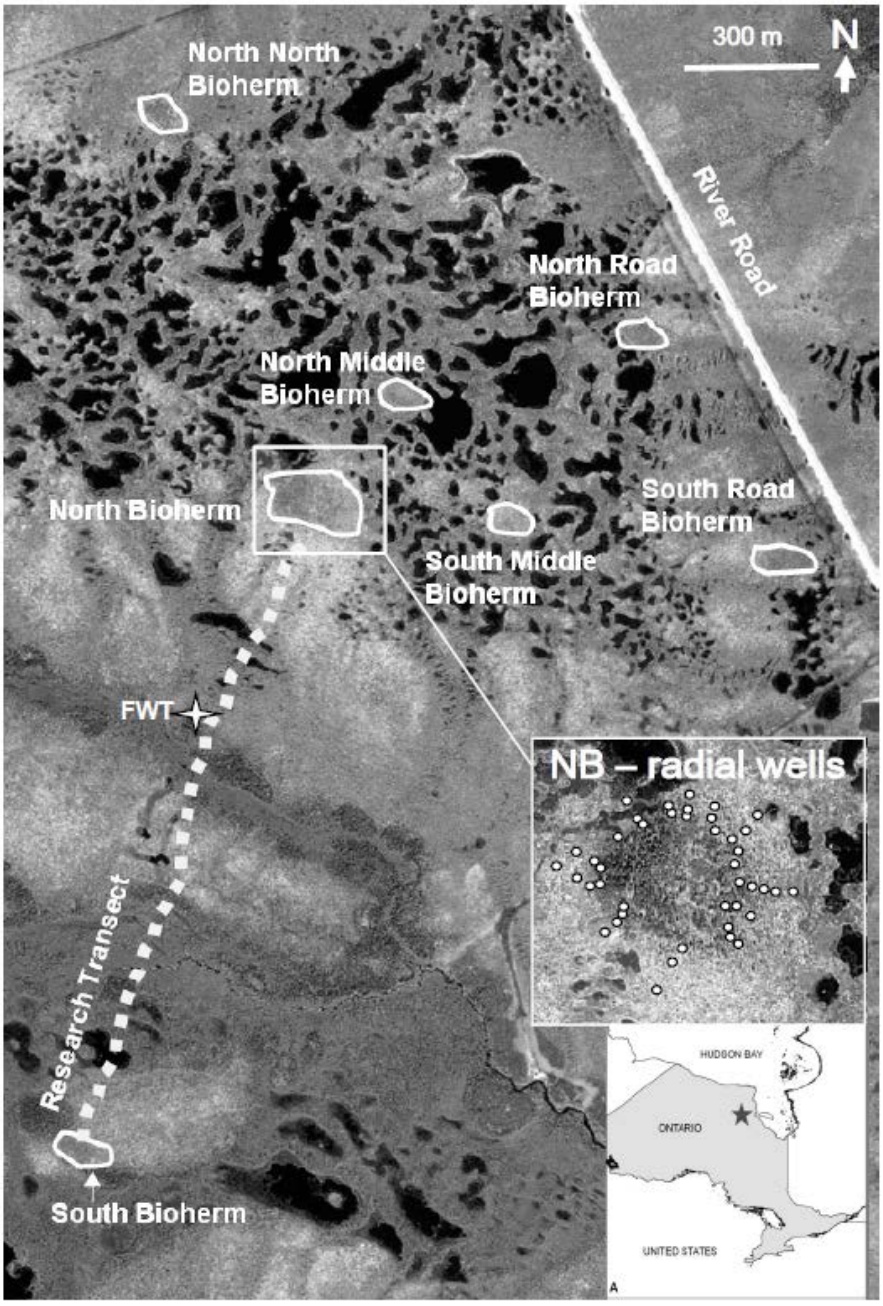

Figure 3-1 Bioherms located in the study area. Note: the dashed line (research transect) between SB and NB is approximately 1500 m long. FWT is the fen water track location. The open pit is located ~2km from the lower right hand corner of the image. The Control Bioherm is located ~25 km south west.

Table 3-1 Bioherm instrumentation table. The numbers in the Peat piezometer column indicate the distance, in meters, from the edge of the bioherm each nest is located, and on which side. e.g., the NRB has 6 nests; 4 on the east side and 2 on the south side, with the south side nests being 10 and 20 m from the edge (a value of 0 indicates the only nest is located in the middle of a subcropping bioherm). Nests with distances in bold font also include a drive point piezometer. Dimensions are maximum bioherm height above surrounding peatland (0 indicates subcropping); length and width dimension

Name		Dimensions (m)	Peat piezometers
South bioherm	SB	3.5; 43 × 80	N + 5, **15**, **35**, **70**
North bioherm	NB	4; 100 × 115	S + 2, **10**, **30**, **50**
South road bioherm	SRB	1.5; 30 × 30	S + 10; N + 5, 10, 15
North road bioherm	NRB	1.5; 60 × 77	E + 5, 10, **20**, 50; S + 10, **20**
North north bioherm	NNB	1; 100 × 60	E + 20
Control bioherm	CB	3; 100 × 130	S + **5**, **20**
North middle bioherm	NMB	0; 77 × 80	0
South middle bioherm	SMB	0; 80 × 53	0

3.4 Methods

To determine the near surface stratigraphy surrounding the NB three transects were selected that extended outwards from the edge of NB to ~25, ~35 and ~40 m respectively. These transects were located on the north-west, south-west and east sides of NB close to a nearby well transect (see below). Along each transect a hand auger was used to determine the thickness of the peat and marine sediments as well as the depth to bedrock. NB was selected as it is the most heavily instrumented of all the bioherms (see below).

Bedrock monitoring wells were installed using a drill rig that created a 15 cm diameter hole. PVC (2.5 cm diameter) standpipes were installed with 3 m screens open at specified depths, sand packed, and sealed with bentonite. At the NB the screened openings were centred at 25.5, 58.5 and 64.5 meters below ground surface (mbgs) in the upper Attawapiskat limestone formation. At the SB the screened openings (3 m) were also located in the upper Attawapiskat limestone formation at 10 and 30 mbgs. At the CB they were at 1.3 and 10.85 mbgs, respectively in the lower Attawapiskat limestone. These wells were equipped with a pressure transducer set to record every 12 hours.

Peat piezometers and wells were constructed from 2.5 cm diameter PVC pipes and were installed in the peat by pre-auguring a hole using a hand auger slightly smaller than the diameter of the well. Each nest typically had three piezometers (with 30 cm slotted intakes) usually centered at 0.9 m, 1.5 m and 2+ m (with the deepest near the peat/marine sediment interface; which ranged in depth from 1.9 m to 3.0 m, with the majority in the 2.1 – 2.7 m range). Piezometers were located within ~50 cm laterally of each other. In fine-grained mineral sediments 20 cm diameter stainless steel drive point piezometers (Solinst

Model 615) were installed using a compression rock hammer (Pionjaar 120). At select locations two drive points were installed, one just below the peat/mineral sediment interface and the other to refusal (typically between 4 and 8 m). Flexible plastic tubing connected to a nipple in the drive-point passed though sections of steel pipe to the surface. Hydraulic conductivity (*K*) was determined using bail tests (Hvorslev, 1951) by evacuating water with a Waterra foot valve and measuring the head recovery with a blow stick.

Pipe top elevations were surveyed using a dual frequency survey-grade GPS in real time kinematic survey mode (Topcon GMS-2). The base station was setup over a known benchmark near the mine and the rover was never further than about 4 km from the base. The acceptable precision for the DGPS was manually selected within the software and set at 0.003 m vertical and 0.005 m horizontal. The DGPS only records the point when these conditions are met. The 0.003 m software setting is misleading, as in practise, the relative accuracy of the DGPS was ~ 1 cm.

Well networks (see inset NB – radial wells in Figure 3-1 for an example of their arrangement) radiating out from the bioherms were installed using the same techniques and materials as the peat piezometers described above, however, the wells were slotted along their entire length and were ~1 m long. Wells were located in a radial pattern away from the bioherms at distances of i) 1-5 m from the bioherm; ii) ~5-10 m away from that; and iii) ~15-30 m from that. Each of the instrumented bioherms (NB, NRB, SRB) had ~9 of these mini-transects and labelled as Transect 1 – 9.

3.5 Results

The subsurface stratigraphy was similar in pattern but differed in depth and lateral extent around NB (Figure 3-2). At each location there was a zone (ranging from 5 to 22 m from the bioherm edge) where the peat mantled the bedrock directly. After this distance a layer of marine sediment started to emerge (ranging in thickness from 0.15 m to 1.8m) between the peat and the bedrock.

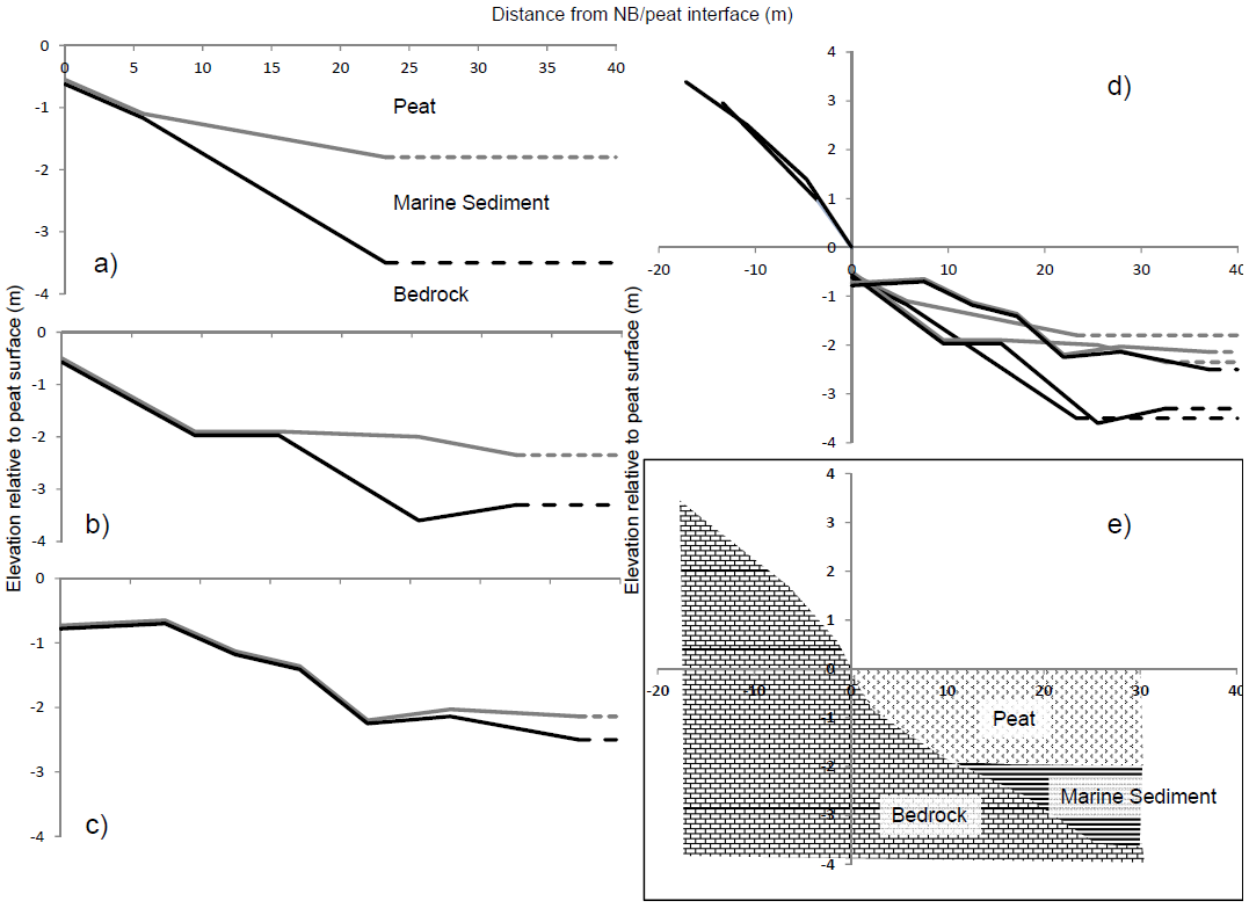

Figure 3-2 NB stratigraphy cross section on the a) east side, b) southwest side), c) northwest side. The surface is assumed to be flat and is represented by the x-axis. The area below the x-axis and above the grey line is peat, between the grey and black lines are marine sediments (ranging from sand to clay), and below the black line is bedrock. Dashed lines begin where auguring ended. d) Cross section with all three transects as well as the bioherm elevation profile. Note there are two lines for the bioherm elevation profile and are the north and south sides of NB. e) Idealized stratigraphy of bedrock (brick shade), peat (speckled) and marine sediments (horizontal shade).

Bedrock water levels at all sites show a seasonal pattern of snowmelt recharge followed by drawdown over the duration of the year. At NB and SB water levels have decreased between 2 and 4 m from April 2007 to January 2010 (Figure 3-3) but have not declined at CB.

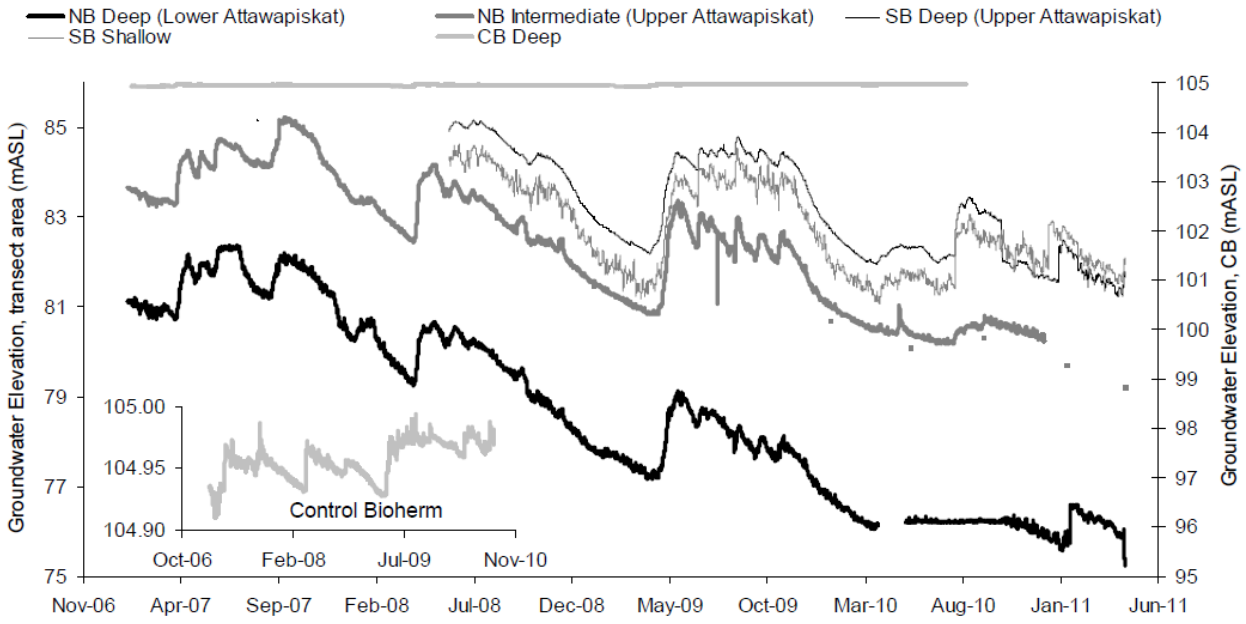

Figure 3-3 Bedrock water levels at NB and SB (primary Y-axis) and CB (secondary Y-axis). The inset graph is the CB on its own scale: note Y-axis scale difference between main (10 m) and inset (0.1 m) graph

The 2010 field season had an atypically shallow snow pack, which melted early and provided little groundwater recharge to the system. By the end of June the peatland and creek water levels were at the lowest of the 4 field seasons (2007-2010). However, after heavy rain (58 mm on July 28, 2010) and cooler temperatures, water levels rebounded to typical seasonal conditions. The lowest water tables in the radial wells surrounding the bioherms occurred at the end of June (Figure 3-4 a). During the dry period (e.g., June 29, 2010), water levels within the first 25-30 m around NB, NRB and SRB were lower than that at CB, but beyond this distance water table depths were similar and were generally within 30 cm of the surface. (*n.b.* Water table depths plotted at depths less than -100 cm represent the bottom of a dry well, actual water table is unknown.) During the wet period (e.g., July 30, 2011) some of the transects had water tables similar or higher than at CB and the majority of the transects had water tables within 30 cm of the surface within ~10 m (Figure 3-4 b). The SRB still experienced slightly more drawdown than NB and NRB. However, all transects had water tables near the surface within 30 m, and most by 20 m of the bioherm.

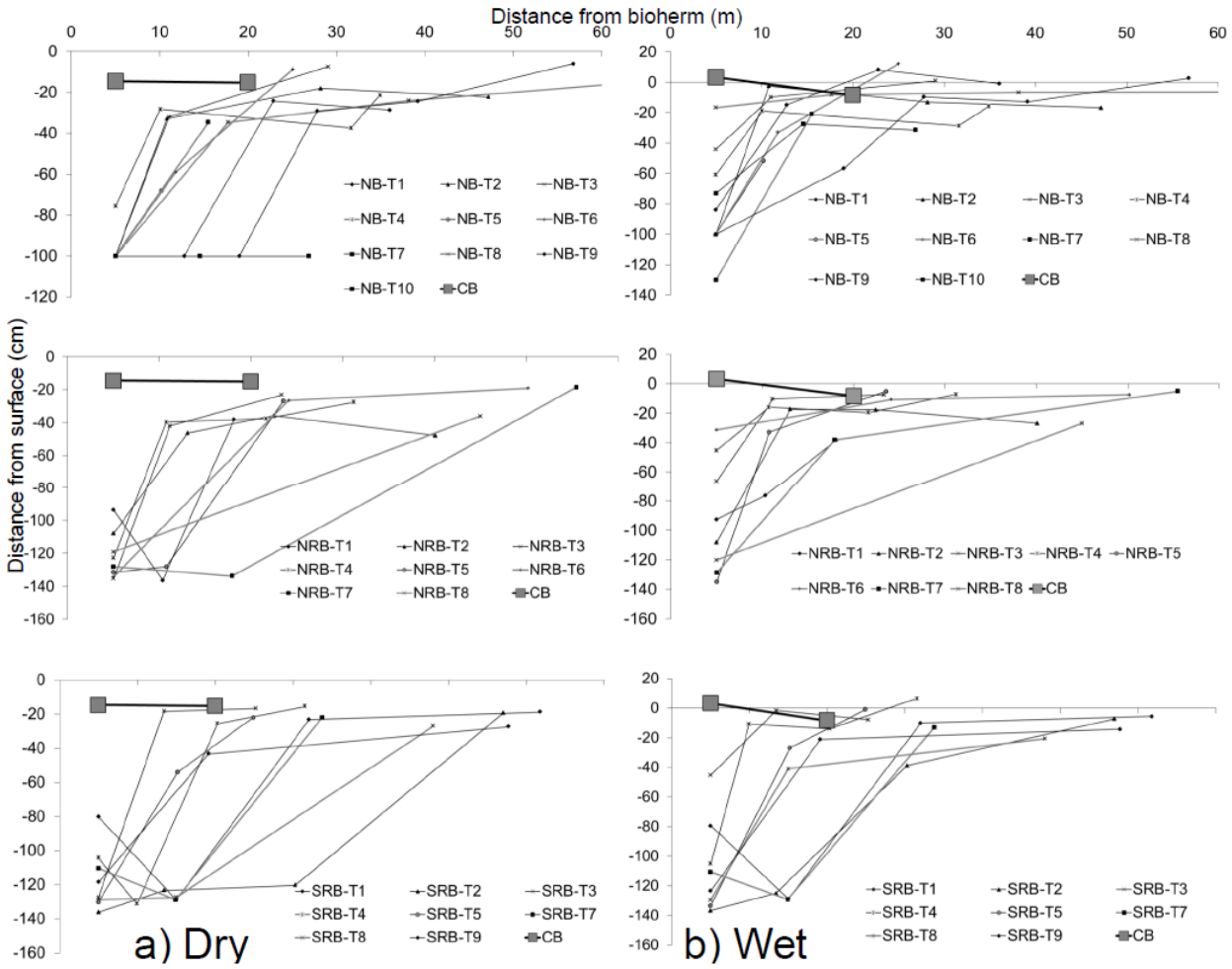

Figure 3-4 Water table drawdown in the radial wells around the NB, NRB, and SRB for a) dry (June 29, 2010) and b) wet (July 30, 2010) periods. CB dates were June 30, 2010 and August 14, 2010 for dry and wet, respectively. The later wet date at CB reflects the difficulty in accessing the remote site (via helicopter) and would likely be higher than shown. The T# is the transect number around the respective bioherm.

Gradients (calculated from the deepest to the shallowest piezometers) were downward (negative) at every bioherm nest in the impacted area for the entire study period (Figure 3-5). At the impacted bioherms (Figure 3-5 b - f) the hydraulic gradients generally decreased over the season but became stronger (more negative) from year to year. Gradients at 6 locations exceeded 1.0 (Eaton, 2010; Hart et al., 2008) for some period of time, as head in the deep piezometers adjacent to the mineral sediment dropped markedly (not shown). At all sites these gradients are 1-3 orders of magnitude larger than at CB (Figure 3-5 a) where gradients were between -0.017 and -0.002. These trends were not universal throughout the impacted area; the Fen Water Track (FWT) is located within the impacted area, though ~500 m from the

closest bioherm. Gradients (not shown) at this site were positive (albeit small) for parts of each year, likely due its location along the edge of the domed bog.

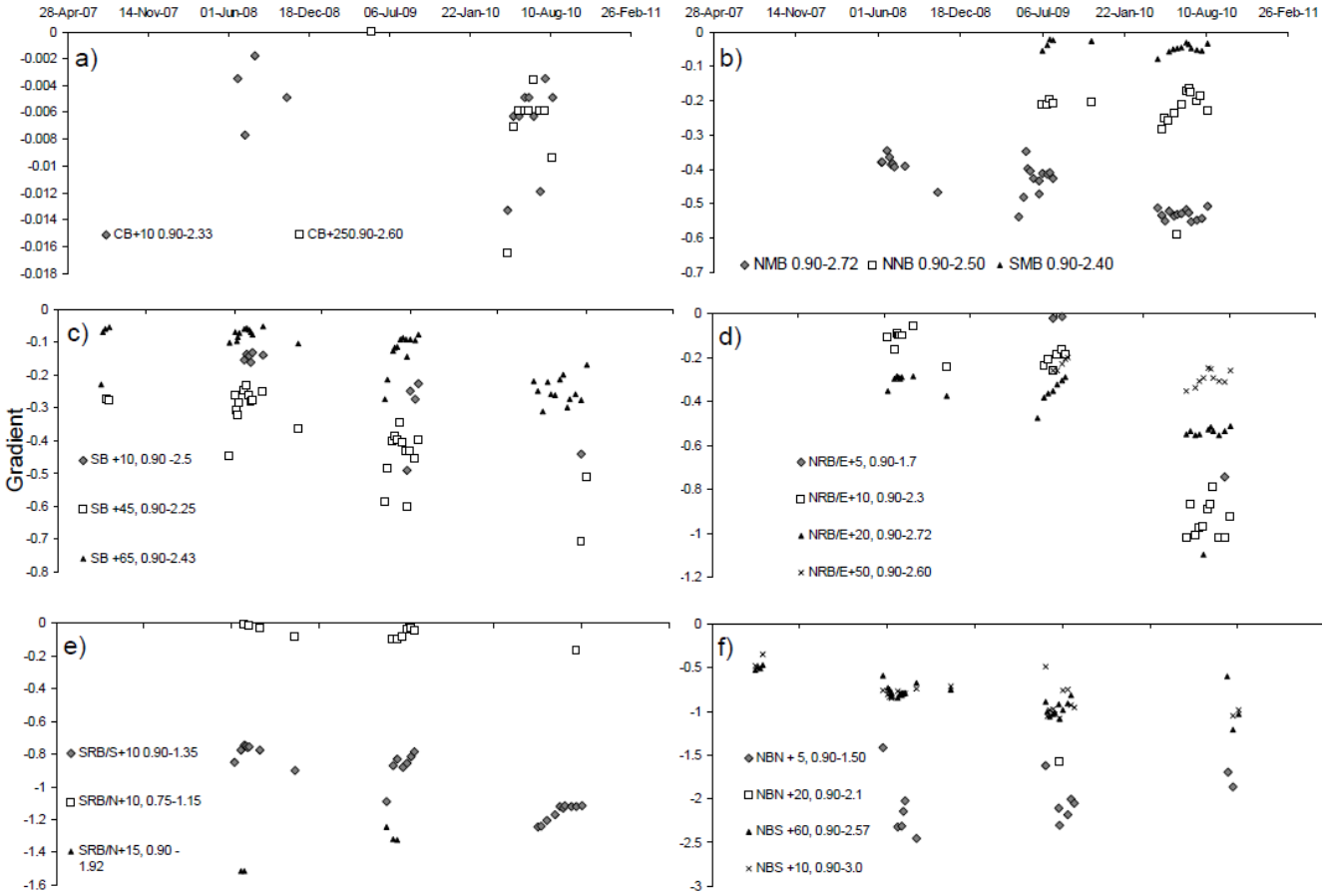

Figure 3-5 Head change from shallowest to deepest peat piezometer at the bioherm peat nests at all sites, through time. The distance from the edge of the bioherm is reported as the +X value followed by the depths of the piezometer midpoints used to calculate the gradient. Note the scale of the vertical axes are not the same between graphs, increasing from a) to f).

Hydraulic conductivity (horizontal unless noted otherwise) values in the peatland ranged 5 orders of magnitude and offered few trends (Figure 3-6a). Locally (with a nest), *K* did tend to decrease with depth. However this was not universal at all nests. A slight trend of decreasing *K* with increasing distance from a bioherm was observed within the first 20 m from a bioherm. After this distance, *K* appeared to increase with increasing distance. The marine sediments in the study area and in the CB area were similar with most *K* values around 0.1 cm/day. Bedrock *K* values were similar at all sites and ranged from ~300 to ~1000 cm/day (Figure 3-6 b).

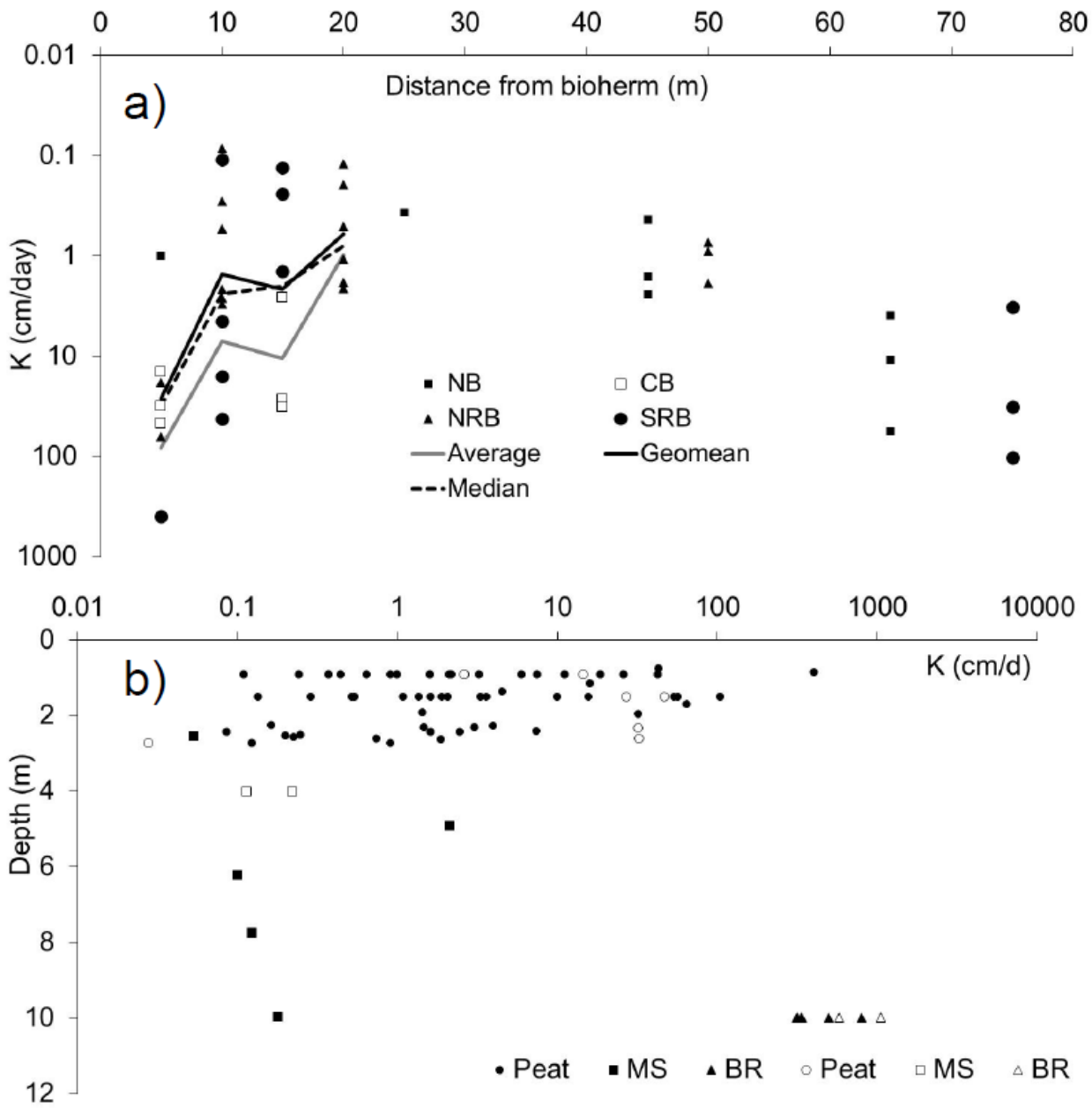

Figure 3-6 Hydraulic conductivity values for piezometers and wells installed near or in bioherms. Note the peat K values are the same between a) and b) but shown with different metadata. a) Peat K with distance from the respective bioherm. b) All peat K values from near the bioherms, as well as marine sediments (MS) (not necessarily near a bioherm) for the study area (dark) and near CB (white), as well as bioherm (BR, bedrock) K values from NB, SB and CB. Note that the bioherm values are artificially placed at 10 m depth for graphing purposes.

3.6 Discussion

During the study period the water table in the pit decreased to a depth of ~60 m below the local surface which is only a third of the projected final drawdown of >150 m. Recent modelling reports (Itasca Denver 2011) (*n.b.* HCI was renamed Itasca Denver Inc.) predict the depressurization of the bedrock in the North Granny Creek Zone will range from -10 to -30 m, meaning that the current drawdown (~ -2 to -4 m, Figure 3-3) experienced in the bioherms is between 10 to 40% of the projected final value. Regardless, it is clear from the results that aquifer dewatering is already impacting the peatlands surrounding the bioherms, though perhaps only fractionally compared to the eventual drying, since the water levels in the bedrock have not reached their final drawdown. What is unclear is whether is drawdown experienced in the surrounding peatlands is a result of horizontal drainage to the bioherm, vertical drainage as a result of a thinner or absent marine sediment layer (Figure 3-2), or both. First, however, it will be useful to determine the theoretical maximum lateral extent of drawdown with a relatively impermeable marine sediment layer.

In this hypothetical scenario a similarity exists between the drawdown experienced at a pumping well (see Theis, 1935) and the drawdown experienced around the bioherm where the bioherm behaves like a large diameter pumping well. There is a well-established logarithmic decrease in drawdown with distance from a pumping well given the transmissivity and storativity of the medium being dewatered (see Fetter, 1994; Freeze and Cherry, 1979). Some simple modelling (not shown) of the Theis (1935) equation suggests that even under extreme drawdown (much greater than the predicted impact from the mine) in the bioherm, the drawdown in the surrounding peat becomes asymptotic to a water level of ~-0.08 m at ~25 m from the edge (assuming the water table was initially at the surface). Thus for the following section we will limit our analyses to within 30 m surrounding NB on the date of the driest condition (June 29, 2010).

Using the information from the stratigraphic transects we can develop an idealized cross section and partition the horizontal and vertical fluxes within it (see Figure 3-2e). (The cross section is divided into three 10 m annular segments (0-10, 10-20, 20-30 m), the first (i.e., closest to the bioherm) with no marine sediments, the second with thin (1 m thick) marine sediments and the third with thick (2 m) marine sediments. Peat depths are 2 m throughout.) The specific discharge (q, L/T) version of Darcy's Law will be used to calculate the fluxes of water from the various compartments and distances using equation 3-1,

$$q = \frac{Q}{A} = K\frac{dh}{dl} \quad \text{[3-1]}$$

where Q is discharge (L^3/T), K is the hydraulic conductivity (L/T) and dh and dl (dimensionless) are the change in head and length between the measurement points, respectively.

Hydraulic conductivity in peat surrounding the bioherms is highly variable (Figure 3-6). For all calculations of horizontal flow the geomean and median K value for the appropriate distance from the bioherm will be used. The average was omitted as it is very susceptible to outliers. For vertical fluxes the lowest value in the profile will be used as that layer will ultimately control the vertical seepage losses.

Table 3-2 Horizontal and vertical specific discharge values for the three zones surrounding an idealized bioherm.

	K (cm/day)			*q* (mm/day)	
	Geomean	Median	*dh/dl*	Geomean	Median
Horizontal					
Average	1.5	2.4	0.07	1.1	1.7
Max	1.5	2.4	0.15	2.3	3.6
Min	1.5	2.4	0.05	0.8	1.3
Vertical					
No marine sediments					
Average	0.58	0.63	0.47	2.7	3.0
Max	0.58	0.63	1.13	6.6	7.1
Min	0.58	0.63	0.03	0.2	0.2
Thin marine sediments					
Average	0.19	0.12	2	3.8	2.5
Thick marine sediments					
Average	0.19	0.12	1.5	2.8	1.8

The average, minimum and maximum gradient (*dh/dl*) used for the horizontal flow were calculated from the 9 radial well transects surrounding NB (Table 3-2). Horizontal specific discharge ranged from 0.8 mm/day to 3.6 mm/day. The average, minimum and maximum vertical gradients as well as the geomean and median K for the no marine sediments zone were obtained from the relevant nests in Figure 3-5. Vertical loses through the peat (no marine sediment zone) ranged from 0.2 to 7.1 mm/day. The gradient in the thin marine sediment zone was calculated assuming the water table was near the surface in the peat with an elevation of 87 masl, which is 6 m higher than the NB intermediate water level (81 masl, Figure 3-3). It was assumed that the NB water level under the marine sediments would be the same as in the bioherm where it is measured, and over the scale of less than 30 m is a reasonable assumption. As the peat is 2 m thick and the marine sediments assumed to be 1 m thick, the *dl* is 3 m, which yielded a gradient of

2 and specific discharges of 2.5 and 3.8 mm/day (Table 3-2). Where the marine sediments were thicker (i.e., 2 m), the gradient decreased decreasing the specific discharge to 1.8 to 2.8 mm/day (Table 3-2).

The idealized bioherm specific discharge values (Table 3-2) are similar to those that were calculated using actual *in situ* gradients and *K* values for that particular nest (Table 3-3), rather than assumed or averaged (e.g., geomean or median) values for the idealized bioherm. These "real" values range from 0.41 mm/day to 4.8 mm/day and thus the idealized bioherm offers good agreement with field observations.

Table 3-3 Specific discharge and K values for piezometer nests near bioherms on June 30, 2010 (dry day). The distance from the edge of the bioherm is reported as the +XX value followed by the depths of the piezometer midpoints used to calculate the gradient.

Location	*dh/dl*	*K* (cm/day)	*q* (mm/day)
CB + 10, 0.90–2.33	*−0.006*	*14.5*	*0.91*
CB + 25, 0.90–2.60	*−0.004*	*2.6*	*0.09*
NMB, 0.90–2.72	−0.526	0.9	4.72
NNB, 0.90–2.50	−0.164	0.2	0.41
NRB E + 10, 0.90–2.3	−0.866	0.5	4.67
NRB E + 20, 0.90–2.72	−0.517	0.1	0.63
NRB E + 50, 0.90–2.60	−0.252	0.7	1.85
SB N + 10, 0.90–2.43	−0.299	1.6	4.80
SMB, 0.90–2.40	−0.035	7.4	2.61
SRB S + 10, 0.90–1.35	−1.131	0.1	1.24

Ultimately we are interested in the loss of water from the peatland system as it relates to the water balance; large losses that are unmatched with recharge will result in desiccation of the peat, and damage to its ecological and carbon storage function. Annual precipitation is estimated to be 690 mm/year (Environment Canada, 2008) and actual evapotranspiration 431 mm/year (Singer and Chen, 2002) (averages of Moosonee and Lansdowne House), which is about 3 mm/day during the growing season. AMEC (2004) estimated runoff in nearby basins to be 260 mm/year. These figures essentially balance (i.e., precipitation vs. evapotranspiration + runoff) and thus the groundwater recharge of 10 mm/year estimated by HCI (2004) is in order. Therefore, since the majority of the calculated specific discharges (i.e., groundwater recharge) are between 1 and 4 mm/*day* these represent a significant loss to the local, near bioherm, system (in the order of annual evapotranspiration).

It is also evident that the vertical losses are a larger and more important component of the water lost from the system. The horizontal losses are limited to the zone closest to the bioherm as beyond 10-15 m the

water table begins to flatten rapidly with increasing distance (flattened by 20 m), greatly reducing the gradient and thus horizontal flow. The North Granny Creek Zone was identified as an enhanced recharge zone because of the localized abundance of bioherms. This abundance is due the bedrock being closer to the surface (and thus the bioherms are able to protrude) with the corollary being a thinner marine sediment layer. Therefore, the distance to bioherm (horizontally) is likely not as important as distance to bedrock (vertically) for the impacted area as a whole. The horizontal distance of impacted peat to bedrock range between 0-30 m, however, vertically this distance is simply the depth of the marine sediments (~ 0-2 m in the bioherm zone), an order of magnitude smaller. The *K* of the marine sediments was similar to that of the deepest peat samples and thus does not provide the protection of a very low permeability aquitard (e.g., clay); instead, it is the thickness of the marine sediments that provides the protection. In the FWT location (Figure 3-1) gradients were positive for periods of the 2010 season, despite being within the impacted zone and only several hundred meters from NB. The marine sediment in this location, however, is estimated to be well over 100 m thick, providing the protection required to keep the peatland wet, minimizing vertical seepage losses.

3.7 Conclusion

The area studied was predicted to be an enhanced recharge zone because the bedrock is much closer to the surface, on average, than in other areas. The bioherms are draining the peatlands in the immediate area surrounding them and are acting as efficient drainage nodes and the lateral extent appears to be limited to ~30 m. However, the proximity to bedrock (non-bioherm or bioherm) is perhaps more important as vertical recharge rates in well-connected areas (i.e., thin marine sediments) are similar or larger than immediately adjacent to the bioherms. These losses represent a significant, and irreplaceable (until aquifer recovery following the end of mine dewatering), loss in the water balance both within a peatland form and within the peatland complex. The area that the bioherms occupy is very small (~0.5% of the impacted area), however, the area that the enhanced recharge zones occupy is much larger (~8%), further supporting that proximity to bedrock as the more important factor.

The geological and hydrological connection found in this study between the upper peatland aquifer and the groundwater bedrock aquifer provides background for future research, and provides valuable information for regulators and industry concerning how to manage proposed mining activity in the James Bay Lowland. It is particularly pertinent given the “Northern Ontario Ring of Fire” development occurring a few hundred kilometres west of our study site.

3.8 Acknowledgements

We would like to thank C. Cook, S. Ketcheson, M. Leclair, the “Fox”, PAM, and P. Jeffries for help with data collection. Thanks to Dr. Richardson for GIS related help. Thanks also to K. Tindale for stratigraphy coring. Special thanks to the Environment Crew (esp. B. Steinback and the Env. Monitors) at De Beers for all the help. Funding was provided from an NSERC CRD and De Beers Canada. Thanks also to the comments of two anonymous reviewers.

4 Effect of mine dewatering on the peatlands of the James Bay Lowland: the role of marine sediments on mitigating peatland drainage

This chapter is submitted as:

Whittington, P., and Price, J.S. submitted September 19, 2012. Effect of mine dewatering on the peatlands of the James Bay Lowland: the role of marine sediments on mitigating peatland drainage. Submitted to Hydrological Processes, HYP-12-0656.

4.1 Overview

The wetlands of the James Bay Lowland comprise one of largest wetland complexes in the world, in part due to the properties (thickness and hydraulic conductivity) of the marine sediment that underlay them. Dewatering of an open-pit diamond mine is depressurizing the surrounding Silurian bedrock below the marine sediments. Prior to mining it was assumed that these marine sediments would largely isolate the overlying peatlands from the depressurized regional bedrock aquifer. To assess this we instrumented a 1.5 km long transect of wells and piezometers located within the zone of the mine's influence that crossed a sequence of bogs, fens and bedrock outcrops (bioherms). Results were differentiated between those areas with no marine sediment (near bioherms) and those with marine sediment (non-bioherm) along the transect. Between 2007 and 2010 at near-bioherm and non-bioherm locations, average peat water tables declined 71 and 31 cm, and hydraulic head declined 66 and 32 cm, in bioherm and non-bioherm locations, respectively. Gradients varied from near zero (-0.001) at the start of dewatering to -0.03 (after 5 years) in non-bioherm areas and from -0.20 to -0.45 in near-bioherm areas. These corresponded to fluxes (groundwater recharge) of approximately -0.26 mm/day and -2.1 mm/day, in non- and near-bioherm areas, respectively. Specific discharge (recharge) determined using the known mine dewatering rate and drawdown cone hydraulic head values and surface areas corresponded well with measured recharge determined in the non-bioherm transect locations. A simple rearrangement of Darcy's Law used to calculate the specific discharge highlighted how the ratio of hydraulic conductivity to the thickness of the marine sediments can be used to assess vulnerable areas.

4.2 Introduction

The world's second largest wetland complex, the Hudson James Bay Lowland (HJBL), exists because high water tables are maintained by the extremely low relief which delays lateral runoff; the subarctic climate which limits evapotranspiration losses and provides adequate rain and snow melt; and the thick,

relatively impermeable (Price and Woo, 1988a), marine sediments that prevent vertical seepage losses. These marine sediments (MS) were deposited as the Laurentide Ice sheet melted about 8000 years ago, allowing the Tyrell Sea to flood the lowlands (Lee, 1960a). This resulted in a very large and flat basin underlain by a clayey silt (Dredge and Cowan, 1989; Glaser et al., 2004c) which is up to several hundreds of metres thick, mantling Silurian bedrock of the Upper and Lower Attawapiskat formation. Higher isostatic rebound at the coast continues to decrease the regional slope (Glaser et al., 2004b).

Until recently, little was known about the origin of the wetlands in the HJBL due to their remote and generally inaccessible setting. Sjörs (1963) offered one of the earliest assessments as to the origin of the wetlands, and Klinger and Short (1996) provided a more comprehensive assessment essentially confirming Sjörs' and both agree that large domed bogs are the terminal point of the successional pathway, which require an isolated or perched water table to maintain a high acidity which decreases fen species and favours bogs species. The perched (or domed) water table in bogs has been explained by two relatively contrasting models (Clymo, 1984; Ingram, 1982) and regardless of which model is used, both either imply (Clymo, 1984) or specify (Ingram (1982), i.e., the Dupuit-Forcheimer assumption) that vertical flow is negligible (Belyea and Baird, 2006) in the development of these bog systems, from which we can assume would require a relatively impermeable base layer, and/or no (large) vertical gradient.

Discovery of kimberlite (diamondiferous) deposits in an area of the James Bay Lowlands has led to open-pit diamond mining which requires substantial groundwater pumping to dewater the mine thus causing depressurization of the regional bedrock aquifer beneath the marine sediments. Whittington and Price (2012) found that this depressurization caused a localized water table drawdown in the peat around exposed or sub-cropping bedrock features (ancient coral reefs called bioherms (Cowell, 1983)) which was limited to ~30 m from the edge of the bioherms where there are little or no MS. In a 12 km radius around the mine approximately 100 bioherms can be found occurring in three distinct lateral bands (Whittington and Price, 2012), suggesting that their cumulative impact may be larger. Beyond this zone the presence of marine sediments was expected to play a role in protecting the peatland from excessive (vertical) recharge and desiccation (HCI, 2004a) but has yet to be properly assessed. Modelling simulations (supported with field data from both the Albany River Basin (HJBL) and Glacial Lake Agassiz (northern Minnesota), peatlands) by Reeve (2000) indicated that vertical flow was negligible in large peatland complexes when the hydraulic conductivity of the MS (i.e., the base) was low (10^{-7} m/s or 8.6 mm/day); when the MS had a higher hydraulic conductivity, vertical flow became more important. However, in all of these cases no

significant vertical hydraulic gradients were present because the horizontal gradient was assumed to be much greater than the vertical (Belyea and Baird, 2006).

In the feasibility study for the mine, HCI (2004a) used three field samples to determine the vertical hydraulic conductivity of the marine sediments and found the mean to be 0.025 mm/day, which is several orders of magnitude lower than that specified by Reeve (2000) as important to recharge, and on the high side of literature values for clay. Freeze and Cherry (1979) report "unweathered marine clay" to range between 0.086 to 0.000086 mm/day. The K of the marine sediment is only one aspect of its potential protective ability, the other being its thickness. In their model (HCI, 2004a) HCI varied both the thickness (from 0.5 m to 15 m) and the *K* (from 0.1 mm/day to 0.007 mm/day) and the corresponding rates of recharge from the peatlands ranged from 181 mm/year to 3 mm/year (or 70% and 1% of annual runoff). In addition, HCI (2004b) defined enhanced recharge zones that generally corresponded with the localized clusters of bioherms (in the bands noted earlier) and found that depending on the *K* of the limestone and MS, recharge in these zones could range from 21 to 148 mm/year.

With evidence that depressurization is occurring (Whittington and Price, 2012) the assumption of no vertical flow in these large peatland systems surrounding the mine is now invalid. Therefore, the impermeable nature, as well as the thickness of the MS will be assessed. The objective of this paper is to determine the impact of aquifer dewatering to peatlands surrounding the mine and to use this information to make inferences about the protective properties of the MS.

4.3 Study Site

The study site is located at the De Beers Canada Victor Diamond Mine, which is located ~90 km west of Attawapiskat and 500 km north of Timmins, Ontario, Canada. The James Bay Lowland is typified by a complex arrangement of bogs and fens, which comprise the majority of the landscape (60%) and when combined with open water and other wetland types, make up >90% of the landscape (Riley, 2011). Peat deposits range in thickness from 0 m where exposed bedrock is present (Cowell, 1983; Whittington and Price, 2012), to ~4 m (Glaser et al., 2004b; Sjörs, 1963).

A 1500 m long transect was instrumented with wells and piezometers between 2007 and 2010 (Figure 4-1, Table 4-1). The transect runs roughly south-north and is anchored at both ends by bioherms. The start of the transect is the South Bioherm (SB) and nests along the transect are named according to the distance

away from the SB, e.g., SB+1485 is a nest located 1485 m north from SB (note: as the transect is 1500 m long, SB+1485 is located very close to the North Bioherm). In 2009 five additional nests were installed north of the transect area in the North Granny Creek enhanced recharge zone (ERZ) (HCI, 2004b) called 8-1-D, Landbridge (LB), North Middle Bioherm (NMB), South Middle Bioherm (SMB), and North North Bioherm (NNB). In 2010 two nests were installed on the west side of the North and South Road Bioherms (NRB, SRB), approximately 75 m from the edge of the bioherm, outside of the zone of direct peat-bedrock influence (Whittington and Price, 2012), but within the ERZ.

The average annual January and July temperatures for Lansdowne House are -22.3 and 17.2 °C, respectively, and for Moosonee are -20.7 and 15.4 °C, respectively (Environment Canada, 2008). Lansdowne House (inland 300 km west-south-west) and Moosonee (250 km south-east near the coast) are the closest stations with long-term meteorological records available. Annual precipitation for Lansdowne House is 700 mm with ~35% falling as snow; and for Moosonee is 681 mm with ~31% falling as snow.

4.4 Methods

Local weather conditions have been measured at an on-site 10 m meteorological tower since March 2000 and include air temperature and relative humidity, rainfall, net radiation, photosynthetically active radiation, wind speed and direction.

Bedrock monitoring wells (PVC, 2.5 cm diameter) were installed with 3 m screens open at specified depths, sand packed, and sealed with bentonite. Screened openings were centred at 25.5, 58.5 and 64.5 meters below ground surface (mbgs) in the upper Attawapiskat limestone formation at the North Bioherm. At the SB they were also located in the upper Attawapiskat limestone formation at 10 and 30 mbgs (3 m screens). All bedrock wells had a pressure transducer set to record every 12 hours. Marine sediment wells (PVC, 2.5 cm diameter) were installed at various points along the transect in a similar fashion to the bedrock wells, however the slotted openings were only 0.3 m.

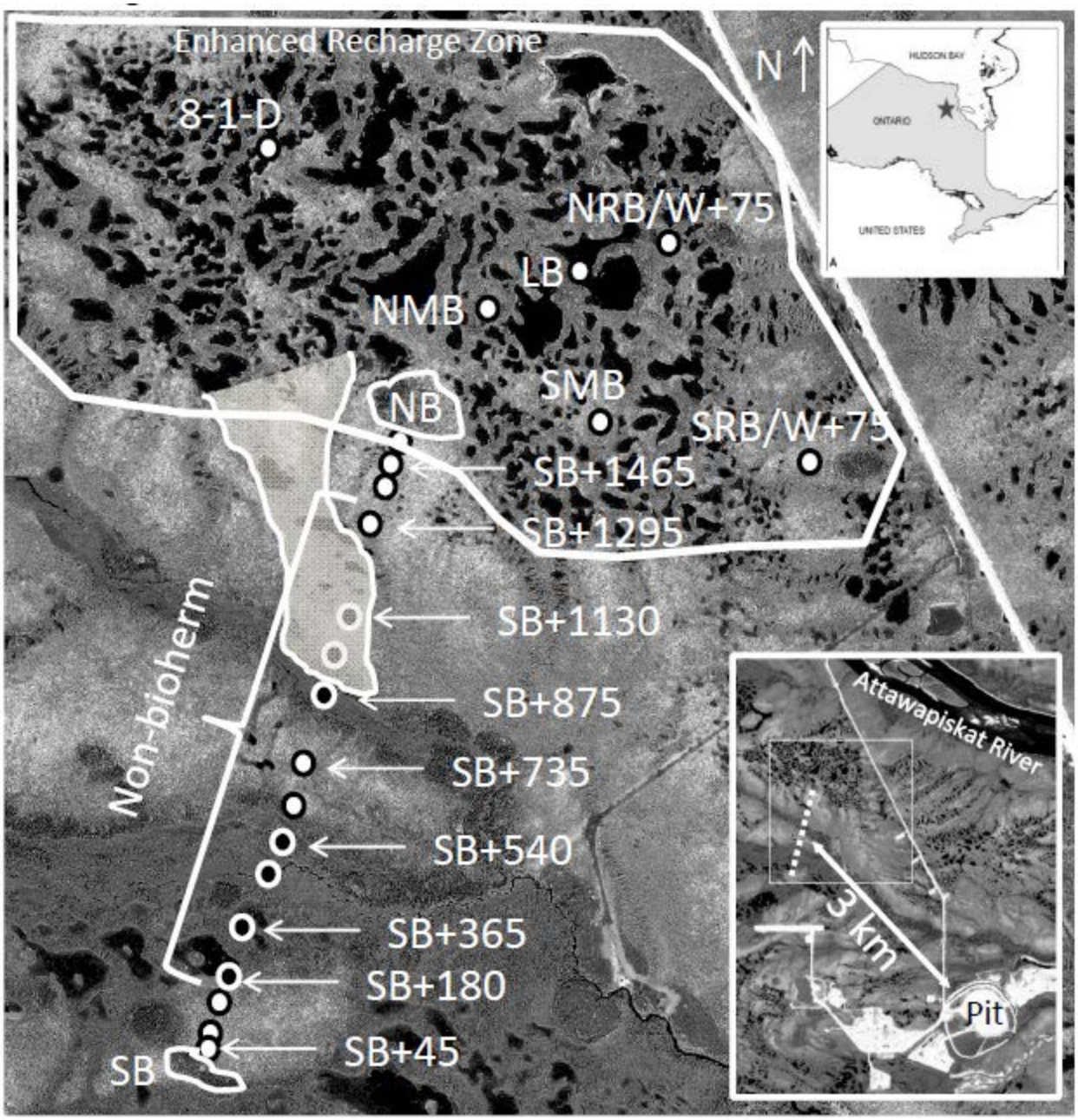

Figure 4-1 Location of selected nests along and north of the transect. White-centred circles are bog locations, black-centered circles are fen locations. The reader is directed to Table 4-1 for a complete list of the transect nest locations. Top inset: Site location within Ontario; bottom inset: location of the research area relative to the mine. The shaded section shows one of the fen water tracks coming off of the domed bog. North North Bioherm (NNB, not shown) is just out of the image above the word "Enhanced".

Table 4-1 Installation year, name (nest), peatland type, piezometer depths (meters below ground surface), elevation sensor rod (ESR) and whether the nest is in a Bioherm/Non-bioherm (BH/NBH) or enhanced recharge zone (ERZ) location. For the Nest column S = south, B = bioherm, N = north, M = middle, R = road, W = west, and LB = land bridge.

Year	Nest	Type	Piezometers (mbgs)	ESR	Location
2007	SB+45	Bog - domed	0.9, 1.5, 2.4	No	BH
2007	SB+65	Bog - domed	0.9, 1.5, 2.25	Yes	BH
2007	SB+100	Bog - domed	0.9, 1.5, 2.43	Yes	BH
2007	SB+180	Fen - floating mat	0.9, 1.5, 1.9	Yes	NBH
2007	SB+365	Fen - channel	0.9, 1.5, 1.7	Yes	NBH
2007	SB+430	Fen - channel	0.9, 1.5	Yes	NBH
2007	SB+540	Fen - channel	0.9, 1.5, 1.7	Yes	NBH
2007	SB+645	Bog - domed	0.9, 1.5	Yes	NBH
2009	SB+735	Bog - domed	0.9, 1.5, 1.9	No	NBH
2007	SB+875	Fen - channel	0.9, 1.4	Yes	NBH
2007	SB+1005	Fen - water track	0.9, 1.5, 1.8	Yes	NBH
2007	SB+1130	Fen - water track	0.9, 1.5, 2.4	Yes	NBH
2007	SB+1295	Bog - domed	0.9, 1.5, 2.38	Yes	NBH
2007	SB+1445	Bog - domed	0.9, 1.5, 2.57	Yes	BH
2007	SB+1485	Bog - domed	0.9, 1.5, 3	Yes	BH
2009	8-1-D	Bog - domed	0.9, 1.5, 2.3	No	ERZ
2009	LB	Bog - domed	0.9, 1.5, 2.5	No	ERZ
2009	NMB	Bog - domed	0.9, 1.5, 2.72	No	ERZ
2009	SMB	Bog - domed	0.9, 1.5, 2.4	No	ERZ
2009	NNB	Bog - domed	0.9, 1.5, 2.5	No	ERZ
2010	NRB/W+75	Bog - domed	0.9, 1.5	No	ERZ
2010	SRB/W+75	Bog - domed	0.9, 1.5, 1.95	No	ERZ

Peat piezometers and wells were constructed from 2.5 cm diameter PVC pipes and slotted at the bottom 30 cm (piezometers) or their entire length (wells). The peat wells and piezometers were installed by manually pre-auguring a hole using a hand auger slightly smaller than the diameter of the well. Each nest typically had three piezometers and a well with the shallowest piezometer installed to 0.9 m below ground surface. The next piezometer was installed to 1.5 m below ground surface (1.4m at one location) and the deepest peat piezometer (when possible) was installed below that. The depths of the third piezometer ranged as they were installed near the peat/marine sediment interface, which varied with location and ranged in depth from 1.7 m to 2.75 m, (see Table 4-1). Piezometers were located within ~1 m laterally of each other. Hydraulic conductivity (*K*) was determined using bail tests (Hvorslev, 1951) by evacuating water with a Waterra foot valve and measuring the head recovery with a blow stick. For measuring *K* in

the marine sediment piezometers a pressure transducer was used to record the water table rise of the period of recovery, which ranged from <1 to 2 days.

Pipe top elevations were surveyed using a Topcon GMS-2 dual frequency survey-grade GPS in real time kinematic survey mode with the base station setup near the mine over a known benchmark; the rover was never further than about 4 km from the base. The acceptable precision for the DGPS was manually selected within the software and set at 0.003 m vertical and 0.005 m horizontal. The DGPS only records the point when these conditions are met. The 0.003 m software setting is misleading, as in practise, the accuracy of the DGPS was ~ 1 cm, although with better than 1 cm precision (e.g., pipes in a nest relative to one another).

Laboratory assessment of *K* anisotropy in peat was made from samples collected from three locations along the transect including two bog (SB+65, SB+1485) and one fen water-track (SB+1005). A Wardenaar™ corer was used to collect relatively uncompressed 0.8 m x 0.13 m x 0.1 m cores that were placed into a rigid wooden box of the same dimensions, sealed with plastic wrap and transported back the laboratory. The cores were sectioned into roughly 0.1 m sections (attempting to keep any obvious horizontal layers intact) and then were encapsulated in wax (Hoag and Price, 1997). Hydraulic conductivity (*K*) in both the horizontal (K_h) and vertical (K_v) directions were determined by cutting an opening in the respective ends of the waxed core and ponding water on the surface until a steady discharge (and constant head) from underneath was reached. Once this was achieved the core was resealed, rotated, and the process repeated for the other direction. Darcy's Law was used to determine *K*.

4.5 Results

Aquifer dewatering officially began in January 2007, however, following a 60-day pumping test in October and November 2006 the depressurization of the bedrock underlying the research transect on Nov 28, 2006 was predicted to result in an *interpreted* drawdown of ~5 m on Nov 28, 2006 in the area around the research transect (HCI, 2007). Since instrumentation for this study began July, 2007, water pressure in the deep aquifer (i.e. in bioherms) was potentially already impacted (see Whittington and Price, 2012) for which we have no data. When dewatering of the pit began, pumping rates were ~8 200-18 000 m^3/day and increased to ~85 000 m^3/day by February 2010 (Itasca Dever Inc, 2011) and averaged ~80 000 m^3/day for 2011 (ranging from ~3000 to 97 000 m^3/day). At the end of August 2011 (the end of these data presented in this paper) the pit was ~90 m deep (-10 masl) with a water table ~93 m deep (-13 masl) (Patrick Rummel, 2012, De Beers Canada hydrogeologist, personal communication). The final pit is expected to

be 220 m deep with a corresponding depth to water table, indicating that in 2011 the mine depth was less than halfway completed.

The average monthly temperature of the onsite weather station generally fell between that of Lansdowne House and Moosonee, suggesting an average of those two stations offer a good surrogate for the long-term (30-year climate normals) climate at the study site. During the 2008 and 2009 field season (May 1 to August 31) the average temperature was cooler than the long-term average, whereas 2007, 2010 and 2011 were close to the long-term average (Table 4-2). Most years were slightly drier than average (2008, 2010, 2011), with 2007 being much drier (220 mm rain) and 2009 being a lot wetter (380 mm rain) (Table 4-2). Of note is that 2010 had no real melt period due to a very shallow snow pack and early melt (February/March) that provided little recharge to the system in the spring.

Table 4-2 Meteorological variables from May 1 to August 31 for 2007 to 2011, respectively. LH and M are based on the 30 year (1971-2000) Canadian Climate Normals from Environment Canada for Lansdowne House (LH) and Moosonee (M), respectively (snow depth is the end of March).

	2007	2008	2009	2010	2011	LH	M
Average air temperature (°C)	13.0	11.9	10.4	13.0	12.5	13.4	12.0
Precipitation (mm)	220	298	380	276	284	333	294
*Snow (cm)	37	43.0	75	0.0	39	56	35
Snow date	April 9	April 5	April 9	-	April 12	March 31	

***Snow depths are from: 2007/ 2008 from unpublished field data; 2009/2011 from Whittington and Price (2012); 2010 no snow was present in April (and most of March).**

The hydrostatic pressure in bedrock wells from spring 2007 to spring 2011 declined between 4 and 5 m in NB and from summer 2008 to spring 2011 declined ~3.5 m in SB (see Figure 3 in Whittington and Price, 2012; Figure 3-3 this thesis). Along the transect (i.e., non-bedrock) peat water tables from 2008 to 2011 in bioherm and non-bioherm locations declined 0.71 and 0.31 m, respectively, and within bogs and fens declined 0.52 and 0.35 m, respectively (Figure 4-2). In the ERZ water levels declined 0.32 m from 2008 to 2011. Data shown for 2007 in Figure 4-2 are from August only (due to study site installation timing) and thus are not an average for the season, however, examination of some of the De Beers' regional compliance monitoring wells has shown the same trend, with 2007 being drier than 2008/2009 and thus despite the later sample time, is representative of the conditions for that field season. The similarity between the non-bioherm and fen sites, and the higher absolute water tables in bioherm and bog locations,

are because the bioherms are surrounded by bogs (in this study area) which are naturally raised above the surrounding landscape (Clymo, 1984; Ingram, 1982).

Figure 4-2 Water tables elevation through time for both bioherm/non-bioherm and bog/fen nests, and the ERZ. Points are shown offset in time (x-axis) for display purposes only. Data are the average of the field season measurements, generally from April/May to August (except 2007). Error bars are +/- 1 standard deviation.

Between 2007 and 2011 the average hydraulic head in each nest of peat piezometers declined between 0.12 and 1.0 m. In bogs and fens the decline was 0.54 and 0.33 m, respectively, and in bioherm and non-bioherm locations was 0.66 and 0.32 m, respectively. These changes were calculated as an average across the peat profile (i.e, of the 3 (or 2) piezometers) at each nest.

Hydraulic gradients in the peat profile (calculated from the water table to the mid-point of the deepest piezometer in the nest) declined along the transect (average of all nests), through time (Figure 4-3). The gradients in the bioherm nests were 4 to 9 times larger than in the non-bioherm nests. When the two nests in the FWT are removed (rationale given in discussion) hydraulic gradients are near zero (range -0.001 to -0.007) for 2007-2009, but increase an order of magnitude to -0.03 in 2010 and -0.01 2011. The ERZ maintained a relatively steady average gradient of 0.2 from 2009 to 2011, being less than the bioherm nests, but more than the transect area.

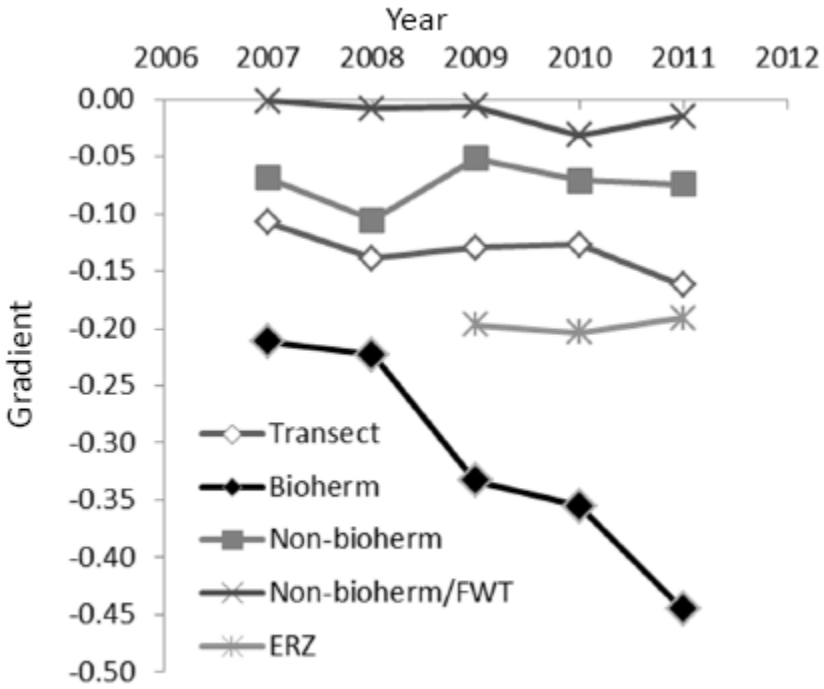

Figure 4-3 Average hydraulic gradient (from well to mid-point of deepest piezometer) from 2007 to 2011 along the transect, in bioherm nests, non-bioherm nests, and non-bioherm/non-fen water track (FWT) (see Figure 4-1) nests.

The marine sediments subsided at every point along the transect, ranging from 4 to 34 cm, with an average subsidence of ~12 cm along the transect since 2007 (Figure 4-4). The difference between bioherm and non-bioherm marine sediment subsidence, as well as between bog and fen marine sediment subsidence, were both < 1 cm. Peat subsidence averaged 6 cm along the transect (Figure 4-4). At bioherm and non-bioherm locations, peat subsidence was 7.3 and 5.5 cm, respectively, and between bog and fen locations peat subsidence was 6.9 and 5.3 cm, respectively.

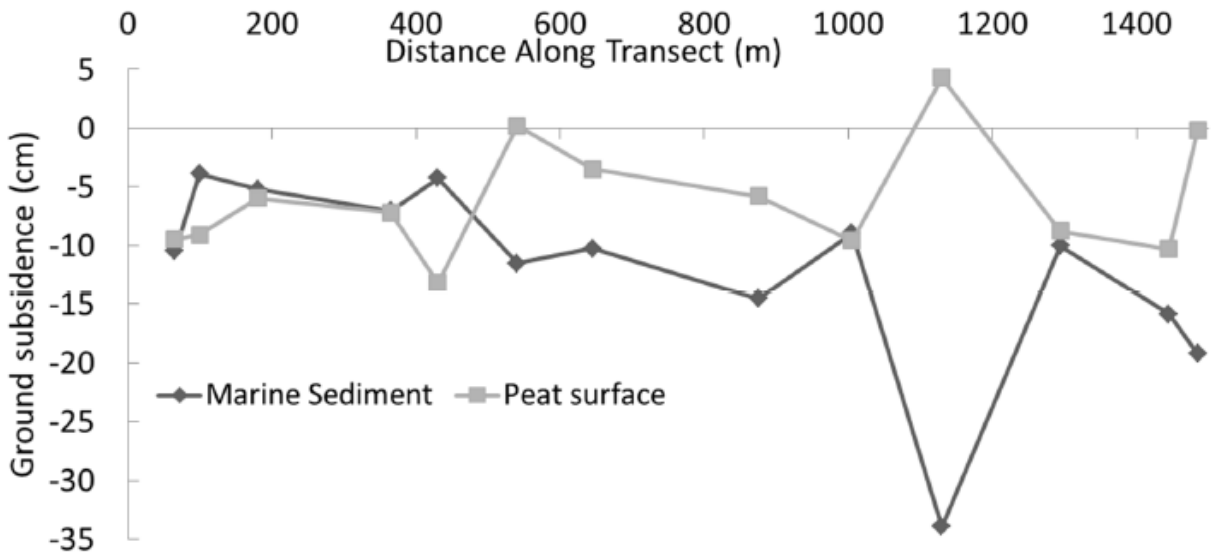

Figure 4-4 Marine sediment and peat elevation changes along the transect from 2007 to 2011.

Hydraulic conductivity in the peat varied 4 orders of magnitude between ~4 and 4000 mm/day with ~90% between 10 and 1600 mm/day and a transect average of 340 mm/day (Figure 4-5). *K* generally trended 0.90 m > 1.50 m > 2+ m (deepest piezometer) with average values for those depths of 698, 230 and 58 mm/day, respectively. *K* in the (elevated) bogs tended to be less than the *K* in (lower lying) fens; *K* in bogs averaged 85 mm/day whereas in fens it averaged 597 mm/day. Hydraulic conductivity in the marine sediments ranged 0.5 mm/day to ~30 mm/day, with an average of ~10 mm/day and median and geomean of ~5 mm/day.

Hydraulic conductivity (vertical and horizontal) of the upper 0.75 m of peat determined from the cores ranged between 20 and 10,000 mm/day with the majority (~80%) between 20 and 1100 mm/day, which makes the upper portion of the peat profile within a similar range to those depths determined with piezometers. In ~90% of the samples $K_h > K_v$ (n = 18), with a median anisotropy value (*log* K_h/K_v) of 0.23, or K_h being 1.8 x K_v.

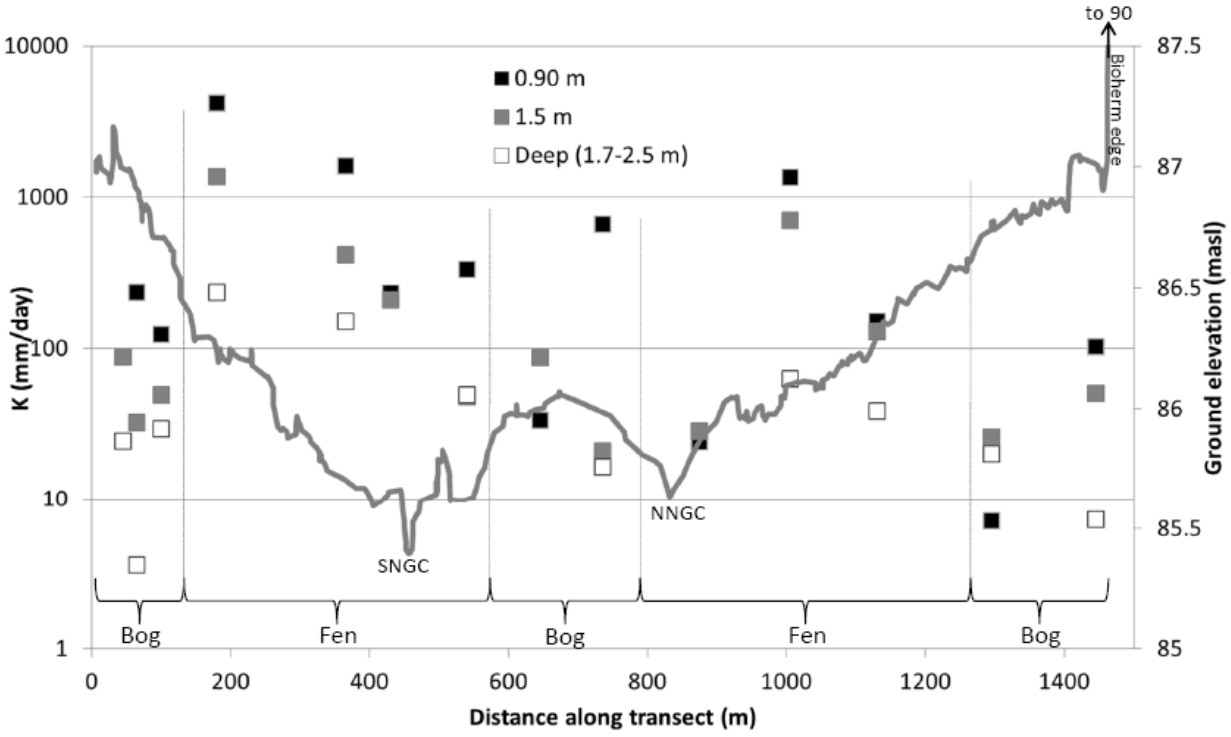

Figure 4-5 Average (2007-2011) hydraulic conductivity per piezometer (points) and ground elevation (2008) (grey line) along the transect. Ground elevation was determined using an 8-point-moving-average from a DGPS survey with points taken every 4-5 m; the NB is clearly seen at the far right of the figure and extends upwards to 90 masl over ~10 horizontal meters. The locations of bogs and fens are shown along the X-axis. SNGC and NNGC are the stream channels for South- and North-North Granny Creek.

4.6 Discussion

The study period presented here covered 5 years of dewatering, from shortly after dewatering began to slightly less than half of the anticipated drawdown. Over this time period annual weather conditions varied considerably and likely masked some of the effects that can be attributed solely to aquifer dewatering. The summer of 2007 was warm and dry (Table 4-2); however the effect of pumping was only seen in the near-bioherm nests (Figure 4-3). In summer 2008 it was cool and wet resulting in higher water tables than in 2007, but still relatively unaffected by the mine in non-bioherm areas (Figure 4-2). The summer of 2009 was cold, very wet and had a large early-season snowpack, which may have masked any dewatering in non-bioherm areas due to the 'surplus' of water, despite being the third summer of dewatering. As there was essentially no spring recharge in 2010 (no snow), large drops in water tables in 2010 were likely more a response to the minimal spring recharge event due to the absence of snow, than due to dewatering; the average temperature and slightly less precipitation maintained the initial conditions

of the season, but by this time 4 years of aquifer dewatering had also occurred and even the non-bioherm areas of the transect were beginning to be affected with lower water tables and larger gradients.

As noted previously in Figure 4-3 two of the fen water track (FWT) nests were removed from the non-bioherm classification as these two nests are impacted, albeit indirectly, by the bioherm. The ponds on the top of the domed bog (i.e., the ERZ, Figure 4-1) feed the fen water track which comes down off the bog to the stream channels, and as hydraulic gradients were higher in the bioherm and ERZ areas (the area supplying the FWTs), water in the fen water track was cut off, drying these nests despite these nests being 100s of m from a bioherm.

The larger scale surficial flow systems also help to explain the different responses seen between bogs and fens to dewatering. Both water tables and hydraulic heads (Figure 4-2, Figure 4-3) declined more in the bog locations than in the fen locations. This is due to the ombrogenous nature of bogs – they receive inputs through precipitation only. Fens, however, may receive inputs of water from numerous sources. In this study area, the majority of the Granny Creek watershed is non-impacted, meaning the headwaters for NNGC and SNGC (the streams that feed the majority of the fens in the study area) are supplying (lateral) water to the (vertically) impacted fens, helping mitigate the effects of dewatering. The ERZ, however, is dominated by bogs and therefore ombrogenous and not additionally protected by the lateral flows of water.

At a study site located ~150 km south of Victor in the HJBL, Reeve (1996) found the peat *K* to vary between 10^{-7} to 10^{-4} m/s (~9 to ~9000 mm/day), however, the majority of Reeve's *K* values were between ~10 and ~1000 mm/day, which is very similar to the ~10 to ~1600 mm/day range found in this study area. Similarly, Reeve et al. (2000) use a value of 10^{-7} m/s (~8.6 mm/day) for the marine sediment *K*, taken from Reeve (1996), which compares well with the values of ~5 to 10 mm/day found along the research transect. The *K* anisotropy value found in this paper (median was log(0.23)) is lower than the values reported by Beckwith et al. (2003), 0.55, and Schlotzhauer and Price (1999), 0.57, however, it is similar to those reported by Whittington et al. (2007), 0.35, as well as Chanson and Siegel (1986), 0.3.

As noted earlier, Reeve et al. (2000) found that no vertical flow (bog) occurred where there was a marine sediment *K* of ~9 mm/day or less, implying that this would be similar at our study site under natural conditions, as the range of *K* values are very similar. Whittington and Price (2012) found near-zero gradients at a control bioherm, confirming this finding. However, the aquifer dewatering is increasing the natural, near-zero, vertical gradients to ~-0.5 in bioherm areas, -0.2 in the ERZ, and ~-0.03 in non-

bioherm areas. Using these gradients and the *K* at each nest, it is possible to calculate the flux of water leaving the peat at each nest along the transect (Figure 4-6).

When considering the anisotropy-adjusted (0.23) hydraulic conductivity profile and gradients in the peat no significant trends in the vertical flux of water (Figure 4-6) along the transect or through time are observed. This is due, in part, to the large range in *K* values found along the transect. Even through the gradients are small in the fens areas (Figure 4-3), the *K* is high (Figure 4-5) resulting in a calculated flux of water similar to those at bioherm sites, where the gradients are large but the *K* is low. Fluxes are higher in the bioherm or bog areas and lower in the fen areas; in 2011 the non-bioherm/FWT nests averaged -0.26 mm/day and for the same year, the bioherm nests averaged -2.1 mm/day based on calculations made with peat *K*. The ERZ fluxes averaged -1.2 mm/day in 2011 (Figure 4-7).

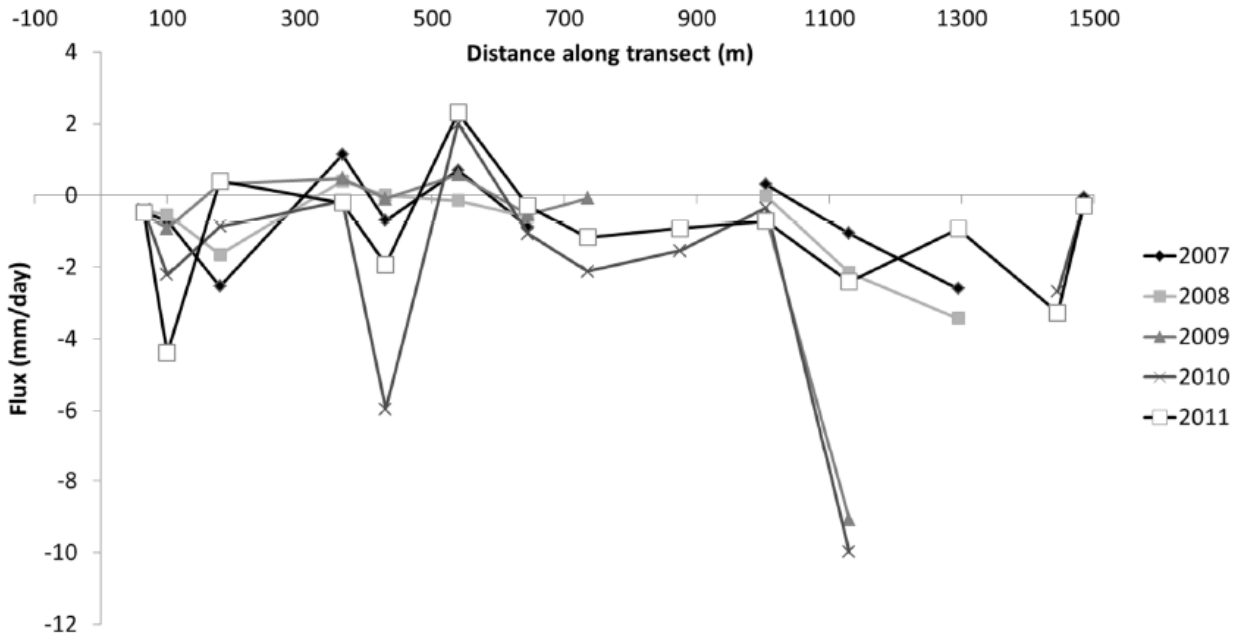

Figure 4-6 Fluxes of water through the peat, through time, along the transect.

It is clear that the impacts of dewatering are being seen along most of the transect and that the marine sediments are not isolating the peatlands from the aquifer below, but have been delaying or muting the impact as evidenced by relatively high recharge in the bioherm and ERZ areas (no or little MS) vs. relatively small impact in non-bioherm (MS) areas.

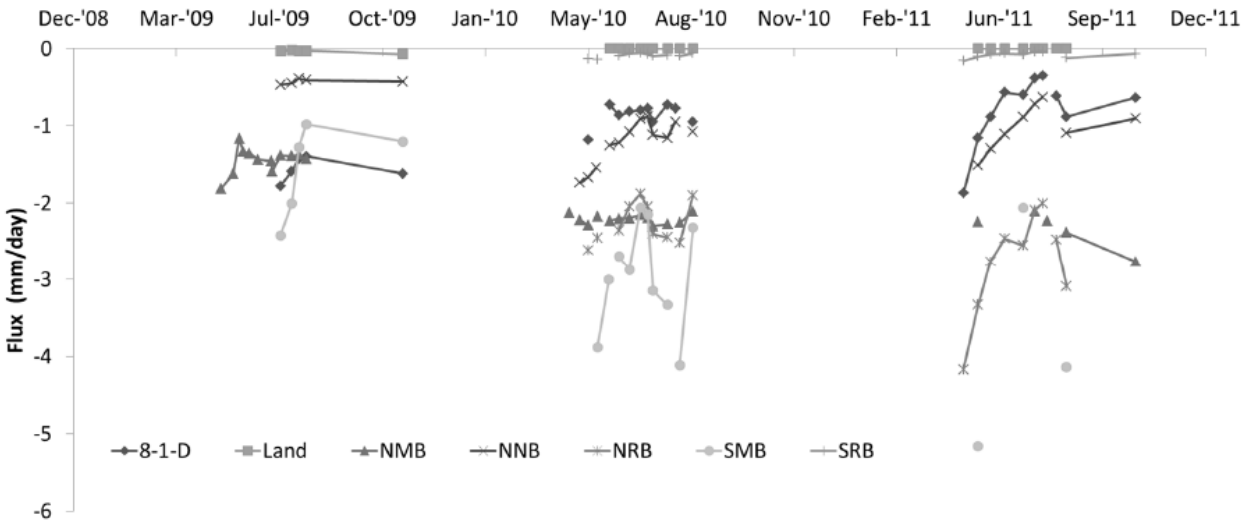

Figure 4-7 Fluxes of water through the peat in the ERZ from 2009 to 2011.

Using current (August 2011) drawdown data, Itasca (2011) created a drawdown cone map (not shown). The shape of the current drawdown cone, as defined by the depressurization in the Upper Attawapiskat Limestone (i.e., the layer directly below the marine sediment), is irregular, with the 2 m drawdown line extending out between 2 and 8 km from the mine. The area for each drawdown ring was found and from that the total area of drawdown was found to be ~65 km^2 (A_T). Knowing that the total dewatering rate averaged ~85,000 m^3/day in 2011 (Patrick Rummel, 2012, De Beers Canada hydrogeologist, personal communication) and that ~50% of that was attributable to "recharge from surface water" (Itasca Dever Inc, 2011), the total muskeg dewatering would be about 42,500 m^3/day (Q_T). (n.b. The pumping rate is a very reliable value as it can be directly measured at the pump house; unfortunately, it is unclear from the report (Itasca Dever Inc, 2011) how they arrived at the 50% figure and what assumptions were made, however, different predictions in numerous reports dating back to 2004 have all hovered around the 45,000 m^3/day for 2011.) Therefore, knowing the total dewatering amount and area, as well as the change in head (Δh) as defined by the Upper Attawapiskat Limestone it was possible to determine the specific discharge (q_i) for each "ring" of drawdown around the mine using a simple rearrangement of Darcy's Law,

$$\boldsymbol{Q_T = K A_T \frac{\Delta h}{\Delta l}} \qquad \textbf{[4-1]}$$

where K is the hydraulic conductivity and Δl is, effectively in this case, the thickness of the marine sediment. Isolating the ratio of K and Δl allows the calculation to be made without knowing (or assuming) a value of either and will be discussed more below. Rearranging [1] yields

$$\boldsymbol{Q_T = \frac{K}{\Delta l}\sum_{i=1}^{n} A_i \Delta h_i} \qquad \textbf{[4-2]}$$

where the total area has been re-defined as the sum of each ring and rearranging [2] by solving for the ratio of K and Δl gives

$$\boldsymbol{\frac{K}{\Delta l} = \frac{Q_T}{\sum_{i=1}^{n} A_i \Delta h_i}} \qquad \textbf{[4-3]}$$

The discharge at each individual ring, Q_i, follows from [4-2] and substituting [4-3]

$$\boldsymbol{Q_i = \frac{Q_T}{\sum_{i=1}^{n} A_i \Delta h_i} A_i \Delta h_i} \qquad \textbf{[4-4]}$$

And finally, dividing by the area of each specific ring gives

$$\boldsymbol{q_i = \frac{Q_i}{A_i}} \qquad \textbf{[4-5]}$$

The transect falls on roughly the 4 m drawdown line and from equation 5 yields a value of about -0.21 mm/day, which matches remarkably well with the non-bioherm/FWT 2011 average of -0.26 mm/day with peat K noted above. The bioherm and ERZ fluxes, however, were half to an order of magnitude higher, though represented much smaller total areas. It is worth noting specifically that the values used to generate Table 4-3 are independent of those measurements presented in Figure 4-6 and Figure 4-7. The only overlapping data would be those from the NB and SB bedrock water levels, which were used to determine the drawdown cone along the research transect; those values were not used in the calculation of the vertical fluxes along the transect.

The value of $K/\Delta l$ has dimensions of 1/[T], and in the case reported here has a value of 5.2×10^{-5}/day. As noted earlier, it is the combination of K and thickness of the marine sediments that would provide its protective properties, and thus determining a relationship linking the two variables could prove extremely useful in making inferences about marine sediments. Solving this equation (K of MS (mm/day) = 0.052 * marine sediment thickness (m) determined solely from the drawdown data) for the three important values of K discussed in the paper (see caption) and the corresponding MS thickness is shown in Figure 4-8.

Ratios plotting below the best fit line would indicate more protective properties than currently exist (i.e., a lower *K* for the same thickness), whereas above the regression line (black line) would indicate less protective properties (i.e., shallower thickness for the same *K*). For example, near the bioherms the MS are thinner (a few meters) and with a *K* of 5 mm/day would plot in the upper left hand corner of the graph, above the regression line. The curve becomes asymptotic to an infinitely thin and low *K* MS layer, at which point the flow would no longer be governed by Darcy's Law (Freeze and Cherry, 1979), and instead osmotic processes (Neuzil and Provost, 2009) as the "marine sediment" would essentially be an impermeable membrane.

Table 4-3 Specific discharge (q) within the 2011 drawdown cone. The bold row (h = 4) indicates the row that best matches the transect distance.

Drawdown (h)	Area (km^2)	q = mm/day
2	17.53	0.10
4	**20.15**	**0.21**
10	11.39	0.52
20	5.26	1.04
30	3.51	1.56
40	2.63	2.08
50	1.75	2.60
60	0.88	3.12
70	0.88	3.64
80	0.88	4.16
	64.8	

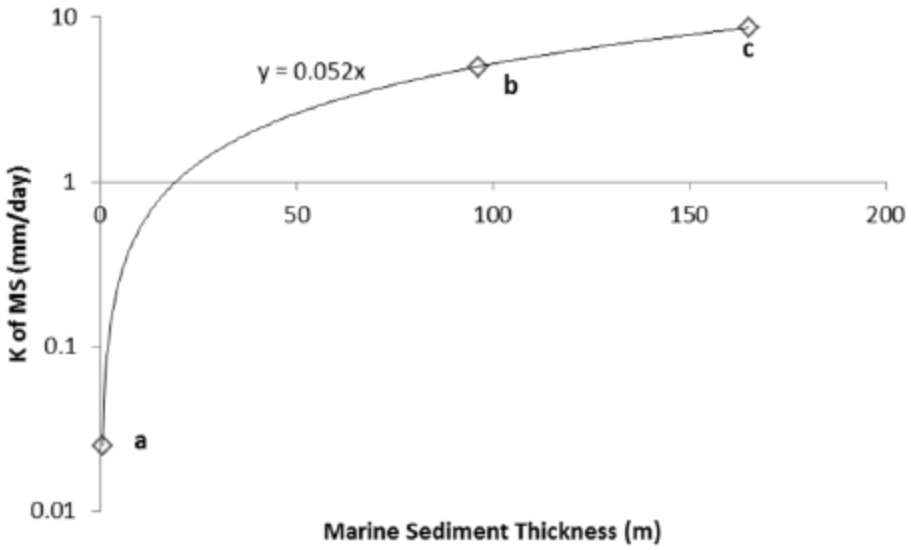

Figure 4-8 K vs. marine sediment thickness using the K/ΔL ratio = 5.2×10^{-5}/day. The K values used are: a) 0.025 mm/day, value used by HCI (2004a); b) 5 mm/day, median value of MS found in this paper, c) 8.6 mm/day, Reeve's (2000) "no flow" base.

4.7 Conclusion

Considerable attention is given to the hydraulic conductivity of aquitards when their protective properties are important, e.g., a liner in a landfill or the MS presented here; however, the thickness is almost equally as important. Under normal field conditions (i.e., no depressurization of the regional aquifer) the properties of the marine sediments are rarely tested, in fact, high water tables can be maintained directly beside bioherms where no MS are present. In the post-glacial landscape the MS likely played a critical role in reducing recharge to more permeable deposits (like sand) and thus allowing for the establishment of the wetlands, however this would have occurred with a minimal vertical gradient. When determining the effects of (vertical) dewatering in peatlands, the lateral transmission of surface waters must also be considered, as the fens in this study area appear to be less impacted due to their hydrogeomorphic setting (i.e., non-ombrogenous). Currently, because of regional aquifer depressurization, the MS are being stressed and are not acting as a perfect aquitard as assumed in the original feasibility studies.

4.8 Acknowledgements

We would like to thank the De Beers Canada Environment Lab for allowing us access to the site. We would like to thank A. Nicol, C. Cook, S. Ketcheson, M. Leclair, the "Fox", PAM, P. Jeffries, T.

Ulanowski, E. Perras, K. Ali (nee Tindale), M. Glover and A. Warnock for help with data collection over the years. Special thanks to Dr. M. Kompani-zaire for the insightful discussion about Darcy's Law.

5 Fire, rock and ice: a fire risk assessment of dewatered organic soils surrounding a bioherm at an open-pit diamond mine

This chapter is submitted as:

Whittington, P., Thompson, D.K., Price, J.S. submitted December 6 2012. Fire, rock and ice: an fire risk assessment of dewatered organic soils surrounding a bioherm at an open-pit diamond mine in the James Bay Lowlands. Submitted to Canadian Journal of Forest Research. CJFR-2012-0499

5.1 Overview

The Hudson-James Bay Lowlands are the world's second largest wetland and is undergoing rapid environmental changes both naturally (large scale climate change) and anthropogenically (small scale industrial developments, such as the De Beers Victor Diamond Mine). Both stressors will cause a decline in the water table (climate change increase evapotranspiration and industrial developments require aquifer dewatering) but how this water table decline will impact the lowlands' fire risk (and carbon cycle implications) is unknown. Bioherms, ancient coral reefs, are exposed bedrock outcrops and are showing the most impact from aquifer dewatering with water tables >1 m below pre-mining levels. We sampled three 10 x 10 m quadrats for fuels loads on the bioherm, immediately adjacent to the bioherm, and 20 m away from the edge of the bioherm and found that little fuel existed (0.38 kg/m^2) beyond 10 m from the bioherm. Historical indices for Initial Spread Index (ISI) and Drought Code (DC) were determined and showed that little overlap between high ISI and DC occurred indicating a low fire risk for the area. Lastly, we used soil moisture contents adjacent to the bioherm and a depth of burn model and determined that under ideal conditions the burn would be limited to ~1 cm.

5.2 Introduction

The Hudson-James Bay Lowlands (HJBL) are one of the world's largest wetland complexes and represent about a tenth of the globe's cooling benefits derived from carbon accumulation in peatlands; the HJBL peatlands sequester about a third of Ontario's total carbon emissions (Riley, 2011). The HJBL is typified by saturated conditions due to the low topographic relief and subarctic climate limiting evaporative losses; the peatlands generally overlay a thick, relatively impermeable layer of marine sediments which minimize vertical seepage losses separating the peatlands from the regional limestone aquifer. Despite the

HJBL's size and relative importance, there is a lack of knowledge about the lowlands, particularly pertaining to the carbon cycle, and more specifically peatlands' fire risk and how increased industrial development in the area might increase the fire risk.

The HJBL is also undergoing an unprecedented period of rapid climate change (Gagnon and Gough, 2001; Gough and Wolfe, 2001) which Roulet et al. (1992) predicted could cause a water table drawdown of 14-22 cm. The discovery of kimberlite (diamondiferous) pipes in an area of the HJBL has led to the development of an open-pit diamond mine which requires dewatering of the regional limestone aquifer. The effect on the surrounding peatland has generally been localized to areas where the bedrock is close to the surface (i.e., locally thinner marine sediments), or exposed such as those areas surrounding bioherms, the fractured limestone bedrock exposures that rise above the surround peatlands (Cowell, 1983). Aquifer dewatering has caused local water table drawdown (> 1 m) in the peat immediately surrounding the bioherms, though this is limited to about 30 m from the bioherm edge (Whittington and Price, 2012). As the bioherms are local topographic highs in an otherwise flat landscape, they are also at increased risk for lightning strikes (Petrov et al., 2003), the dominant ignition mechanism in these environments.

Despite the high moisture contents commonly found in peatland systems like the HJBL, laboratory studies have found that peatland smouldering combustion can occur at depth in peat with water contents upwards of 15% volumetric moisture content (VMC) if the overlying combusting peat is of sufficiently high bulk density (Benscoter et al., 2011). The inverse relationship between water table and fire risk has been established in experimentally-drained peatlands in the Boreal Plain of Alberta (Turetsky et al., 2011), suggesting that a drying of the peatlands would increase its fire risk; however, few, if any, fire studies have been conducted in the HJBL and so the fire risk (and carbon cycle implications) remains essentially unknown. The water table drawdown caused by resource extraction could provide insight into how the fire risk in these environments may respond to a warming climate on a large (ecosystem) scale, rather than merely the local (near the extraction) scale. In addition, the cumulative impacts of a changing climate as well as localized dewatering must be addressed as this information would be very useful for natural resource and fire management agencies, as well as carbon cycle studies as the fire risk has implications for vegetation recovery, permafrost stability and the post-fire energy and water balance.

The Canadian Forest Fire Danger Rating System (CFFDRS) is used throughout Canada to quantify fuel moisture and the potential for fire spread in a variety of fuel types (corresponding to vegetation communities). The weather component of the CFFDRS, the Fire Weather Index System, comprises six standard components: Fine Fuel Moisture Code (FFMC), Duff Moisture Code (DMC), Drought Code

(DC), Initial Spread Index (ISI), Buildup Index (BUI) and Fire Weather Index (FWI). The first three are codes that follow daily changes in moisture contents, and are based on meteorological variables; the last three are fire behaviour indexes (Van Wagner, 1987) and are calculated, in part, with the first three. Waddington et al. (2012) note that while these were parameterised in upland soils, the DMC and DC are most representative of the surface and deeper peat, respectively. DC was shown to correlate well with VMC (ranging in the upper 5-15 cm of the profile depending on the site) during dry periods at numerous wetland types (bog and fen) and years across boreal Canada suggesting that the DC could be used to characterize the VMC of peat (Waddington et al., 2012). For full details on the calculations of all of the components the reader is directed to Van Wagner (1987). In brief, the DC was originally formulated as 1/100 of inches of water in a BC Douglas fir forest, but has been modified and is now largely considered a unitless drought indicator. The DC is calculated daily as an index of the water stored in the soil and is calculated using a rainfall phase and a drying phase (potential evapotranspiration based on noon temperature and a monthly coefficient). The starting value of the DC each spring is determined with fall and winter precipitation amounts following standard methods (Lawson and Dalrymple, 1996) such that the DC is started higher with a dry spring and low snow winter. The ISI combines noon measurements of air temperature and humidity with wind speed to determine fire spread potential. Beyond fuel moisture, potential fire behaviour is determined using the ISI and fuel-type specific regression in order to estimate a forward rate of spread and fire intensity.

Therefore, the objectives of this paper are to determine 1) what the historical ISI and DC values are and, 2) existing peat fuel loads around bioherms, and 3) to compare these with changes in soil moisture to determine the fire risks, if any, as a result of dewatering (or potential climatic warming).

5.3 Study Site

The study site is ~500 km north-north-west of Timmins, Ontario, at the De Beers Canada Victor Diamond mine (N 52.854° W 83.924°) (Figure 5-1a). A research transect anchored at both ends by bioherms, traverses a complex arrangement of bogs and fens, indicative of the regional landscape. Peat depths range between 0 and ~4 m and overlie fine-grained marine sediments. The marine sediments range in thickness from 0 (e.g., bioherms) to over 100 m and overlie Silurian bedrock of the Upper and Lower Attawapiskat formation.

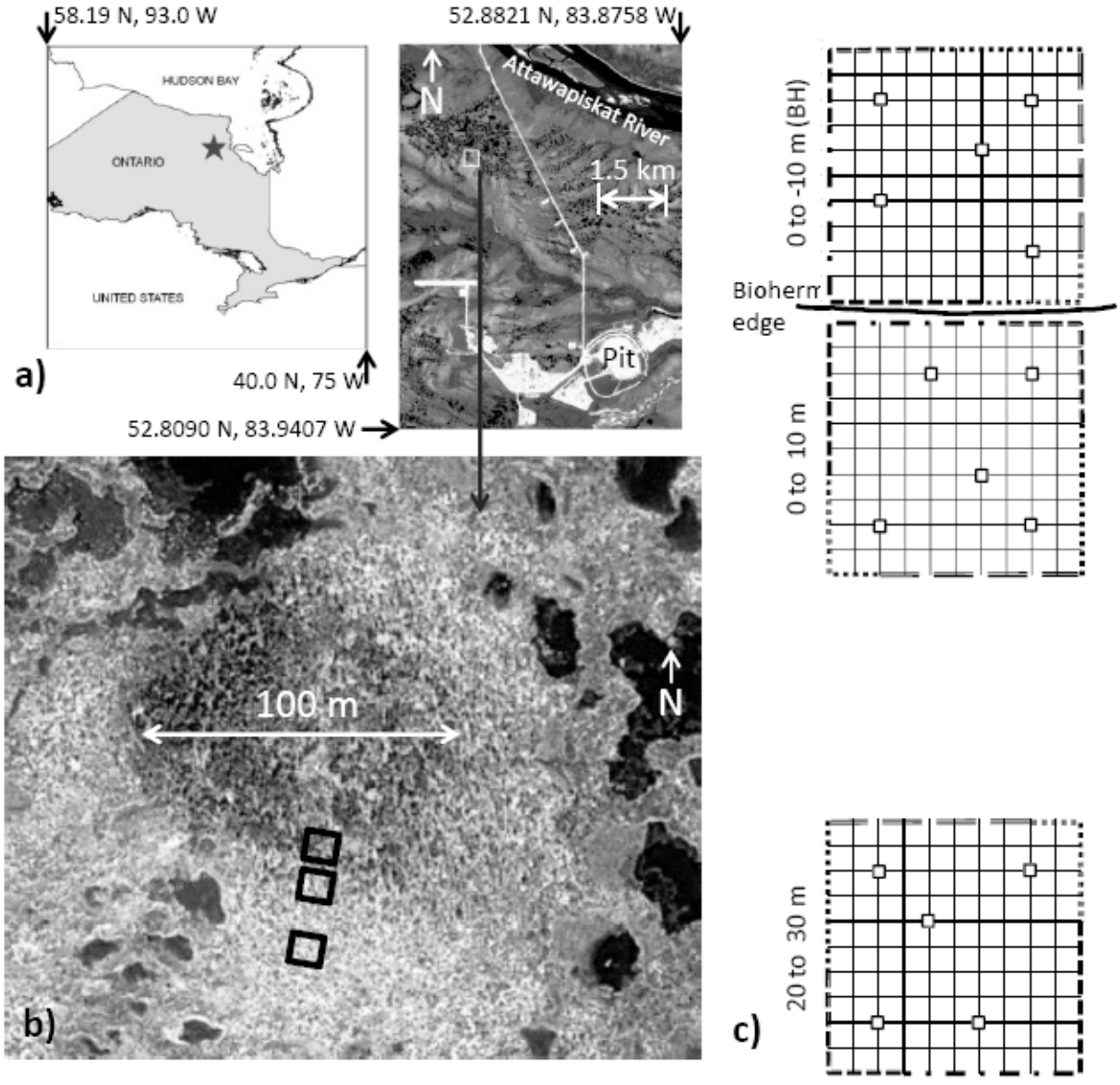

Figure 5-1 a) Study site in reference to Ontario (left) and the open-pit diamond mine (right). b) IKONOS image of the North Bioherm with approximate locations of the quadrats (black squares). c) Example quadrat showing the dead-down woody fuel sampling locations (changes in line pattern around border, with the first and last size classes shown), as well as the five surface fuel sampling locations (small, thick black squares. Entire quadrat was 10 x 10 m, shown with 1 m grid spacing d) locations of the quadrants in relation to the edge of the bioherm.

Lansdowne House (inland 300 km west-south-west) and Moosonee (250 km south-east near the James Bay coast) are the closest stations with long-term meteorological records available. Whittington et al. (2012) and Whittington and Price (submitted) found that an average of the 30 year climate normals

(Environment Canada, 2008) for Lansdowne House and Moosonee could be used to determine a long term average for the Victor Mine site. The average annual January and July temperatures for Lansdowne House are -22.3 and 17.2 °C, respectively, and for Moosonee are -20.7 and 15.4 °C, respectively (Environment Canada, 2008). Annual precipitation for Lansdowne House is 700 mm with ~35% falling as snow; and for Moosonee is 681 mm with ~31% falling as snow. The field season (May 1 – August 31) average temperature and precipitation at Victor are therefore 12.7 °C and 314 mm, respectively.

The Hudson Plains ecozone (spanning from Churchill, Manitoba to the east shores of James Bay) experiences on average 255 large wildfires (defined as those greater than 200 ha) per year with an geometric mean area of 1500 ha. Annual area burned in the Hudson plains is 97 000 ± 151 000 ha per year (Parisien et al., 2006), though this number is likely an underestimate, as approximately one-third of the ecozone is not subject to observations or cataloguing of fire scars.

At the northern end of the research transect is the North Bioherm (NB). NB is approximately 4 m high and is ~100 m in diameter. Ground cover at NB is lichen dominated and the dominant tree cover is black spruce.

5.4 Methods

A weather station was installed at the mine site (~5 km from the bioherm) during site construction in March 2000 and recorded wind speed/direction, temperature, and precipitation.

5.4.1 Soil Properties

To determine the moisture content profile in the peat, a Campbell Scientific TDR 100 system was installed (~10 m) adjacent to the edge of NB in October 2007. A pit was excavated so that lateral insertion of the probes was possible. Probes were installed at 0, -10, -20, -30 and -40 cm below base of the lichen (i.e., top of the peat) and the hole repacked carefully to minimize destruction to the peat. Moisture contents were recorded every hour and waveforms every 12 hours. A 2.5 cm diameter PVC well was installed near the pit and manual measurements of water table in the peat were recorded during the summer months.

The dielectric constant (K_a) values determined from the TDR100 were converted to moisture contents (θ) using the third order polynomial of Kellner and Lundin (2001) for peat soil:

$$\theta = 0.039 + 0.0317\,Ka - 0.00045\,Ka^2 + 0.0000026\,Ka^3 \quad [5\text{-}1]$$

To determine bulk density a narrow (~10 x 10 cm) column of the upper 50 cm of the peat was taken from an area near the TDR installation using a hand saw. The core was transported back to the laboratory, sectioned into 5 cm sections, weighed, dried and weighed again.

5.4.2 Fuel Loads

Fuel sampling was completed using the methods outlined in McRae et al. (1979) and Johnston (2012) but modified to determine the relative fuel loads from the edge of the bioherm. Three, 10 x 10 m quadrats (Figure 5-1 b, c) were used: the first was located 20 to 30 m from the edge of NB, the second 0 to 10 m from the edge of the bioherm, and the third was located on the bioherm, 0 to -10 m from the edge of the bioherm. (Note, the 0 to 10 and 0 to -10 were offset slightly (~50 cm) from the edge of the bioherm so that they did not share a common edge.)

Five surface fuel sampling (0.3 m x 0.3 m) locations were selected at random within each of the 3 quadrats (small black squares (Figure 5-1c). Surface fuel was sorted into 6 categories: live shrub, dead shrub, litter, ground lichen, shrub lichen, and live herbaceous plants. The samples' field weights were recorded and then the samples were dried in an oven at 95 °C until dry, then dry masses were recorded.

Dead-down woody fuel (i.e., downed woody debris laying on the ground) was sampled along the edge of each quadrat using the class size criteria in McRae et al. (1979) but for 6 m (8 m for the last class) intervals, rather than 5 m. Size classes from 1 to 6 were 0-0.49, 0.5-0.99, 1.0–2.99, 3.0–4.99, 5.0–6.99, and > 7.0 cm in diameter, respectively, and are shown in Figure 5-1c as changes in the border line style around the quadrat. The reader is directed to either McRae et al. (1979) or Johnston (2012) for details on the calculations.

Stand characterization was completed within each 10 x10 m quadrat by recording the following characteristics for all trees > 0.5 m in height: tree species, condition (dead or alive), height, diameter at breast height (1.4 m), basal diameter, crown base height (measured from ground surface to the lowest continuous branch <0.5 cm diameter), and a qualitative rating of the foliage and lichen load from 0-3, where 0 is an absence of lichen and 3 is heavily loaded with lichen. The diameter at ground level was used to calculate the fuel mass based on the equations in Table 2.7 of Johnston (2012). Crown bulk density was calculated as the canopy fuel load (kg/m^2) divided by the canopy height (m) to get kg/m^3 (canopy height was determined as the 90^{th} percentile).

5.4.3 Historical indexes and depth of burn

Weather data collected at Lansdowne House was used to calculate historic daily Fire Weather Indices (DMC, DC, ISI) for the period 1978 to 2011. Empirical distribution functions for the ISI and the DC were calculated for each of the months of the fire season May through to September.

The energy input from a flaming front to the peat surface is the sum of radiative and convective exchange between the approaching flaming front and peat surface, which is pre-heated by the flaming front and is cooled marginally by increases in its longwave emissions and convective cooling prior to the arrival of the flaming front. While individual heat transfer processes are modelled in Thompson et al. (submitted) the net heat flux to the surface (E_{net}, kJ m^{-2}) can be expressed as a function of the *ISI*:

$$E_{net} = 11804\, ISI^{-0.2} \quad \textbf{[5-2]}$$

In order to calculate the depth of burn, first the energy required for the ignition of the peat (E_{ign}, kJ m^{-3}) must be calculated following Benscoter et al. (2011), including the energy required to evaporate all the water and increase the temperature of the dry peat to the ignition temperature of 300ºC:

$$E_{ign} = \left(c_w \theta \left(T_V - T_A\right)\right) + \left(L_V \theta\right) + \left(c_{peat}\, \rho_b \left(T_{ign} - T_A\right)\right) + \left(S\, \rho_b\right) \quad \textbf{[5-3]}$$

where c_w is the heat capacity of water, θ is the volumetric water content (m^3 m^{-3}), T_v is the boiling point of water (100ºC), T_A is the ambient temperature, L_V is the latent heat of vapourization, c_{peat} is the heat capacity of peat, ρ_b is the bulk density of the peat (kg m^{-3}), T_{ign} is the ignition temperature for smouldering (300ºC from Van Wagner, 1972), and *S* is the energy required to liberate water molecules sorbed to organic material (50.4 kJ kg^{-1}) from Van Wagner (1972).

While Benscoter et al. (2011) used discrete peat horizons 3 cm in thickness and modelled total depth of burn at 3 cm resolution with depths of burn in excess of 20 cm, the relatively high water contents in HJBL peat allow for a simple approximation of shallow (<3 cm) depth of burn, assuming minimal conduction into deeper horizons:

$$z_{DOB} = \frac{E_{net}}{E_{ign}} \qquad \textbf{[5-4]}$$

where z_{DOB} is in metres following the units given above.

5.5 Results

Using a minimum ISI of 10 in order to achieve a surface fire of moderate intensity (Alexander et al., 1991) that is difficult for fire crews to contain, the ISI exceeded this critical value on 12% of days in the historical record in May (1978-2011), but only on 8% of days in June and less than 2% of days in the remainder of the fire season (Figure 5-2a). The DC followed an inverse trend with May values of the DC less than 100 in 90% of cases (Figure 5-2b). Low snow years caused the DC to initiate above the standard value of 25, and as such DC values in excess of 200 are observed are seen above the 90th, and are mainly all from the same dry springs. In late summer the 90th percentile of the DC in August and September did not exceed 400.

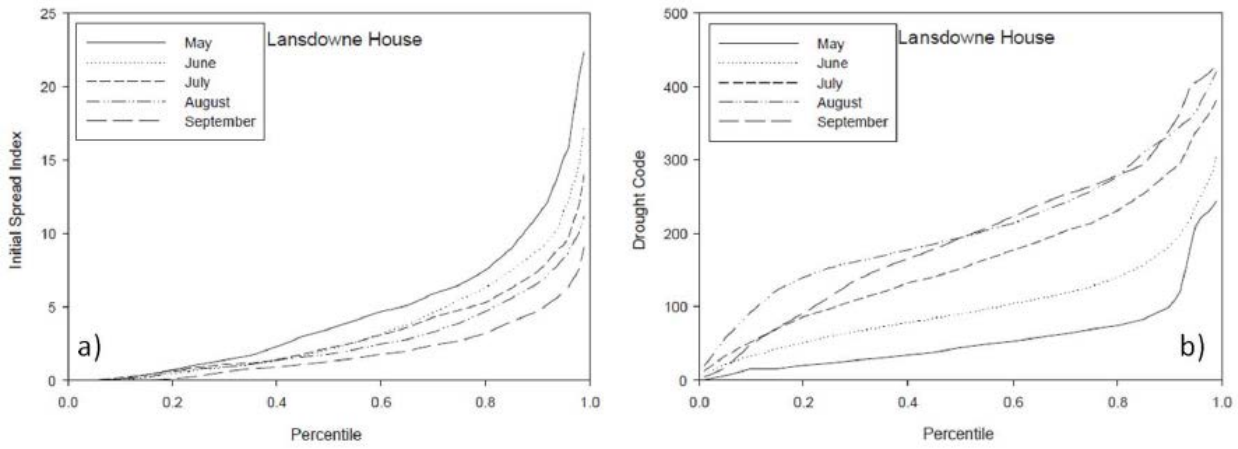

Figure 5-2 Historical Initial Spread Index (ISI; a) and Drought Code (DC); b) for Lansdowne. Lansdowne House's record extends from 1978 to 2011.

Fuel loads trended 20 to 30 m from bioherm < 0 to 10m from bioherm < 0 to -10m on bioherm (BH) for surface and dead-down woody fuel types; stand fuel was highest near the bioherm (0 to 10m) and lowest away from the bioherm (20 to 30 cm) (Figure 5-3, Table 5-1). Surface fuel loads on the bioherm (0 to -10)

were twice that of the 20 to 30 m quadrat (0.32 vs. 0.16 kg/m^2) (Figure 5-3, Table 5-1). Dead-down woody were similar between the 0 to 10 and 0 to -10 quadrats (0.17 and 0.19 kg/m^2) and both were several orders of magnitude higher than the 20 to 30 quadrat (0.002 kg/m^2). This was similar to the stand fuel, only the difference between the near- and on-bioherm locations were ~10x larger (0.22 vs. 2.13 and 1.85 kg/m^2).

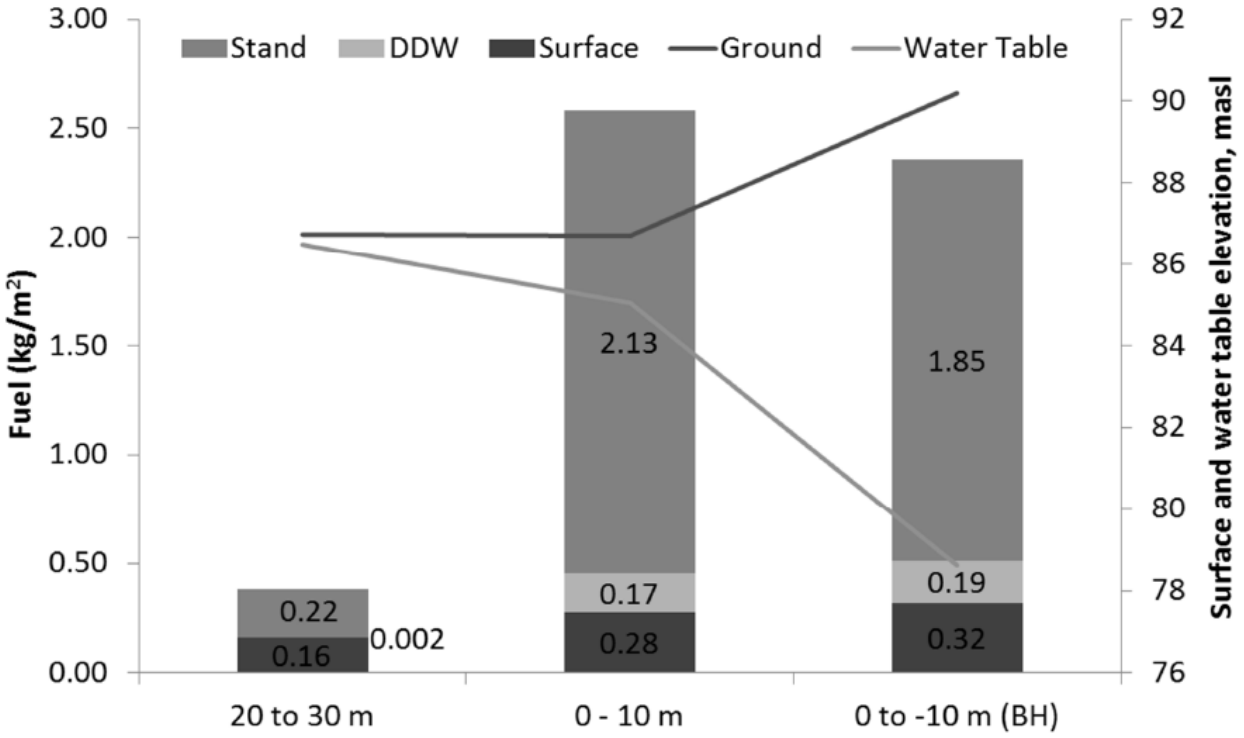

Figure 5-3 Fuel loads (Stand, Dead Down Woody (DDW) and surface fuel) for each quadrant (also shown are the actual values in kg/m^2). The ground surface and water table on July 27, 2012 are also shown for reference.

Table 5-1 Fuel loads (Stand, Dead Down Woody (DDW) and surface fuel) for each quadrant as well as canopy characteristics

	Surface Fuel Load	Dead Down Woody		Canopy characteristics					Total
				Stand fuel	Density	Stem Density	Basal area	90th Pct height	
Location	kg/m2	tonnes/hectare	kg/m2	kg/m^2	kg/m^3	stems/ha	m^2/ha	m	kg/m2
20 to 30 m	0.16	0.02	0.002	0.22	0.13	2900	4.0	1.6	0.38
0 to 10 m	0.28	1.74	0.17	2.13	0.66	6800	33.4	3.2	2.58
0 to -10 m (BH)	0.32	1.92	0.19	1.85	0.82	4100	30.1	2.2	2.36

From 2007 to 2011 the field season (May to August) weather varied compared to the 30 year climate normal with 2007 being the warmest and driest (lowest seasonal precipitation) field season and 2009

being the coolest and wettest (Figure 5-4a). 2008, 2010 and 2011 were slightly cooler and drier than average. Snow data are shown as typically snow melt occurs throughout April (Whittington et al., 2012), but in 2010 the snow pack was minimal and melted early providing little recharge to the system.

Water tables in the bedrock of North Bioherm declined ~5 m over the study period (for more details the reader is directed to Whittington and Price, 2012; Whittington and Price, submitted). In the peat surrounding the bioherm the field season average water table declined ~1.4 m from 2007 to 2011 (Figure 5-3 and Figure 5-4b).

a)

2007	2008	2009	2010	2011	
13.0	11.9	10.4	13.0	12.5	Ave. Air Temp. (°C)
220	298	380	276	284	Rain (mm)
37	43	75	0	39	*Snow (cm)

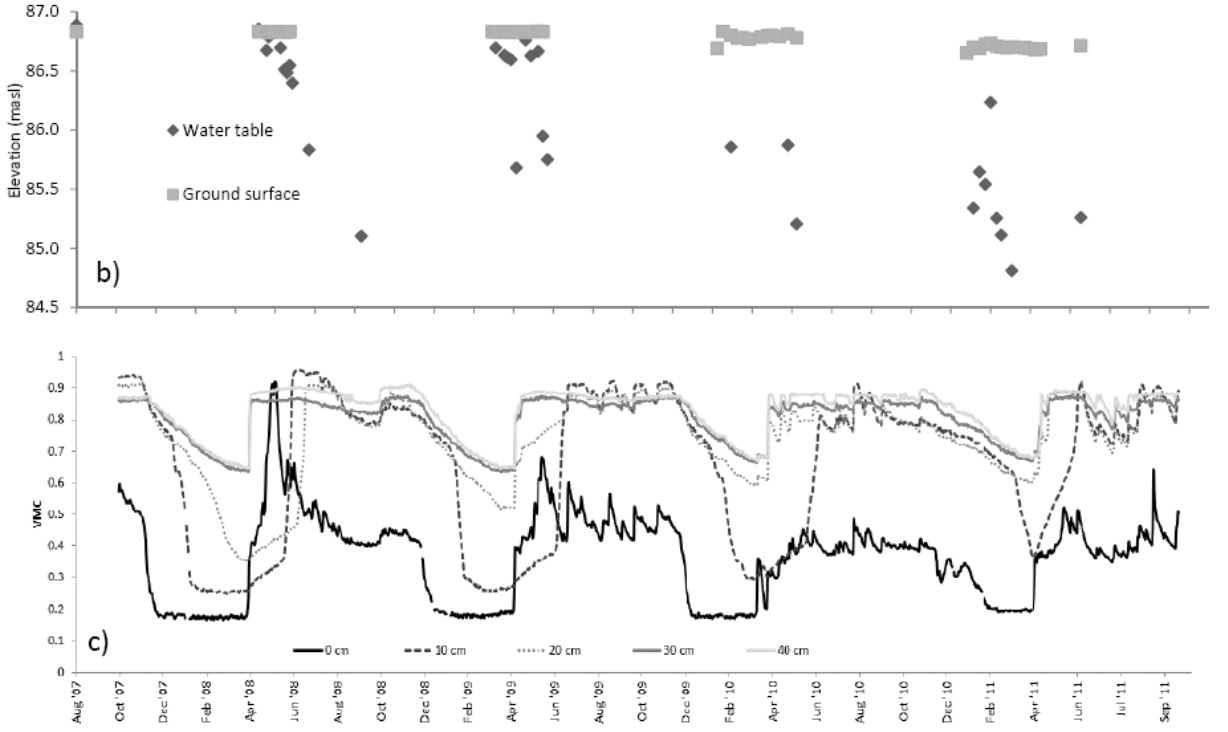

Figure 5-4 a) seasonal (May to August) weather from 2007-2011. Snow depth represents the approximate depth of snow at the start of melt (generally early to mid April). b) Water table and surface elevation near the TDR pit, through time. c) VMC from 0 to 40 cm below the surface from Oct. 2007 to Oct. 2011.

Volumetric soil moisture contents showed a similar pattern year to year with an increase in soil moisture in April and May followed by a slow decline through the summer in the upper probes (0 and -10 cm; Figure 5-4c). During relatively rain-free periods of the summer, the DC was a good predictor of surface

VMC. For example, between June 2-28 2010, VMC declined from 43.4 to 36.0% as DC increased from 112-267. Moisture contents were fairly consistent throughout the summer for the lower probes (-20, -30, -40 cm) but did show more variability in 2010 and 2011 versus 2008 and 2009. Beginning in December each year moisture contents decreased during freeze up until the spring wet up.

The r^2 value of DC vs. daily average VMC for each VMC probe (0 cm to 40 cm) for each month from 2008 to 2011 were calculated and are shown in Table 5-2. In 2008 and 2009, when it was particularly wet, strong relationships were seen at almost all depths for the entire season (darker coloured cells). In 2010, which was very dry, these relationships were only strong in June and weak to non-existent for the remainder of the season. In 2011, only June offered strong relationships with July-September being mostly weak.

5.6 Discussion

The historical weather record show the infrequency of the ISI exceeding 10 and the DC to exceeding 400 and, more importantly, rarely at the same time (Figure 5-2); generally the ISI was higher in the early summer when wind speeds would be higher, but due to spring melt the DC usually started low and did not exceed 400 until later in the season when the wind speeds decreased.

The poor relationships between DC and VMC found in the drier years (2010/2011) suggests that in the future in under-drained areas the DC may not be a good approximation of peat VMC and therefore smouldering risk. However, the DC can be started at a higher value to reflect overwinter drying (Lawson and Armitage, 2008), but this is usually reserved for variations in weather conditions (i.e., low snow fall or unusually dry fall the year prior), rather than for artificial (e.g., mining) causes. This suggests that in order to accurately characterise the fire risk and compare the ISI with the DC, the DC would need to be corrected (i.e., started at a higher value) which could promote more overlap with the higher ISI found earlier in the year and reflect the true fire risk for anthropogenically dried areas. It is likely that under climate change conditions (lower water tables) the DC would be started at a higher point as the lower water tables are the result of the changing climate (and hence seasonal weather used to calculate the DC) and would create the need for a higher spring DC to account for drier falls and shorter/less snowy winters.

Table 5-2- The r^2 values of DC vs. daily VMC of TDR probes for May to September from 2008 to 2011 at Lansdowne House and are coloured such that the darker the cell the better the relationship is: the black and grey cells represent r^2 values of 0.75 to 1.0 and 0.5 to 0.74, respectively, whereas the lighter grey or non-shaded represent r^2 values of 0.25 to 0.49 and 0 to 0.25, respectively.

2008	0 cm	10 cm	20 cm	30 cm	40 cm
May	0.93	0.80	0.72	0.49	0.03
June	0.72	0.01	0.63	0.05	0.02
July	0.21	0.47	0.04	0.92	0.91
August	0.74	0.80	0.73	0.61	0.49
September	0.46	0.48	0.52	0.25	0.58
2009					
May	0.74	0.15	0.76	0.64	0.70
June	0.66	0.81	0.47	0.80	0.56
July	0.74	0.78	0.75	0.60	0.55
August	0.85	0.73	0.76	0.74	0.19
September	0.42	0.73	0.58	0.45	0.41
2010					
May	0.21	0.69	0.23	0.00	0.02
June	0.84	0.43	0.89	0.90	0.84
July	0.47	0.50	0.31	0.22	0.00
August	0.16	0.03	0.01	0.01	0.00
September	0.18	0.11	0.08	0.01	0.00
2011					
May	0.33	0.42	0.18	0.03	0.21
June	0.93	0.90	0.97	0.93	0.82
July	0.16	0.13	0.25	0.38	0.23
August	0.36	0.39	0.41	0.51	0.50
September	0.22	0.40	0.15	0.61	0.60

The tree basal area on and nearby (0-10 m) the bioherm is similar to that found in an poorly-drained but non-peatland black spruce stand in northern Manitoba by Gower et al. (1997) and exceeds the 28 m^2/ha found in black spruce bogs in northern Ontario by Stocks (1980). The stand structure is substantially different, however, as the stem density is greater and the canopy height is substantially lower compared to the above studies. The plot 20-30 m distant to the bioherm showed a basal area and stem density lower than even the sparsely-treed spruce-lichen woodlands from Alexander et al. (1991).

Alexander et al. (1991) notes that the dead-down woody material at Porter Lake were “exceedingly low” with a mean value of 0.38 kg/m^2 which is twice that of the dead-down woody at the near bioherm

locations (0 to 10 and 0 to -10) and several orders of magnitude higher than away from the bioherm (20-30 m) suggesting that there is little fuel on the ground near the bioherms (Table 5-1). This is likely due to a combination of low above-ground biomass, accompanied by the ability of *Sphagnum* mosses to grow at approximately 3 mm per year (Vitt et al., 2003), meaning that much of the woody debris is overgrown by mosses within a few years of deposition on the moss surface.

The fuel loadings on and near the bioherm as a result of the high stem density and basal area (2.36-2.58 kg/m^2, Table 5-1) are similar to the ~2.5 kg/m^2 loadings measured by Stocks (1980), but are greater than the loadings of no more than 1 kg/m^2 measured by Johnston (2012) in black spruce bogs in central Alberta. The 20-30 m plot showed a fuel loading only slightly more than a black spruce bog 27 years since fire in northern Alberta, as measured by Johnston (2012). The net result of moderate fuel loadings and low canopy heights (2.2-3.2 m) on and near the bioherm is that canopy bulk density was actually rather high at 0.66 kg/m^3 on the bioherm edge and 0.82 kg/m^3 on the bioherm (Table 5-1).

While the fire risk is relatively low given the historical ISI and DC, the chances of it spreading off of the bioherm and into the surrounding peatland is also quite low as the peatlands surrounding the bioherms contain little fuel (Figure 5-3) to carry a fire beyond the 20-30 m distance. Given the very high moisture contents (>75%) found at depths as high as 20 cm (Figure 5-4c) and the ~ 40% VMC at the surface (0 cm; Figure 5-4c), the depth of burn, even if a fire were to occur, would be limited to the overlying lichens and no more than 1 cm of peat (Figure 5-5). Figure 5-5 shows the relationship between the DC and ISI for the soil profile; the deepest burn possible in this peat profile (>0.9 cm) requires a high DC (~275) but can occur at a lower ISI (e.g., 5).

It is possible that with prolonged drying due to mining tree growth could be enhanced on the edges of bioherms, which would increase both fuel loads as well as potentially drying peat in the rooting zone (Lieffers and Macdonald, 1990). However, as Whittington and Price (2012) have shown the drawdown around the bioherm is limited to ~30 m. In the current case, the Victor mine is expected to last only ~12-15 years, minimizing any long-term impacts due to increased tree growth.

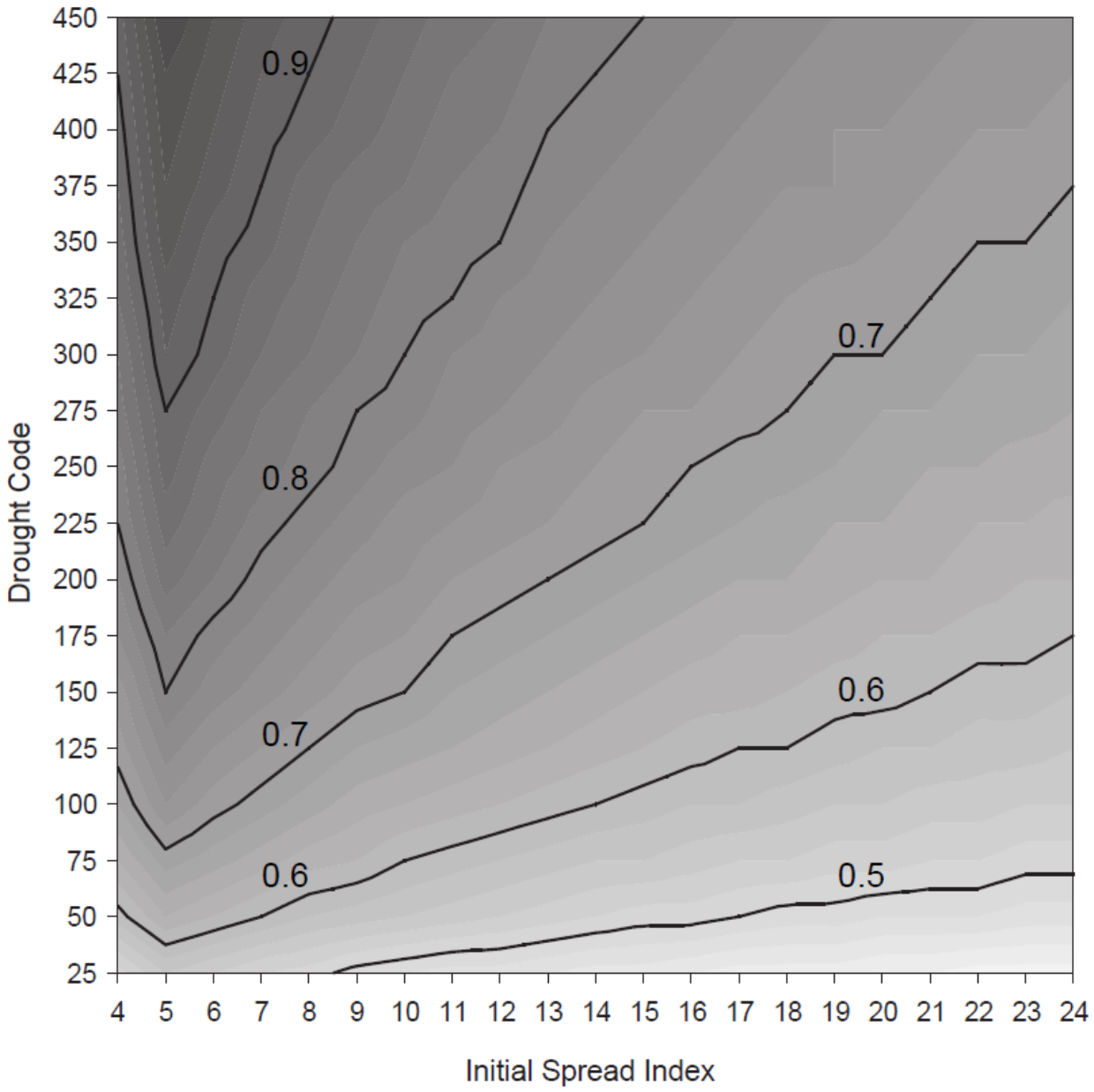

Figure 5-5 DC vs. ISI and associated depth of burn (contours) in cm. The observed DC-VMC relationship during June 2010 (VMC = 1.131 $DC^{-0.207}$; R^2 = 0.96) was used as the input for E_{ign}, while *ISI* controlled E_{net}. Depth of burn was calculated using equation 5-4.

5.7 Conclusion

While other studies have shown peatlands in drier boreal plain to be particularly vulnerable to multiple disturbances (fire after drainage (Turetsky et al., 2011)), the combination of wildfire and dewatering of

the underlying aquifer does not appear to pose the same risk of deep smouldering during wildfire. While the explicit impacts of the mine operation on the groundwater and saturated hydrology of the peatland are apparent (Whittington and Price, 2012; Whittington and Price, submitted) the high water retention capacity of the peat despite water tables in excess of 1 m maintains sufficiently high water contents to limit peat combustion to a very shallow depth. It would appear that another fundamental change to the water balance (enhanced evaporation or transpiration) in addition to the water table changes observed here would be required to shift the peat to a drier state where extensive smouldering would be possible.

The similarities between an under-drained peatland and a climate change affected peatland extend only to the result of a decline in water table and certainly not the cause of the decline. When using traditional fire indices such as DC to predict depth of burn, managers of anthropogenically affected areas need to exercise caution as the DC only incorporates the seasonal weather, and not the under-drainage due to dewatering. In a climate change scenario the DC would likely better account for the soil's drought (caused by weather) and increase the temporal period that the ideal ISI and DC conditions coincide by increasing the initial DC. However, regardless of the increased temporal period that a lower ISI and DC (i.e., greater than 10 and 400 respectively) may occur simultaneously, the peatlands surrounding the bioherms just do not contain enough fuel to carry a fire.

5.8 Acknowledgements

We would like to thank the De Beers Canada Environment Lab for allowing us access to the site. The authors would also like to that C. Davidson, T. Despault, M. Kline, M. Leclair, E. Perras, J. Sherwood, T. Ulanowski, and A. Warnock for help in the field.

6 The role of permeable marine sediments in peatland-dewatering around a bioherm outcrop, James Bay Lowlands

This paper is submitted as:

Ali, K., Whittington, P., Remenda, V., and Price, J.S. submitted December 20, 2012. The role of permeable marine sediments in peatland-dewatering around a bioherm outcrop, James Bay Lowlands. Submitted to Hydrological Processes, HYP-12-0907

6.1 Overview

Peatlands in the Hudson-James Bay Lowlands (HJBL) exist, in part, due to minimal vertical seepage losses through the low hydraulic conductivity (*K*) Tyrrell Sea sediments and small vertical gradients between the surface and the bedrock aquifer. Recent development of an open-pit diamond mine within the HJBL requires the dewatering of the regional limestone aquifer in the area of the mine. This creates downward gradients near the surface, increasing the importance of low *K* sediments that help retain water in the peatlands. There are areas within the mine's impacted area where exposed bedrock outcrops (bioherms) puncture the sediment layers and increase vertical drainage, which has resulted in partial desiccation of the overlying peatlands. This paper investigates the characteristics of the sediments and the flow regime surrounding three of these bioherms and proposes a conceptual model of flow. In general, the sediments in profiles near bioherms were either highly stratified showing 3-4 layers with distinct hydraulic properties; or poorly stratified with only a mix of silts and sands. In a suite of nested piezometers the vertical Darcy flux from the peat to the sediment and from the shallow to deep sediments indicated one of two patterns: either less water flowed downward in the sediment than was supplied from the peat layer above, or significantly (100 times) more water was flowing down in the sediment than was being received from the overlying peat. The conceptual model presented hypothesizes that in the first case flow in the sediment is primarily horizontal until proximal to flow channels in the bioherm rock at which point the second case is observed as both water from the peat above and water flowing laterally in the sediment drains downwards into the dewatered bedrock. The flow regime around bioherms has relevance in predicting the impact of dewatering programs on the surface ecosystem as well as anticipating the recharge to the bedrock aquifer, which is an important factor in designing a dewatering program.

6.2 Introduction

The Hudson-James Bay Lowlands comprises one of the world's largest wetland complexes and exists primarily because of a delicate balance of water inputs and outputs. The cool subarctic climate limits evapotranspiration losses while providing sufficient precipitation, and the low regional slope delays lateral runoff. The simplified stratigraphy of peat over marine sediments over bedrock is also important as the hydraulic heads in the marine sediments/bedrock are close to or above those in the peat, minimizing any vertical seepage losses. Discovery of kimberlite (diamondiferous) pipes in an area of the James Bay Lowlands has led to the establishment of the De Beers Canada Victor Diamond Mine which requires dewatering of the regional bedrock to maintain a dry open-pit. Whittington and Price (submitted) have shown that dewatering of the bedrock surrounding the mine has resulted in partial drainage of the peatlands in this area; this is particularly true in areas near bioherms (ancient coral reefs) which are exposed bedrock outcrops in the lowlands. Currently there is an inadequate description of the hydrogeological connectivity of peatlands to the bedrock aquifer near bioherms, because of the complicated stratigraphy associated with their genesis in the littoral zone and subsequent isostasy.

The stratigraphy in the area of the mine is shaped by glacial events and current climate (Glaser et al., 2004a; Glaser et al., 2004d). The upper 2-3 metres is covered by peat deposits overlying Tyrrell Sea marine sediments. The Tyrrell Sea sediments are underlain by glacial tills deposited over several events onto the top the Silurian limestone. The combined thickness of the till and Tyrrell Sea deposits varies from 200 m in areas of gouged trenches to 0 m in areas where bioherm (reef mound) structures rise to surface (AMEC, 2003).

Under dewatering conditions bioherms in the area have been shown to act as drainage nodes (Whittington and Price, 2012). The hypothesis of this work is that the drainage through the bioherms is enhanced by aprons of relatively high hydraulic conductivity sediments *and* that the characteristics of the bioherms themselves results in non-uniform radial flow. While they represent only 1% of the landscape (Whittington and Price, 2012), their potential contribution to desiccation of peatlands may be much higher depending on the vertical hydraulic conductivity (K_v) of the bioherm and the horizontal hydraulic conductivity (K_h) of the sediment surrounding it.

Bioherms or reef mounds are the geologic product of coral reefs that typically have a massive/structureless core with breccia along the sides (Hills, 1963) and in the HJBL are visible at the surface as partially vegetated mounds of exposed bedrock (Cowell, 1983). Drilling at the bioherms in the

HJBL indicate micro-karst “vuggy” features that are generally unconnected. Glacial erosion in the region likely removed much of the beccia but the resistant mounds have persisted as both outcropping and subcropping (no surface elevation expression) limestone (HCI, 2004b). Considering the alteration of flow around the bioherm features on the floor of the Tyrrell Sea and the effect of the shifting shoreline during deposition it is suspected that the sediments proximal to the bioherms vary from the typical low permeability Tyrrell Sea clay deposits.

Karst is the formation of channels in carbonate rock through dissolution; karstic features have been identified at bioherms in the region (Cowell, 1983). Field observations of bioherms near the deeply incised Attawapiskat River and pools of standing water along the edge of many bioherms indicate that drainage through bioherms does not always occur. The aperture and connectivity of these features evolves over time (Worthington and Ford, 2009) creating significant scalar effects in the hydrogeologic regime (Worthington, 2009).

This paper presents a conceptualization of groundwater flow proximal to bioherms in response to mine dewatering in the HJBL based on a more detailed assessment of the stratigraphy than that presented by Whittington and Price (2012). The potential impacts of drainage nodes within the dewatering drawdown cone have been shown to be (Whittington and Price, 2012) because these peatland ecosystems depend on restricted basal water losses (Martini, 2006; Riley, 2011). Therefore the objectives of this paper are to define, in detail, the subsurface stratigraphy surrounding bioherms, characterize the hydraulic properties of the different layers, and use these findings to define a conceptual model and determine the fluxes of water (both magnitude and direction) around bioherms.

6.3 Regional Geology

Multiple glaciation events have occurred in this region, the last of which was the Laurentide Ice Sheet. The glaciers eroded the limestone surface and deposited layers of glacial tills and glacial lake deposits across the area, infilling most depressions (Drege and Cowan, 1989). When Hudson Bay became ice free 7000-8000 years BP the isostatically depressed area was rapidly inundated by the Tyrrell Sea (Roy et al., 2011). The subsequent isostatic rebound (Glaser et al., 2004d) caused the regression of the Tyrrell Sea towards the current Hudson Bay coastline and the deposition of fine-grained marine sediments overlaying the glacial tills (Lee, 1960b). Due to the shifting shoreline the Tyrrell Sea low permeability deposits are upward coarsening (Drege and Cowan, 1989). The Tyrrell Sea deposits across the region can vary from 60 m thick in estuarine depositional sinks to zero in high elevation till areas (King and Martini, 1984;

Martini, 1981). Isostasy resulted in the emergence of a relatively flat, low permeability coastal environment where tidal marshes became established (Price and Woo, 1988b) which were eventually replaced by swamp forests and then forested and non-forested bogs (Klinger and Short, 1996; Sjors, 1963) as the system prograded.

6.4 Study Site

The De Beers Canada Victor Diamond Mine is located 500 km north-north-west of Timmins and approximately 90 km west of Attawapiskat (near the James Bay coast) in northern Ontario (Figure 6-1). There are at least 100 bioherms outcropping in three distinct bands (~2 km wide) running northwest to southeast, approximately 10 km apart, in a 12 km radius around the mine site (Whittington and Price, 2012). There are also an un-quantified number of sub-cropping bioherms, which are overlain by relatively thin overburden and/or peat. Elsewhere, the overburden there is commonly 10 metres (maximum of 20 m) of Tyrrell Sea deposits that create a low permeability aquitard between the surface system and the bedrock aquifer. Glacial gouging or ancient fluvial erosion of the limestone in some areas has resulted in up to 180 m of till (AMEC, 2003), but not in the immediate vicinity of the study sites reported here.

The study area is located ~3 km north-west of the open pit mine and is within one of the bioherm bands noted earlier. Whittington and Price (2012) studied 7 bioherms, the three with more detailed instrumentation; North Bioherm (NB), North Road Bioherm (NRB), and South Road Bioherm (SRB) are the focus of this study (see Figure 6-1). The bioherms are slightly elliptical in shape with the major axes being 115, 77 and 30 m, respectively, for the NB, NRB and SRB. The height of the bioherms range from 4 m at the NB to 1.5 m at NRB and SRB. The bioherms in this study area are surrounded by bogs dominated by *Sphagnum* species and lichen.

6.5 Methods

Subsurface stratigraphy around each bioherm was determined in two sets of transects (northwest to southeast, and northeast to southwest) of hand augered boreholes that extended across the top of the bioherm and out from the edge approximately 30-60 m (i.e., there are 4 peatland/bioherm-edge transitions at each bioherm; see black and white lines, Figure 6-1). The boreholes were advanced to bedrock; where sediment was found detailed observations were made and samples were collected. Sediment classifications are based on field descriptions and laboratory results of Atterburg limits and grain size distribution as set by the Unified Soil Classification System (ASTM D2487, 2011; ASTM D6913, 2009 for the fraction >63 µm). A Fritzch Laser Particle Analyzer was used to determine the distribution of the

finer grained portion (<63 µm). The stratigraphic information gathered through the boreholes was digitized as individual points and anchored to LiDAR generated surface topography of each bioherm.

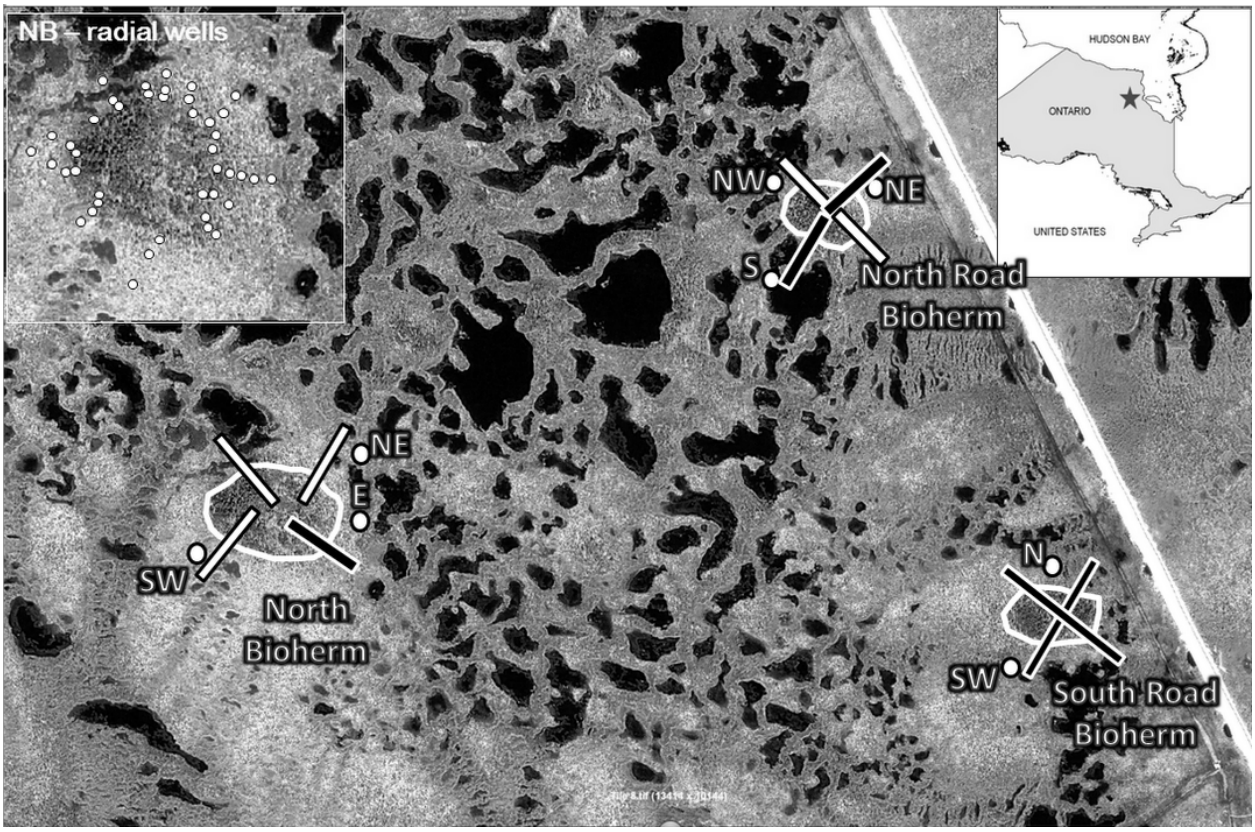

Figure 6-1 The position of the transects of stratigraphy surveys are shown with lines and are exaggerated in length. White lines are highly stratigrafied and black lines are poorly stratified (see Results). Piezometer nests installed in 2011 are shown with the white circles. Top left inset: example of radial well transects around the North Bioherm. Top right inset: location of study site within Ontario.

Bedrock monitoring wells installed in the middle of NB consisted of 2.5 cm diameter PVC standpipes, sand packed and sealed with bentonite in late 2006 or early 2007. Slotted intakes were 3 m long and the top of the slotted intakes were located at 24, 57 and 63 meters below ground surface (mbgs), all in the upper Attawapiskat formation (AMEC, 2011). Two transects of piezometer nests were installed to monitor the peat unit in the summer of 2007, one on the south side of NB, and one on the northwest side (not shown). In 2008 transects were installed on the east and south side of NRB and on the north and south side of SRB (not shown). The outermost nest of piezometers in these transects ranged from 15 to 75 m from the edge of the bioherm. Piezometers were constructed from 2.5 cm diameter PVC pipes and installed by pre-auguring a hole slightly smaller than the diameter of the pipe. Slotted intakes were 0.3 m

and were generally centred at 0.9 and 1.5 mbgs. A third piezometer was also installed (where peat thickness permitted) in each nest and was located at the peat/marine sediment interface, generally between 2 and 3 mbgs. Table 6-1 provides a summary of piezometer nests installed in the sediments.

Additional marine sediment piezometer nests with 10 cm screens were installed during the summer/early fall of 2011 using a thin filter pack around the screen and a bentonite seal above. Following installation any standing water was removed using a bailer to ensure that future water levels reflected pressures at each screen, not artefacts of installation. Each nest generally consisted of two piezometers in the marine sediments (shallow and deep), as well as one in the peat directly above. Three nests were installed at NB (SW, E, NE) and NRB (S, NW, NE) and two at SRB (SW, N) (Figure 6-1, white circles in the non-inset map). Hydraulic conductivity was determined from rising head tests using the Hvorslev (1951) method for unconfined aquifers.

Radial transects of wells (construction and installation same as piezometers, but slotted their entire length, ~1 m) were installed in 9 mini-transects around NB, NRB and SRB (see inset Figure 6-1). These transects generally had 3 wells: the first well was located ~5 m from the edge of the outcropping bioherm, the second 5-10 m and the third 15-30 m from that.

6.6 Results

The sediments are present in an apron structure around the bioherms; as the bedrock depth drops away from the centre of the bioherm the peat thickens to a maximum of ~3.3 m and the sediment thickness increases, reflecting the relatively consistent thickness of the peat and the decreasing elevation of the limestone. The borehole logs indicate each transect can be classified as either highly stratified or poorly stratified. The highly stratified type is shown in cross section on the left side of Figure 6-2 and the poorly stratified type on the right side. On Figure 6-1 the locations of highly stratified transects are indicated with white lines and the poorly stratified with black lines. The highly stratified areas present three to four sediment layers with distinct hydraulic properties and were identified on the southwest and northeast transects of NB and the northwest transect of NRB. Poorly stratified areas were found at the SRB (all transects), the southeast transect of NB, and the northeast and southwest transects at NRB and showed only silt and sand sediment layers between the peat and limestone.

Table 6-1: Summary of piezometer construction, stratigraphy at nests, vertical gradients, and vertical fluxes. All fluxes are calculated assuming Darcy's Law applies. Peat to sediment gradients and fluxes were calculated between the peizometer installed in the peat and the shallowest of the sediment instalations. Gradients and fluxes indicated as "within sediment" were calculated between the shallowest and the deepest of the sediment pizometer instalations. See the discussion section for furthr detail of flux calculations.

Location	Installation	Stratigraphy		Vertical Gradients		Fluxes mm/day	
		Depth (mbgs)	Layer	Peat to Sediment	Within Sediment	Peat to Sediment	Within Sediment
NB - SW	4 piezometers	0-2	Peat	~ -0.75	+0.3 to -0.5	-1.08	-1.4 to +0.84
	peat @ 1.75 mbgs	2-2.6	Silt				
	silt @ 2.35	2.6-3	Silty clay				
	silty clay@2.95	3-3.2	Sand				
	silty clay@3.55	3.2-3.6	Silty clay				
		3.6	Bedrock				
NB - E	2 piezometers	0-1.8	Peat	Peat is often dry therefore gradients cannot be determined			
	Peat@1.5	1.8-2.5	Silt				
	sand@2.9	2.5-3.2	Sand				
		3.2	Bedrock				
NB - NE	2 piezometers	0-2.7	Peat	Water levels do not appear to reach static levels across layers.			
	Silty clay@3.15	2.7-3	Silt				
	Silty sand@3.85	3-3.8	Silty clay				
		3.8-4	Silty sand				
		4	Bedrock				
NRB - NW	3 piezometers	0-2.4	Peat	-0.4 to -1	fluctuates from -0.4 to +0.06	-1	-0.13 to +0.02
	peat@1.35	2.4-2.6	Silt				
	silt@2.4	2.6-3	Clayey silt				
	clayey silt@2.9	3	Bedrock				
NRB - S	3 piezometers	0-2.3	Peat	Erratic but frequently:		-1.44	1.79
	peat@1.15	2.3-2.5	Silt	~ -1	-0.3 to +1		
	sand/silt@2.6	2.5-3.6	Sand & Silt				
	sand/silt@3.2	3.6	Bedrock				
NRB - NE	3 piezometers	0-2.9	Peat	-0.4	-0.08	0.64	0.04
	peat@1.15	2.7-3.5	Silt				
	silt@2.75	3.5-4	Sand				
	sand@3.9	4	Bedrock				
SRB - SW	3 piezometers	0-1.7	Peat	~ -0.2	~ -0.4	-0.29	-25.6
	peat@1.4	1.7-2.7	Silt				
	silt@1.9	2.7	Bedrock				
	silt@2.6						
SRB - N	3 piezometers	0-2.3	Peat	ranges from -0.6 to -0.8	fluctuate from -0.5 to +0.6	-1.01	-0.07 to +0.08
	peat@1.1	2.3-3.3	Sandy silt				
	sandy silt@2.6	3.3-3.6	Sand				
	sand@3.5	3.6	Bedrock				

Note: "-ve" gradient/flux indicates downward vertical component of flow.

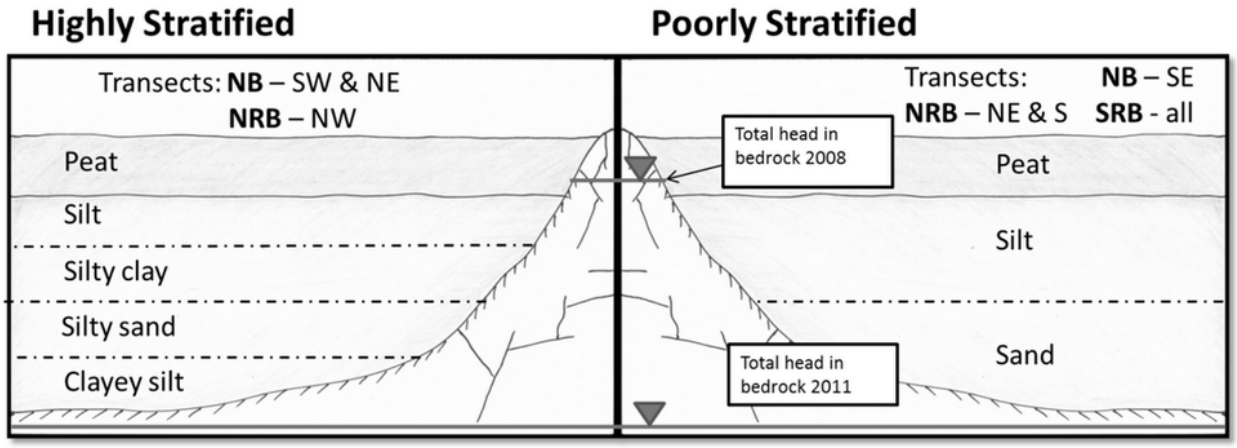

Figure 6-2 The observed stratigraphy at each transect matches one of two generalized stratigraphy types. On the left is the highly stratified type and on the right the poorly stratified type. Not to scale and vertically exaggerated.

The distribution and thickness of the higher hydraulic conductivity units is variable within this area. The K_h measured within the sediments range from $1.4x10^{-3}$ m/day in silty clay to $1.0x10^{-1}$ m/day in silt with some fine sand. There is significant variability among the very silty sediments and coarser grain size was not found to reliably correlate to higher K_h. The sediments with little to no clay fraction had an average K_h of $2.6x10^{-2}$ m/day. The K_h in the peat near the sediment interface was determined generally across the area by examining data collected at many piezometers. Where the peat-sediment interface is relatively shallow (1.5-2.4mbgs) K_h of the peat ranged from $1.7 x10^{-2}$ to $6.0 x10^{-1}$ m/day; however, in the more common case of a deeper interface (2.4-3.3 mbgs) the peat K_h included lower values, ranging from $6x10^{-3}$ to $1.1 x10^{-1}$ m/day. The median value of the deeper interface K_h of $2.6 x10^{-3}$ m/day was used when considering the flow regimes around the bioherms.

Dewatering of the Upper Attawapiskat formation for the mining operations began with a 60 day pumping test conducted in the fall of 2006 and dewatering pumps have been operating since January 2007 (HCI, 2007). Monitoring data from August, 2011 indicates a drawdown cone in the bedrock aquifer of approximately 5-7 m in the area of the study bioherms (AMEC, 2011). Bedrock water levels in NB were monitored as of June, 2007 and declined 2.6 m as of spring 2011. The NRB and SRB are slightly closer to the pumping wells than NB and based on the interpreted drawdown cone (AMEC, 2011) have experienced more drawdown; however no bedrock wells are installed in them. Peat water tables exhibited drawdown in a ~ 30 m zone surrounding bioherms (values showed similar trends to those presented by Whittington and Price (2012)). Outside of this ~30 m zone, the water table was generally 5-30 cm below the surface.

Water levels were monitored in the sediment piezometers in the fall of 2011 and the spring of 2012. The piezometers were occasionally dry, but more commonly showed pressure heads above the sediment/peat interface but below the water table found in the peat.

The piezometers installed in the sediment surround each bioherm; as such there are none near enough to each other to provide horizontal gradient data in units that are verifiably connected. The gradients measured represent either the vertical or horizontal components of the total gradient. Within the sediment layers only the vertical components could be measured. Within the peat around all bioherms downward vertical gradients (i_v) of ~0.57 (median) and horizontal conditions, generally ranging from 0.02-0.08 towards the bioherm were measured, confirming conditions are consistent with those reported by Whittington and Price (2012) under earlier stages of dewatering.

Vertical gradients within the sediments were not consistent (varied in magnitude and direction) compared to those within the peat (consistently downwards) (Table 6-1). Two general trends in the marine sediments were observed: those with large downward gradients (dominantly "vertically draining"), and those with small vertical gradients fluctuating between positive and negative, (probably dominated by lateral "radial flow"). The justification and classification of the vertical and radial flow will be addressed in the discussion section below. Vertically draining conditions were observed at SRB-SW and radial flow conditions were found at found at NB-SW, NRB - NW, NRB - S, and SRB - N. Note: Due to the frequency of recharge and the dewatering in the bedrock unit particular attention has been paid to evaluating if the water levels measured at particular locations reflect static conditions; those deemed not static are not reported here e.g., NB-E and NB-NE.

Figure 6-3 shows cross sections of each of the studied bioherms including, screen locations, K_h for each unit and the total heads and i_v measured on June 27, 2012. Cross sections (Figure 6-3) reflect the stratigraphy relative to the detailed LiDAR topography.

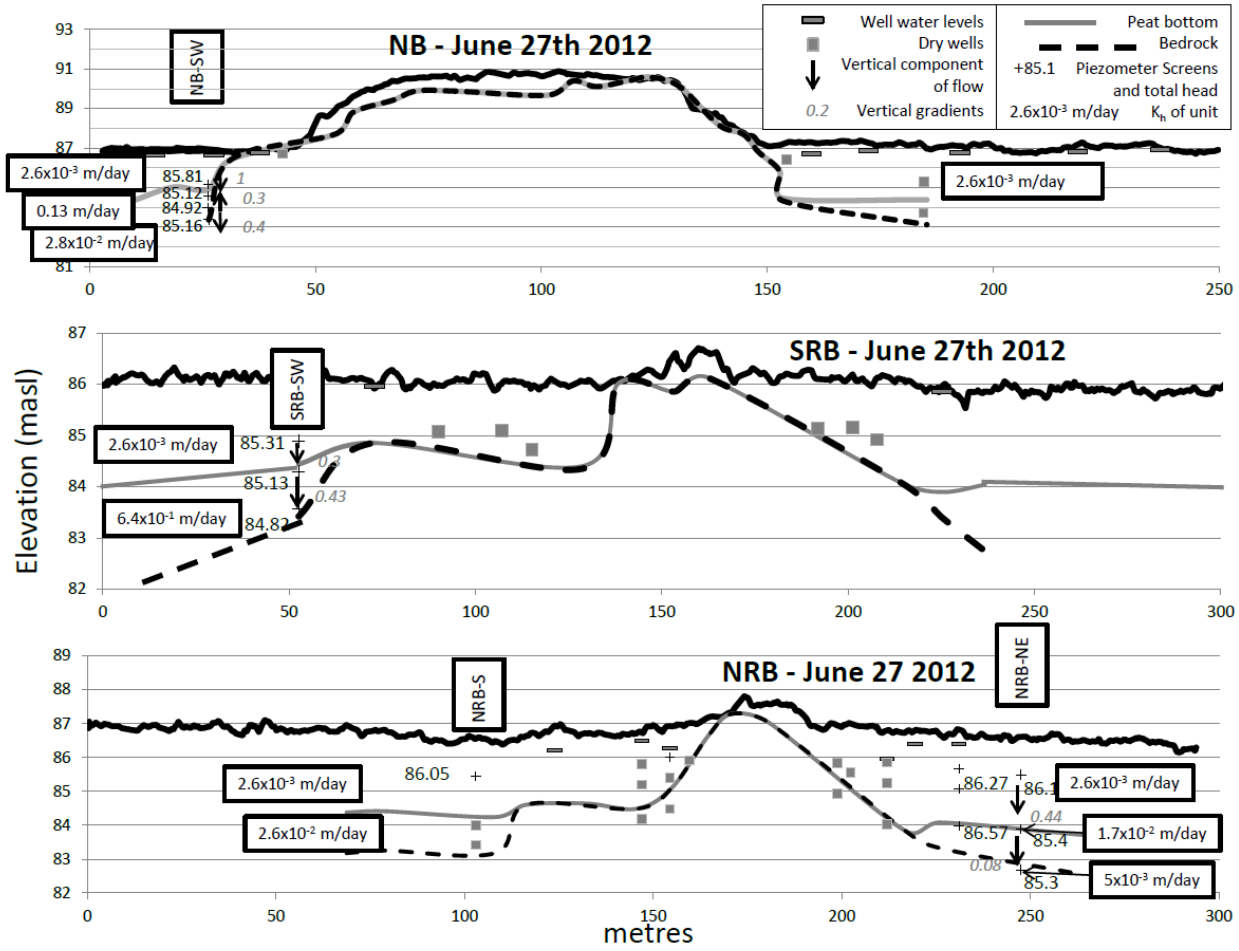

Figure 6-3 Hydraulic data collected around bioherms, a)North Bioherm, b)South Road Bioherm, c)North Road Bioherm.

6.7 Discussion

Prior to the start of pumping the bedrock aquifer had total heads above the sediment-peat interface elevation (HCI, 2006), whereas current bedrock heads are several metres below the base of the sediment (Figure 6-2). This is expected due to the drawdown cone caused by the mine dewatering. Under the new conditions downward gradients between the surface system and the Upper Attawapiskat bedrock aquifer are generated. The degree of peatland drainage is dependent upon the connectivity of these units and the transmissivity of the potential flow paths.

Considering the dominance of horizontal flow paths in limestone, the massive nature of bioherm cores, and the likely erosion of the talus edges, the available primary vertical flow paths are expected to be spatially limited. Secondary features such as karst channels will however have significant impacts. The

flow in a fracture or fissure is proportional to the cube of its aperture (Worthington and Ford, 2009) making massive variations (eight orders of magnitude) of hydraulic conductivity over small scale possible (Zanini et al., 2000). This range of variability makes the regional *K* of the Upper Attawapiskat as determined by pumping tests (HCI, 2007) irrelevant at the scale that is being considered around the bioherms. The vertical connectivity through karst at the bioherms could be spatially sporadic and is supported by the presence of both dry/drained areas and ponds of standing water proximal to the edge of the bioherms, which suggests the general absence in some areas at least of channels in the rock. In the bottom of Figure 6-4 ponds exist very close to the out-cropping bioherm, compared to the upper right portion of the photo where shrinking and drying ponds are visible.

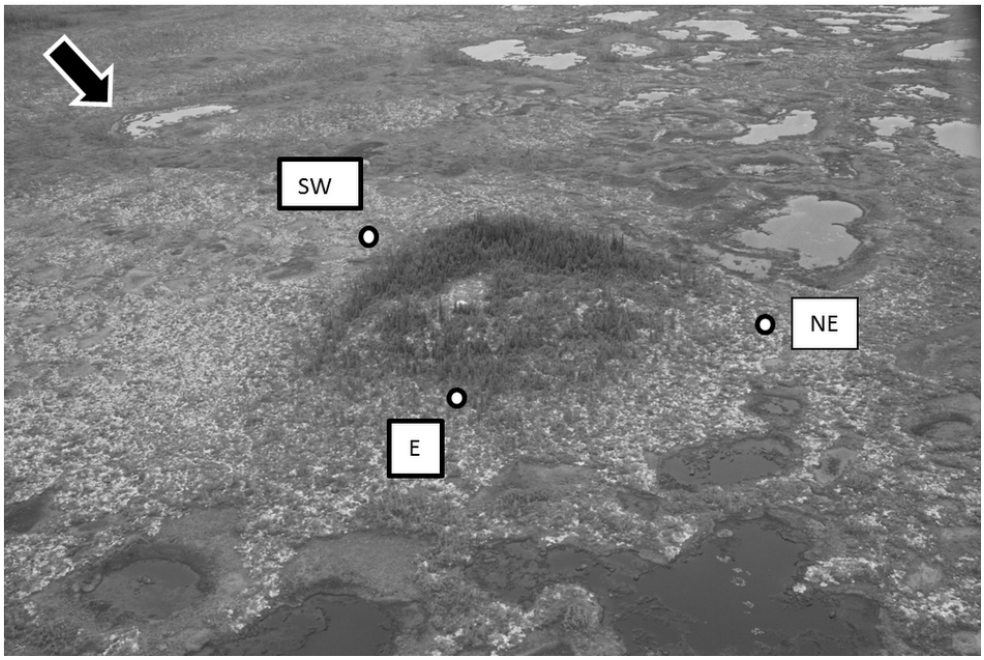

Figure 6-4 North Bioherm (within drawdown cone), August 2011. Outcropping bioherms have denser taller trees than the surrounding peatlands. Along the side of the bioherm both dry/drained condition and pools of standing water are observed. Black arrow indicates direction of North.

The hydraulic stratigraphy has been confirmed to be more complex than assumed by Whittington and Price (2012). The lowest hydraulic conductivity sediments could be reasonably effective in plugging vertical fractures or karstic connections, thus limiting the local influx of water to the Upper Attawapiskat formation. The sediments with little to no clay fraction however had an average K_h of $2.6x10^{-2}$ m/day, six times more conductive than the peat and several (2-5) orders of magnitude more conductive than is

generally expected from a clay layer (Fetter, 2001). Therefore they have the capacity to transmit significantly more water.

The presence of these highly conductive layers has implications for the flow regime around the bioherms. Vertical gradients and fluxes are used here to develop a conceptual model of flow within the sediment aprons consistent with our geological understanding. The vertical fluxes (Table 6-1) are calculated considering anisotropy of $1.8K_v=K_h$ in peat (Whittington and Price, submitted) and assuming $10K_v=K_h$ in the sediment. Determining in-situ anisotropy of *K* in sediments is difficult and expensive, often values are determined by trial and error in numerical modeling to match head data. The assumption of a 10:1 ratio is consistent with measure porous medium values (Barwell and Lee, 1981; Freeze and Cherry, 1979).

The conceptual model (presented in Figure 6-5) is of a flow regime where channels in the bioherms allow significant flow from the sediments into the bedrock, flow that would not have occurred prior to the dewatering (the gradients were not previously present). The drainage locations are supplied by radial (horizontal) flow occurring within the sediments. Each piezometer nest is a window into the flow regime, either near a channel in the rock (vertically draining) or somewhat removed from the channel (radial flow). We will use these names to classify the piezometer nests installed around NB, NRB, and SRB. The conceptual model is provided in Figure 6-5 indicating the relative relationships of K_v, i_v, and vertical flux among the units. The middle diagram shows the overall flow regime and the upper and lower diagrams show the conditions at radial flowing or vertically draining locations.

In the vertically draining marine sediments (e.g., SRB-SW) the i_v is large and indicates downward flow in both the peat and marine sediment units; the fluxes indicate the flow of water in the sediment is two orders of magnitude greater than the flux from peat to sediment (Figure 6-3 and Table 6-1). The much larger flux rate within the marine sediments indicates that water is supplied to the sediments at this location from somewhere other than the peat layer directly above. This nest is installed in a poorly stratified area where no low permeability sediments were observed, the absence of low permeability sediments is likely a control on the presence of vertical drainage conditions. We speculate that NB-E and NB-NE are also vertically draining, representing high fluxes and that the rapid flow makes static water levels rare (only static levels were considered in this study).

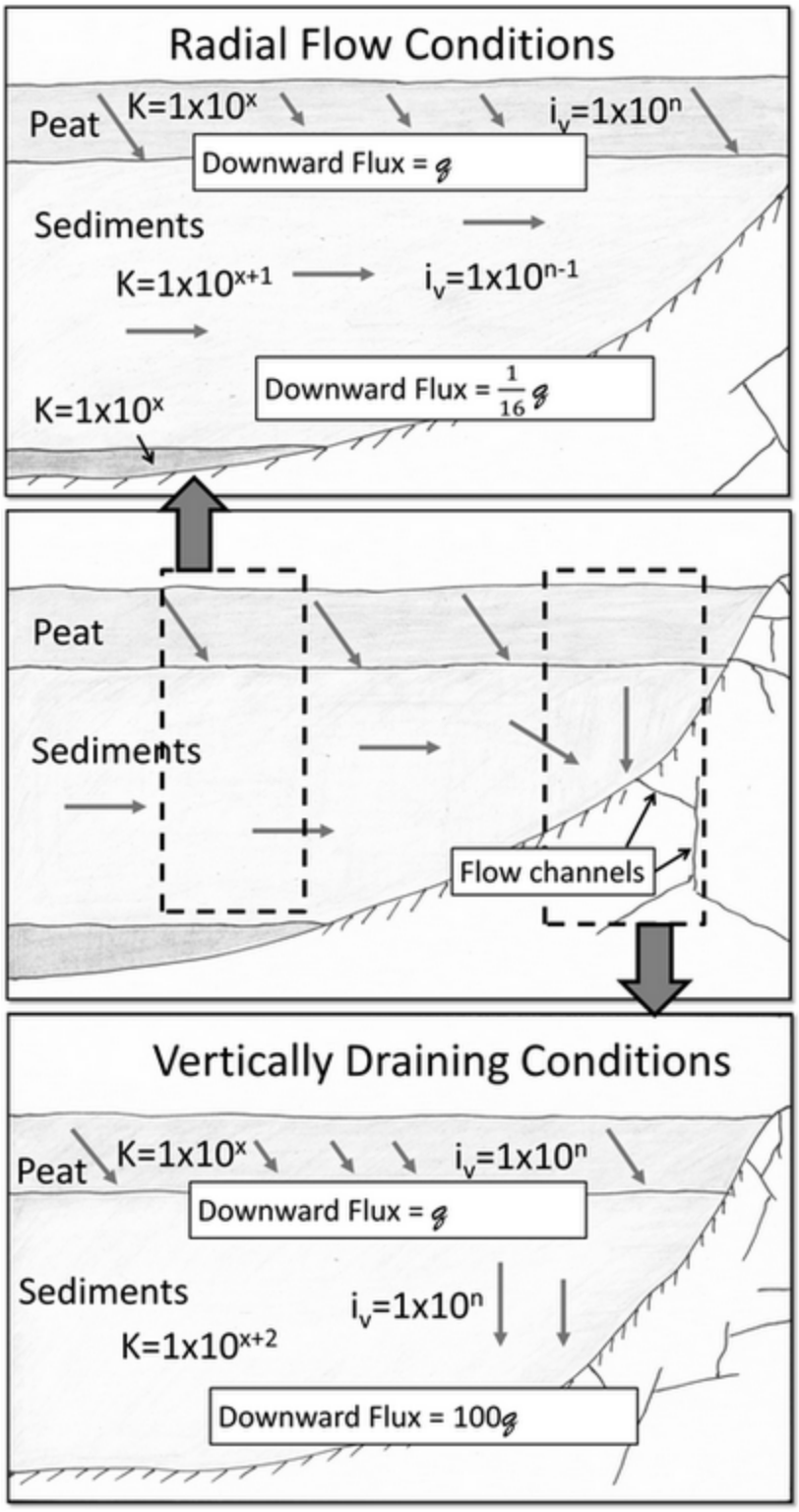

Figure 6-5 Conceptual flow model proximal to the bioherms. Vertically draining or radial flow conditions may be observed in the sediments near the bioherm depending on the position of the observations relative to channels in the rock.

Radial flow is observed much more often (NB-SW, NRB - NW, NRB - NE, NRB - S, and SRB – N) the i_v indicates significant downward flow in the peat layer but much lower, or at times even reversed i_v in the sediment. Based on the lower of the measured sediment K_h at each location (because this would be the limiting factor on vertical flow) and adjusted for anisotropy as discussed earlier, the fluxes at these locations indicate much less vertical flow in the sediments than from the peat to the sediments. For example at NRB-NE the vertical flux within the sediment is 0.04 mm/day and the vertical flux from the peat to the shallow sediment is 0.64 mm/day (see Table 6-1); therefore sixteen times (16:1) more water is flowing into the sediments from above than is moving downward in the sediments. The principle of conservation of mass indicates it must be flowing out horizontally within the sediment. While the difference is small considering the uncertainties of subsurface testing, this same trend is seen at several nests where flow in sediments occasionally reversed but the flux from peat to sediment were always greater than within the sediment; 8:1 at NRB-NW, 2:1 at NRB-S, and 14:1 at SRB-N. The repeatable difference in the vertical flux from the peat compared to that in the sediment suggests poor vertical connection to the bedrock aquifer at these locations (and hence horizontal flow). This may mean that there are no channels in the rock proximal to these nests or flow to the channels is impeded by low permeability sediment.

A conceptual flow net was constructed (Figure 6-5) to show the two flow regimes observed, the way they fit together, and how they relate to the proximity of a vertical flowpath between the sediments and the bedrock aquifer. Where there are highly permeable sediment layers (e.g. top of Figure 6-5) but no vertical pathway the flow is radial until access to the Upper Attawapiskat aquifer is encountered. Where high K_v sediments overly channels in the rock (fractures or karst) vertical drainage occurs (e.g. bottom of Figure 6-5).

6.8 Conclusion

A conceptual model of flow near bioherms combining radial flow in sediment under the peat layer and vertical drainage through channels in rock was presented. The model is consistent with measured hydraulic conductivities, vertical gradients, vertical fluxes and geological understanding. Despite the depressurization of the Upper Attawapiskat aquifer vertical flow is often limited. Drainage of the surface system to the depressurized bedrock aquifer occurs through vertical fractures and/or karstic features where present. Where either vertical pathways are absent or inhibited by low permeability sediments horizontal flow under the peat facilitates flow to the drainage locations. The nature of karst, presence of

low permeability sediments, and the structureless primary character of bioherm cores causes an uneven drainage pattern around the bioherms.

Whittington and Price (2012) identified a 30 m radius of drainage in the peat around the bioherms and assumed low *K* sediments. However, the presence of higher *K* sediments to transport the water laterally to the bioherms could increase this radius beyond 30 m by draining the peat from below, rather than laterally. Channels (karst or fractures) in rock have the potential to have very high transmissivity and so the spatial extent of the sediments layer that supplies water to them controls the extent of drainage that can occur at these locations.

Understanding the mechanisms of these bioherms as drainage nodes is important for current and future development in the area. The spatial distribution of drainage is significant in predicting the ecological impacts of dewatering programs. The location and volume of recharge to the bedrock system is also a key element in designing a dewatering system and predicting the extent and shape of the drawdown cone produced by pumping (HCI, 2004b).

To further validate this conceptual model and to quantify the lateral flow occurring in the sediment layers additional piezometers would be required in the sediments. These would ideally target areas of localized drainage (like the ponds) as well as being positioned in transects near enough to allow measurements of gradients in sediment layers proven to be well connected. Bioherms are the most accessible source of aggregate in the area; assuming future developments use them as such, much could be learned from suitable observations during the extraction, regarding the sediments and the nature of flow paths in the bioherm core and flanks.

6.9 Acknowledgements

The authors wish to thank M. Glover, J. Holloway, and E. Perras for help in the field. Special thanks to the De Beers Environment Lab for everything they do.

7 Conclusion

The factors that combined (climate is cool and wet, topography is flat and low hydraulic conductivity marine sediments widely underlying the peat minimized vertical seepage losses) to create the world's second largest wetland complex are, perhaps not unsurprisingly, the same factors that control the influence of the dewatering. The climate of the area has not changed (appreciably) over the life-span of the mine, however, the seasonal weather varied considerably over the 5 years, including a very wet year (2009) followed by a dry year (2010). The landscape topography and regional gradient remain essentially unchanged. The marine sediments (vertical seepage), however, have been shown to be very important and barring any changes to the marine sediments due to dewatering (some subsidence has been observed which could change some of the marine sediment's properties) the marine sediments are as they were when the peatlands began to develop.

Chapter 4 discussed the properties of the marine sediments, and paid particular attention to the combined effect of both the hydraulic conductivity and the thickness of the marine sediments. As we know from the results of that chapter, the marine sediments are not impermeable, allowing more drainage where the marine sediments are locally thinner (enhanced recharge zone) and less where they are thicker; we can conclude that the marine sediments do not strongly restrict vertical seepage losses as previously thought. If this is the case, then why did the Hudson-James Bay Lowlands grow to such a large extent? The answer requires a third factor, mentioned in Chapter 6 (see Figure 6-2) that shows the pre-dewatering bedrock head level, compared with the current (for this study, 2011) bedrock head and there is a critical difference between these two levels; in 2008 (and prior) the head was above the peat/marine sediment interface and in 2011 it was below the marine sediment/bedrock interface. Thus when considering the mitigating role the marine sediments may play in future developments in the lowlands all three factors must be considered: hydraulic conductivity, thickness, and existing pressure head.

To complicate matters further, the "thickness" factor mentioned above must also have a bedrock condition considered as well. Figure 6-5 shows two flow regimes (radially and vertically draining) that were speculated to be dependant of the presence of flow channels (cracks) in the bedrock. Further supporting evidence of this can been found in Figure 3-4 where several of the transects (e.g., Transect 1 (T1) of SRB and NRB) show a check-mark (e.g., ✓) shape where water levels are actually higher immediately adjacent to the bioherm, lower 5-10 m from the edge of the bioherm, and then returning

close to the surface ~20-30 m from the edge. This could be considered evidence of a flow channel located further away from the bioherm, as drawdown surrounding a pumping well would not exhibit this shape in a uniformly layered aquifer (discussed further below). Thus the conclusion of chapter 3 could be refined to state that it is the distance to accessible bedrock (e.g., flow channels) that was the important factor. The direct effect of exposed bioherms is still limited to ~30 m but this is more due to the properties of the peat, than those of the bioherm. The dramatic (>5 orders of magnitude) change in K over the upper ~50 cm, combined with deep peat hydraulic conductivities that are similar (or lower) than some of the marine sediments is what controls the ~30 m distance. As noted in the discussion of Chapter 3 simple modelling of the Theis (1935) equation showed that even under extreme dewatering in the bioherm (rates likely not physically possible), the water table in the peat was within 8 cm of the surface at ~25 m from the edge and could not show the check-mark pattern noted above.

Only considering the factors of the marine sediments (hydraulic conductivity, thickness, pressure head) as well as the "accessibility" of the bedrock would be imprudent without also considering the properties of the aquifer of concern: the peatland. Peat is a resilient medium with many self-regulating and self-protecting mechanisms designed to hold-on to water both horizontally (e.g., the Theis drainage) and vertically. Evidence of the vertical resiliency (here interpreted as annual water table position) is seen with the inter-annual weather appearing to have more of an effect on the peatlands' water balance than that from dewatering. The bioherms and ERZ do show long-term trends of increased water loss; however, large rain events can temporarily restore water levels to normal, healthy conditions, reducing the risk of long-term *Sphagnum* desiccation and death (as was shown in the near bioherm zone, Figure 3-4). What is unclear with only 5 years of data is how the long-term change in storage will eventually manifest itself with the growing season's water table and peat properties. We can speculate that eventually the spring melt will not be able to recharge the system from the previous year, particularly with over-winter under-drainage creating a large storage deficit. However, the storage deficit within the peat is not infinite; in fact it is quite finite as the depth of peat will not change (meaningfully) from year to year. Using a simple combination of peat depth (2.5 m) and a specific yield (0.15; unpublished field data) a completely drained peatland would need only 375 mm (2500 mm x 0.15) of precipitation to completely wet up; a very snowy winter and wet spring could go a long way to meeting that demand. Another factor is that precipitation comes from the surface and must go through all of the layers of peat before being committed to groundwater recharge (i.e., the water not used for evapotranspiration or lateral processes). Given the nature (the hydraulic conductivity profile mentioned previously) of peatlands, they are able to keep water near the surface delaying vertical seepage losses.

While precipitation essentially falls evenly across the peatland complex, precipitation which fell as snow has the chance to relocate before the spring melt occurs, when it becomes hydrologically active again. Interestingly, the patterns of snow distribution can help and exacerbate the storage deficits noted earlier in the various peatland forms. Chapter 2's main conclusion was snow depths were greater where tree density was higher, but that the density of the trees was not sufficient enough to alter melt rates between treed and non-treed areas. The domed bogs in the lowlands are typified by treeless, heavily ponded tops as the slope at the top of the dome is near 0; towards the side of the bogs the slope increases, allowing for better drainage and larger, more densely packed trees to grow. This edge is also where the edges of the fens are located. Thus the fens, which arguably could be the most affected (compared to bogs) by groundwater dewatering as they receive inputs of water from various sources (e.g., groundwater discharge, surface water inflow) that could be affected by dewatering, are actually situated in areas that receive the most winter precipitation (deepest snow) which could help make-up any overwintering storage deficits. As spring thaw occurs snow at the edges of the domed bogs, as well as within the densely packed riparian zone along the channel fens would supply snow melt water. Bogs, by comparison, have the shallowest snow pack atop the domed bogs and have no other sources of water to supplement any overwintering deficits. The domed bog in our study site is directly underlain by the enhanced recharge zone which would increase the storage deficit over the winter, essentially compounding the impacts. (Note: I am not suggesting that large domed bogs form over areas that have bedrock locally closer to the surface (i.e., enhanced recharge zone), but that in our study area this is the case.) Lastly, the bioherm edges are heavily treed (Figure 5-3) and have a much deeper snow pack than anywhere else on the transect (unpublished field data) which could help reduce the near bioherm spring deficit (i.e., in the ~30 m zone).

The final thing to consider when determining the potential impacts of dewatering to a peatland complex is to determine where in the watershed the cone of depression is anticipated to occur. Leclair (MSc student, personal communication) notes that in 2011 only 15% of the North Granny Creek watershed was impacted, and thus the headwaters were unaffected, allowing the channels fens to contribute water downstream to the affected part of the watershed, again, mitigating the impacts of dewatering.

7.1 The bigger picture

This thesis concentrated mostly on the role of the marine sediments (or lack thereof, i.e., bioherm areas), which the introduction of this thesis speculated would be a control on the runoff processes (i.e., marine sediments would control any subsidence in the peat as it would control the water table drawdown there, as

well as any subsidence with the marine sediments themselves causing larger surficial depressions) important for stream levels (fish habitat) and mercury dynamics.

The subsidence expected within the marine sediments and within the peatland complex did not occur to the extent anticipated. In fact, work done by (Richardson et al., 2012) (of which I am a co-author) found that during dry periods (i.e., 2010) peatland runoff scaled well with watershed size and was largely due to the near stream zone size and geomorphology and not necessarily the connectivity of patterned pools far from the streams. One potential implication of this finding is that the influence of water table drawdown due to mining activities on streamflow may influence watersheds proportionally, regardless of watershed size or landcover composition, at least during low flow periods (Richardson et al., 2012) . As the vast majority of the watershed (85%) was un-impacted (see above) runoff was therefore dependant on seasonal weather. By contrast, during wet periods (when water levels are high) the composition of the landscape (bogs vs. fens) became more important as the relationship between watershed size and runoff broke down (Richardson et al., 2012), however, this would not matter for fish habitat (high stream water levels) as the source of the water to the streams during high-flow periods is not of concern.

The effect of the dewatering on the rest of the water balance for the North Granny Creek watershed (M. Leclair, unfinished MSc thesis and personal communication) was minimal as the majority of the watershed was located outside the cone of depression. In fact, under-drainage accounted for less than 6 mm of the summer (May to August) water balance when areally weighted for the entire basin (precipitation and evapotranspiration ranged between 255-357 mm and 163-217 mm, respectively, for the years studied (2009-2011)).

Understanding the water chemistry and mercury dynamics has also been masked largely by the between-year variation as well as the between-site variation e.g., small scale variation such as hummock vs. hollow (Ulanowski and Branfireun, accepted) and large scale variation such as precipitation vs. bog vs. fen vs. marine sediment vs. bedrock (Orlova, 2012), which makes identifying end members for mixing models difficult (Orlova, 2012). The between-year variation in water chemistry (particularly mercury) due to annual weather patterns appears to trump any affect the mine may be having (Brian Branfireun, personal communication).

Given the Victor Mine's lifespan (~12 years) it is quite likely that the current trends will continue, but that no significant long term damage will occur. Ponds will (have already) drain only to be filled in again when either the pumps are turns off, or after a particularly snowy winter and cool, wet summer.

7.2 A comment about the Ring of Fire

As variable as the properties of peatlands can be across scales of 10s of centimetres (vertically) or 10s-100s of metres (horizontally), they are also somewhat predicable: K generally decreases with depth; bogs generally have thicker peat profiles with lower hydraulic conductivities than fens and that bogs are storage features and fens are the conveyors of the water. The similarities between the properties found in this thesis and in the literature, as well as other HJBL studies, would suggest that the peatlands in the Ring of Fire are also similar, despite a different genesis (these peatlands are more closely linked to their local hydrogeomorphic setting, rather than the regional post-Tyrrell sea/isostatic rebound factors noted earlier); this is further supported by the fact they share the same climate (cool, wet) as the rest of the lowlands. The underlying marine sediments (i.e., restricted vertical seepage factor) is therefore the most critical.

The Ring of Fire is located ~150 km due west of the Victor Mine. The proposed development site at the Ring of Fire straddles the western, feathered edge of the Paleozoic bedrock cover of the Hudson Bay basin and therefore both rocks of Precambrian and Paleozoic age occur beneath the cover of Quaternary sediments. The basic stratigraphy of the Quaternary-age sediments (peat, marine sediments, till and limestone bedrock) is similar but with some important differences: the Tyrrell Sea deposits (marine sediments) are not present in the Ring of Fire area; instead, other fine grained sediments, glaciolacustrine and till, which are, on average, a lot thinner than at Victor (Peter Barnett, Ontario Geological Survey, personal communication), provide a greater chance for enhanced recharge zones like those that were identified at Victor. Larger scale glacial and post-glacial features like eskers, fluted surface topography, as well as iceberg scours (or iceberg keel marks) (not observed at Victor) (Peter Barnett, Ontario Geological Survey, personal communication) could be important pathways for dewatering to impact the peatlands and should be considered very carefully.

Letters of copyright permission

Pete Whittington <whittington.pete@gmail.com>

RE: NON-RIGHTS LINK: copyright waivers

1 message

Permission Requests - UK <permissionsuk@wiley.com> Fri, Jan 11, 2013 at 6:24 AM
To: "whittington.pete@gmail.com" <whittington.pete@gmail.com>
Cc: HYP Editorial Office <hyp-editorial-office@wiley.com>, "Osborne, Jenny - Chichester" <josborne@wiley.com>

Dear Pete,

Thank you for your email request.

Permission is granted for you to use the material requested for your thesis/dissertation subject to the usual acknowledgements and on the understanding that you will reapply for permission if you wish to distribute or publish your thesis/dissertation commercially.

Permission is granted solely for use in conjunction with the thesis, and the article may not be posted online separately.

Any third party material is expressly excluded from this permission. If any material appears within the article with credit to another source, authorisation from that source must be obtained.

Best Wishes,

Verity Butler

Permissions Co-ordinator

Wiley

The Atrium, Southern Gate
Chichester, PO19 8SQ

UK
www.wiley.com

vbutler@wiley.com

References

Adams, W. 1976. Areal differentiation of snow cover in east central Ontario. *Water Resources Research* **12**(6): 1226-1234

Adams, W., Roulet, N. 1982. Areal differentiation of land and lake snowcover in a small sub-Arctic drainage basin. *Nordic Hydrology* **13**(3): 139-156

Alexander, M.E., Stocks, B.J., Lawson, B.D. 1991. Fire behavior in black spruce-lichen woodland: the Porter Lake project (No. NOR-X-310). Forestry Canada, Northwest Region.

AMEC. 2003. Civil Geotechnical Investigation, Victor Diamond Project Feasibility Study, Attawapiskat, Ontario; Geotechnical Investigation Report. Submitted to: De Beers Canada Exploration Inc.

AMEC. 2004. Victor Diamond Project, Environmental assessment comprehensive study.

AMEC. 2011. Correspondence with AMEC staff, water level monitoring data, interpreted drawdown map..

ASTM D2487. 2011. Standard Practice for Classification of Soils for Engineering Purposes (Unified Soil Classification System).

ASTM D6913. 2009. Standard Methods for Particle-Size Distribution (Gradation) of Soils Using Sieve Analysis.

Barwell, V.K., Lee, D. 1981. Determination of horizontal-to-vertical hydraulic conductivity ratios from seepage measurements on lake beds. *Water Resources Research* **17**(3): 565-570

Beckwith, C.W., Baird, A.J., Heathwaite, A.L. 2003. Anisotropy and depth-related heterogeneity of hydraulic conductivity in a bog peat. I: laboratory measurements. *Hydrological Processes* **17**: 89-101

Belyea, L.R., Baird, A. 2006. Beyond "the limits to peat bog growth": cross-scale feedback in peatland development. *Ecological Monographs* **76**(3): 299-322

Benscoter, B.W., Thompson, D.K., Waddington, J.M., Flannigan, M.D., Wotton, B.M., de Groot, W.J., Turetsky, M.R. 2011. Interactive effects of vegetation, soil moisture and bulk density on depth of burning of thick organic soils. *International Journal of Wildland Fire* **20**(3): 418-429

Benson, C.S., Sturm, M. 1993. Structure and wind transport of seasonal snow on the Arctic slope of Alaska. *Annals of Glaciology* **18**: 261-267

Boelter, D. 1972. Water table drawdown around an open ditch in organic soils. *Journal of Hydrology* **15**(4): 329-340

Boon, S. 2009. Snow ablation energy balance in a dead forest stand. *Hydrological Processes* **23**(18): 2600-2610

Boon, S. 2011. Snow accumulation following forest disturbance. *Ecohydrology* **doi: 10.1002/eco.212**

Chason, D.B., Siegel, D.I. 1986. Hydraulic conductivity and related physical properties of peat, Lost River Peatland, Northern Minnesota. *Soil Science* **142**(2): 91-99

Clymo, R. 1984. The Limits to Peat Bog Growth. *Philosophical Transactions of the Royal Society of London. Series B, Biological Sciences (1934-1990)* **303**(1117): 605-654

Cottam, G., Curtis, J.T. 1956. The use of distance measures in phytosociological sampling. *Ecology* **37**(3): 451-460

Cowell, D.W. 1983. Karst hydrogeology within a subarctic peatland: Attawapiskat River, Hudson Bay Lowland, Canada. *Journal of Hydrology* **61**: 169-175

Di Febo, A. 2011. On developing an unambiguous peatland classification using fusion of IKONOS and LiDAR DEM terrain derivatives - Victor Project, James Bay Lowlands, University of Waterloo, Waterloo.

Drake, J. 1981. The effects of surface dust on snowmelt rates. *Arctic and Alpine Research* **13**(2): 219-223

Drake, J., Moore, T.R. 1980. Snow pH and dust loading at Schefferville, Quebec. *Geographica* **XXIV**(3): 286-291

Dredge, L.A., Cowan, W.R. 1989. Quaternary geology of the southwestern Canadian Shield; in Chapter 3 of Quaternary Geology of Canada and Greenland. In: Fulton, R.J. (Ed.). Geological Survey of Canada, Geology of Canada no. 1.

Drege, L.A., Cowan, W.R. 1989. Quaternary geology of the south western Canadian Sheild, Quaternary Geology of Canada and Greenland. Geological Survey of Canada, pp. 214-249.

Eaton, T.T. 2010. Is one an upper limit for natural hydraulic gradients? *Ground Water* **48**(1): 13-14

Elder, K., Dozier, J., Michaelsen, J. 1991. Snow accumulation and distribution in an alpine watershed. *Water Resources Research* **27**(7): 1541-1552

Environment Canada. 2008. Canadian Climate Normals or Averages 1971-2000, accessed June 15, 2011 http://www.climate.weatheroffice.ec.gc.ca/climate_normals/index_e.html.

Fetter, C. 1994. Applied Hydrogeology. Macmillan New York (USA).

Fetter, C.W. 2001. Applied Hydrogeology 4th Edition. Prentice-Hall Inc.

Fraser, C., Roulet, N., Lafleur, M. 2001. Groundwater flow patterns in a large peatland. *Journal of Hydrology* **246**(1-4): 142-154

Freeze, R.A., Cherry, J.A. 1979. Groundwater. Prentice-Hall, Englewood Cliffs, N.J., xvi, 604 pp.

Gagnon, A.S., Gough, W.A. 2001. Trends in the dates of ice freeze-up and breakup over Hudson Bay, Canada. *Arctic* **58**(4): 370-382

Glaser, P.H., Hansen, B., Seigel, D., Reeve, A.S., Morin, P. 2004a. Rates, pathways and drivers for peatland development in the Hudson Bay Lowlands, northern Ontario, Canada. *Journal of Ecology* **6**(92): 1036-1053.

Glaser, P.H., Hansen, B., Siegel, D., Reeve, A.S., Morin, P. 2004b. Rates, pathways and drivers for peatland development in the Hudson Bay Lowlands, northern Ontario, Canada. *Journal of Ecology* **92**(6): 1036-1053

Glaser, P.H., Seigel, D.I., Reeve, A.S., Janssens, J., Janecky, D. 2004c. Tectonic drivers for vegetation patterning and landscape evolution in the Albany River region of the Hudson Bay Lowlands. *Journal of Ecology* **92**(6): 1054-1070

Glaser, P.H., Seigel, D.I., Reeve, A.S., Janssens, J., Janecky, D. 2004d. Tectonic drivers for vegetation patterning and landscape evolution in the Albany River region of the Hudson Bay Lowlands. *Journal of Ecology* **6**(92): 1054-1070.

Glaser, P.H., Siegel, D., Romanowicz, E.A., Shen, Y. 1997. Regional linkages between raised bogs and the climate, groundwater and landscape of north-western Mnnesota. *Journal of Ecology* **85**(1): 3-16

Gorham, E. 1991. Northern peatlands: Role in the carbon cycle and probable responses to climatic warming. *Ecological Applications* **1**(2): 182-195

Gough, W.A., Wolfe, E. 2001. Climate change scenarios for Hudson Bay, Canada, from general circulation models. *Arctic* **54**(2): 142-148

Gower, S., Vogel, J., Norman, J., Kurcharik, C., Steele, S., Stow, T. 1997. Carbon distribution and aboveground net primary production in aspen, jack pine, and black spruce stands in Saskatchewan and Manitoba, Canada. *Journal of Geophysical Research* **102**(D24): 29029-29041

Hamlin, L., Pietroniro, A., Prowse, T.D., Soulis, E., Kouwen, N. 1998. Application of indexed snowmelt algorithms in a northern wetland regime. *Hydrological Processes* **12**: 1641-1657

Hart, D.J., Bradbury, K.R., Gotkowitz, M.B. 2008. Is one an upper limit for natural hydraulic gradients? *Ground Water* **46**(4): 518-520

HCI. 2004a. Dewatering of the Victor Diamond Project. Predicted Engineering, Cost, and Environmental Factors. HCI-1779, Prepared by Hydrologic Consultants Inc of Colorado.

HCI. 2004b. Dewatering of Victor Diamond Project Predicted Engineering, Cost, and Environmental Factors. Addendum I: Update of Ground-Water Flow Model Utilising New Surface-Water Chemistry and Flow Data from Nayshkootayaow River and Results of Sensitivity Analyses.

HCI. 2006. 2005-2006 Hydrogeologic Field Programming Hydraulic Testing and Construction of Monitoring wells Victor Diamond Project, Ontario., Hydrologic Consultants Inc., Hydrologic Consultants Inc.

HCI. 2007. Dewatering of the Victor Diamond Mine. Predicted Engineering and Environmental Factors. HCI-1779, Colorado.

Hedstrom, N., Pomeroy, J. 1998. Measurements and modelling of snow interception in the boreal forest. *Hydrological Processes* **12**(10 11): 1611-1625

Hills, E.S. 1963. Elements of Structural Geology. Jarrold & Sons Ltd., London, England.

Hoag, R.S., Price, J.S. 1997. The effects of matrix diffusion on solute transport and retardation in undisturbed peat in laboratory columns. *Journal of Contaminant Hydrology* **28**

Hvorslev, M.J. 1951. Time lag and soil permeability in groundwater observations, Waterways Experimental Station Bulletin 36. US Army Corps of Engineers, Vicksburg, Mississippi.

Ingram, H.A.P. 1982. Size and shape in raised mire ecosystems: a geophysical model. *Nature* **297**: 300-303

Itasca Dever Inc. 2011. Dewatering of Victor Diamond Project, March 2011 update of March 2008 Groundwater flow model, Denver, Colorado.

Johnston, D.C. 2012. Quantifying the Fuel Load, Fuel Structure and Fire Behaviour of Forested Bogs and Blowdown, University of Toronto, Toronto, Ontario, 149 pp.

Kellner, E., Lundin, L.-C. 2001. Calibration of time domain reflectometry for water content in peat soil. *Nordic Hydrology* **32**(4-5): 315-332

Ketcheson, S.J., Whittington, P., Price, J.S. 2012. The effect of peatland harvesting on snow accumulation, ablation and snow surface energy balance. *Hydrological Processes*.10.1002/hyp.9325

King, W.A., Martini, I. 1984. Morphology and recent sediments of the lower anastomosing reaches of the Attawapiskat River. *Sedimentary Geology* **37**(4): 295-320

Kirk, J.L., St. Louis, V.L. 2009. Multiyear total and methyl mercury exports from two major sub-Arctic rivers draining into Hudson Bay, Canada. *Environmental science & technology* **43**(7): 2254-2261

Klinger, L., Short, S. 1996. Succession in the Hudson Bay lowland, northern Ontario, Canada. *Arctic and Alpine Research* **28**(2): 172-183

Koivusalo, H., Kokkonen, T. 2002. Snow processes in a forest clearing and in a coniferous forest. *Journal of Hydrology* **262**(1-4): 145-164

Lawson, B.D., Armitage, O.B. 2008. Weather Guide for the Canadian Forest Fire Danger Rating System. *Natural Resources Canada, Canadian Forest Service, Northern Forestry Centre, Edmonton, Alberta.* : 84 p.

Lawson, B.D., Dalrymple, G.N. 1996. Ground-truthing the Drought Code: Field verification of overwinter recharge of forest floor moisture. Natural Resources Canada, Canadian Forest Service, Pacific Forestry Centre, Victoria, BC. Forest Resource Development Agreement Report 268.

Lee, H.A. 1960a. Late Glacial and Postglacial Hudson Bay Sea Episode. *Science* **131**: 1609-1611

Lee, H.A. 1960b. Late Glacial and Postglacial Hudson Bay Sea Episode. *Science* **131**: 1609-1611

Lieffers, V.J., Macdonald, S.E. 1990. Growth and foliar nutrient status of black spruce and tamarack in relation to depth of water table in some Alberta peatlands. *Canadian Journal of Forest Research* **20**: 805-809

Martini, I. 1981. Morphology and sediments of the emergent Ontario coast of James Bay, Canada. *Geografiska Annaler. Series A. Physical Geography* **63**(1): 81-94

Martini, I.P. 2006. The cold-climate peatlands of the Hudson Bay Lowlands, Canada: brief overview of recent work, Peatlands: Evolution and Records of Environmental and Climate Changes.

McDonald, B.C. 1989. Glacial and interglacial stratigraphy, Hudson Bay Lowland. In: Fulton, R.J. (Ed.), Quaternary Geology of Canada and Greenland, Geology of Canada. Geological Survey of Canada.

M^{c}Rae, D.J., Alexander, M.E., Stocks, B.J. 1979. Measurement and description of fuels and fire behaviour on prescribed burns: a handbook. Department of the Environment, Canadian Forestry Service, Great Lakes Forest Research Centre. Information Report O-X-287. 44p., Sault Ste. Marie, Ontario.

National Wetlands Working Group. 1997. The Canadian Wetland Classification System - Second Edition. University of Waterloo, Waterloo, Ontario.

Neuzil, C.E., Provost, A.M. 2009. Recent experimental data may point to a greater role for osmotic pressures in the subsurface. *Water Resources Research* **45**: 14

Orlova, J. 2012. Surface Water and Groundwater Contributions to Streamflow in the Hudson Bay Lowlands, University of Western Ontario, London, Ontario, 123 pp.

Parisien, M.A., Peters, V.S., Wang, Y., Little, J.M., Bosch, E.M., Stocks, B.J. 2006. Spatial patterns of forest fires in Canada, 1980-1999. *International Journal of Wildland Fire* **15**(3): 361-374

Petrov, N.I., Petrova, G.N., D'Alessandro, F. 2003. Quantification of the probability of lightning strikes to structures using a fractal approach. *Dielectrics and Electrical Insulation, IEEE Transactions on* **10**(4): 641-654

Pietroniro, A., Prowse, T.D., Hamlin, L., Kouwen, N., Soulis, R. 1996. Application of a grouped response unit hydrological model to a northern wetland region. *Hydrological Processes* **10**(10): 1245-1261

Pomeroy, J., Gray, D. 1995. Snowcover accumulation, relocation and management. *Bulletin of the International Society of Soil Science no* **88**: 2

Pomeroy, J.W., Gray, D.M., Hedstrom, N.R., Janowicz, J.R. 2002. Prediction of seasonal snow accumulation in cold climate forests. *Hydrological Processes* **16**: 3543-3558

Price, J.S., Maloney, D.A. 1994. Hydrology of a patterned bog-fen complex in southeastern Labrador, Canada. *Nordic Hydrology* **25**: 313-330

Price, J.S., Woo, M.-k. 1988a. Studies of subarctic coastal marsh. 1. Hydrology. *Journal of Hydrology* **103**: 275-292

Price, J.S., Woo, M.K. 1988b. Studies of a subarctic coastal marsh: I Hydrology. *Journal of Hydrogeology*(103): 275-292

Quinton, W.L., Hayashi, M., Pietroniro, A. 2003. Connectivity and storage functions of channel fens and flat bogs in northern basins. *Hydrological Processes* **17**: 3665-3684

R Development Core Team. 2009. R: A language and environment for statistical computing. R Foundation for Statistical Computing.

Reeve, A., Siegel, D., Glaser, P. 2000. Simulating vertical flow in large peatlands. *Journal of Hydrology* **227**(1-4): 207-217

Reeve, A., Siegel, D., Glaser, P. 2001. Simulating dispersive mixing in large peatlands. *Journal of Hydrology* **242**(1-2): 103-114

Reeve, A.S. 1996. Numerical and mutlivariate statistical analysis of hydrogeology and geochemistry in large peatlands., Syracuse University, Syracuse, New York.

Reifsnyder, W.E., Lull, H.W. 1965. Radiant Energy in Relation to Forests. In: Service, U.S.D.o.A.F. (Ed.). U.S. Government Printing Office, Washington D.C., pp. 125.

Richardson, M., Ketcheson, S.J., Whittington, P., Price, J. 2012. Runoff generation in a northern peatland complex: the influences of catchment morphology and scale *Hydrological Processes* **26**(12): 1805-1817.10.1002/hyp.9322

Riley, J.L. 2011. Wetlands of the Ontario Hudson Bay Lowland: An Regional Overview. Nature Conservancy of Canada, Toronto, Ontario, Canada, 156 pp.

Roulet, N.T. 2000. Peatlands, carbon storage, greenhouse gases, and the Kyoto Protocol: Prospects and significance for Canada. *Wetlands* **20**(4): 605-615

Roulet, N.T., Moore, T.R., Bubier, J., Lafleur, P. 1992. Northern fens: methane flux and climatic change. *Tellus* **44B**: 100-105

Rouse, W.R., Woo, M., Price, J.S. 1992. Damming James Bay: I. Potential impacts on coastal climate and the water balance. *The Canadian Geographer* **36**(1): 2-7

Roy, M., Dell'Oste, F., Veillette, J.J., Vernal, A.d., Helie, J.F., Parent, M. 2011. Insights on the events surrounding the final drainage of Lake Ojibway based on James Bay stratigraphic sequences. *Quaternary Science Reviews, 30*: 682-692

Schlotzhauer, S.M., Price, J.S. 1999. Soil water flow dynamics in a managed cutover peat field, Quebec: Field and laboratory investigations. *Water Resources Research* **35**(12): 3675-3683

Silins, U., Rothwell, R.L. 1998. Forest peatland drainage and subsidence affect soil water retention and transport properties in an Alberta peatland. *Soil Science Society of America Journal* **62**(4): 1048-1056

Singer, S.N., Chen, C.K. 2002. An assessment of the groundwater resources of Northern Ontario, Environmental monitoring and reporting branch, Ministry of Environment, Toronto, Ontario, Canada.

Sjors, H. 1963. Bogs and Fens on Attawapiskat River, Northern Ontaio., Department of Northern Affairs and National Resources.

Sjörs, H. 1963. Bogs and Fens on Attawapiskat River, Northern Ontario. Canada Dept. of Northern Affairs and National Resources.

Spence, C., Woo, M.-k. 2003. Hydrology of subarctic Canadian shield: soil-filled valleys. *Journal of Hydrology* **279**: 151-166

Steppuhn, H., Dyck, G. 1974. Estimating true basin snowcover, Advanced concepts and techniques in the study of snow and ice resources: an interdisciplinary symposium;[papers]. National Academies.

Stocks, B.J. 1980. Black spruce crown fuel weights in northern Ontario. *Canadian Journal of Forest Research* **10**(4): 498-501

Sturm, M., McFadden, J.P., Liston, G.E., Chapin III, F.S., Racine, C.H., Holmgren, J. 2001. Snow-shrub interactions in Arctic Tundra: A Hypothesis with Climate Implications. *Journal of Climate* **14**: 336-344

Tarnocai, C. 1998. The amount of organic carbon in various soil orders and ecological provinces in Canada. In: Lal, R., Kimble, J., Follet, R., Stewart, B. (Eds.), Soil Processes and the Carbon Cycle. CRC Press, Boca Raton, Florida, pp. 81-92.

Theis, C.V. 1935. The lowering of the piezometer surface and the rate and discharge of a well using ground-water storage. *Transactions, American Geophysical Union* **16**: 519-524

Thompson, D.K., Wotton, B.M., Waddington, J.M. submitted. Heat transfer and the initiation of organic soil combustion during wildfire in forested wetlands. *International Journal of Wildland Fire*

Turetsky, M.R., Donahue, W.F., Benscoter, B.W. 2011. Experimental drying intensifies burning and carbon losses in a northern peatland. *Nature Communications* **2**(51).10.1038/ncomms1523

Ulanowski, T., Branfireun, B. accepted. Small-scale variability in peatland pore-water biogeochemistry, Hudson Bay Lowland, Canada. *Science of the total environment*

Ullrich, S.M., Tanton, T.W., Abdrashitova, S. 2001. Mercury in the Aquatic Environment: A Review of Factors Affecting Methylation. *Critical Reviews in Environmental Science and Technology* **31**(3): 241-293

Van Wagner, C.E. 1972. Duff consumption by fire in eastern pine stands. *Canadian Journal of Forest Research* **2**(1): 34-39

Van Wagner, C.E. 1987. Development and Structure of the Canadian Forest Fire Weather Index System, Canadian Forestry Service, Ottawa. Forestry Techincal Report 35. 35 p.

Vitt, D.H., Wieder, K., Halsey, L., Turetsky, M.R. 2003. Response of Sphagnum fuscum to nitrogen deposition: a case study of ombrogenous peatlands in Alberta, Canada. *The Bryologist* **106**(2): 235-245

Waddington, J.M., Thompson, D.K., Wotton, B.M., Quinton, W., Flannigan, M.D., Benscoter, B.W., Baisley, S.A., Turetsky, M.R. 2012. Examining the utility of the Canadian Forest Fire Weather Index System in boreal peatlands. *Canadian Journal of Forest Research* **42**: 47-58

Whittington, P., Price, J.S. 2006. The effects of water table draw-down (as a surrogate for climate change) on the hydrology of a patterned fen peatland near Quebec City, Quebec. *Hydrological Processes*(20): 3589-3600

Whittington, P., Price, J.S. 2012. Effect of mine dewatering on peatlands of the James Bay Lowland: the role of bioherms. *Hydrological Processes* **26**(12): 1818-1826.10.1002/hyp.9266

Whittington, P., Price, J.S. submitted. Effect of mine dewatering on the peatlands of the James Bay Lowland: the role of marine sediments on mitigating peatland drainage. *Hydrological Processes* **HYP-12-0656**

Whittington, P., Strack, M., Van Haarlem, R., Kaufman, S., Stoesser, P., Maltez, J., Price, J., Stone, M. 2007. The influence of peat volume change and vegetation on the hydrology of a kettle-hole wetland in Southern Ontario, Canada. *Mires and Peat* **2**: 1-14

Whittington, P.N., Ketcheson, S.J., Price, J.S., Richardson, M., Di Febo, A. 2012. Areal differentiation of snow accumulation and melt between peatland types in the James Bay Lowlands. *Hydrological Processes* **26**(17): 2662-2671.10.1002/hyp.9414

Woo, M. 1998. Arctic Snow Cover Information for Hydrological Investigations at Various Scales. *Nordic Hydrology* **29**(4/5): 245-266

Woo, M., Marsh, P. 1978. Analysis of Error in the Determination of Snow Storage for Small High Arctic Basins. *Journal of Applied Meteorology* **17**: 1537-1541

Woo, M., Young, K.L. 1997. Hydrology of a Small Drainage Basin with Polar Oasis Environment, Fosheim Peninsula, Ellesmere Island, Canada. *Permafrost and Periglacial Processes* **8**: 257-277

Worthington, S.R.H. 2009. Diagnostic hydrogeological characteristics of a karst aquifer (Kentucy, USA). *Hydrogeology Journal* **17**: 1665-1678

Worthington, S.R.H., Ford, D.C. 2009. Self-organized permeability in carbonate aquifers. *Ground Water* **47**: 326-336

Zanini, L., Novakowski, K.S., Lapcevie, P., Bickerton, G.S., Voralek, J., Talbot, C. 2000. Ground Water Flow in a Fractured Carbonate Aquifer Inferred from Combined Hydrogeological and Geochemical Measurements. *Ground Water*(38): 350–360